DESIGN AND PERFORMANCE ANALYSIS OF MIMO SPACE-TIME BLOCK CODING SYSTEMS OVER GENERAL FADING CHANNELS

HE JUN

NATIONAL UNIVERSITY OF SINGAPORE

2008

DESIGN AND PERFORMANCE ANALYSIS OF MIMO SPACE-TIME BLOCK CODING SYSTEMS OVER GENERAL FADING CHANNELS

HE JUN

(*B. Eng., Zhejiang University, P.R.China*)

A THESIS SUBMITTED

FOR THE DEGREE OF DOCTOR OF PHILOSOPHY

DEPARTMENT OF ELECTRICAL AND COMPUTER ENGINEERING

NATIONAL UNIVERSITY OF SINGAPORE

2008

Acknowledgment

Numerous people have supported me during the development of this thesis. A few words mentioned here cannot adequately capture all my appreciation.

My supervisor, Professor Pooi Yuen Kam, deserves particular attention and many, many thanks. His passion for research and knowledgeable suggestions have greatly enhanced my enjoyment of this process, and significantly improved the quality of my research work.

I would also like to thank my colleagues and friends in the Communications Lab and the ECE-I^{2}R Wireless Communication Lab for their generous help and warm friendship during these years.

Last, my most tender and sincere thanks go to my family, especially my loving wife, Wang Huan, for her love, understanding, and patience.

Contents

Summary

Space-time block coding (STBC) is a well-known technology to exploit the spatial diversity in multiple-input multiple-output (MIMO) systems, due to its good performance and simplicity of decoding. The existing works on STBC, however, are often based on ideal assumptions, such as channels are identically distributed, or block-wise constant. These assumptions simplify the analysis and design of STBC, but reduce their generality. Therefore, large gaps remain between the real application and the theoretical analysis. The results of STBC obtained so far might not be readily applicable in the real world. Therefore, one purpose of this thesis is to relax some of these unrealistic assumptions, and study STBC in more general channel models. In this thesis, we will examine STBC over general fading channels. Three channel models, namely non-identical channels, time-selective channels and relay channels, are considered.

For STBC over non-identical channels, the performance with both perfect and estimated channel state information (CSI) is investigated. If perfect CSI is available, we derive the exact bit error probability (BEP), together with an upper bound on the BEP. The different effects of non-identical channel statistics on the performance are examined, An optimum power allocation scheme is also proposed. On the other hand, if the CSI is imperfect, we show that the structure of the maximum likelihood (ML) detector is different from the conventional one for the identical channels. The performance of the new ML decoder is analyzed. A new symbol-by-symbol (SBS)

decoder is obtained from the new ML decoder, under certain conditions. A comparison of the performance between the conventional and the new SBS decoders is provided.

For STBC over time-selective channels, we derive the exact BEP. More importantly, we reveal the relationship between the inter-symbol interference (ISI) and the row positions in the code matrix. One proposition is presented for searching for the optimum code, which minimizes the ISI over a time-selective channel. For systems with large numbers of antennas, the code search may become prohibitive, even with the help of the proposition. We then propose two design criteria, following which, the sub-optimum codes can be systematically designed by hand. These sub-optimum codes have a performance close to the optimum one.

For STBC over relay channels, the amplify-and-forward (AF) strategy is examined. Exact BEP results are obtained for the first time, with three different transmission protocols. The exact BEP result is compared with the asymptotic result in the literature, and a great improvement in the accuracy is observed. We also point out that since the noise at the relay is also forwarded in the AF strategy, the relay should keep silent under certain conditions. Adaptive cooperative STBC's are, therefore, proposed and analyzed. Finally, the energy efficiencies of these adaptive schemes are discussed.

List of Tables

List of Figures

Abbreviations

AF	amplify-and-forward
AWGN	additive white Gaussian noise
BEP	bit error porbability
BLAST	Bell lab Layered Architecture of Space-Time
BPSK	binary phase-shift keying
CF	compress-and-forward
COD	complex orthogonal designs
DF	decode-and-forward
EGC	equal gain combining
EPAS	equal power allocation Sstrategy
i.i.d.	independent identically distributed
ISI	inter-symbol interference
MIMO	multiple-input multiple-output
MISO	multiple-input single-output
ML	maximum likelihood
MPSK	M-ary phase-shift keying
MQAM	M-ary quadrature amplitude modulation
LOS	line-of-sight
MMSE	minimum mean square error estimate

MRC	maximum ration combining
OPAS	optimum power allocation strategy
PAM	pulse-amplitude modulation
PASM	pilot-symbol assisted modulation
PEP	pairwise error probability
PIC	parallel interference cancellation
PDF	probability density function
QPSK	quadrature phase-shift keying
RAS	receive antenna selection
SBS	symbol-by-symbol
SC	selection combining
SEP	symbol error probability
SIC	successive interference cancellation
SIMO	single-input multiple-output
SISO	single-input single-output
SNR	signal-to-noise ratio
SR	selection relay
STBC	space-time block code
STC	space-time code
STTC	space-time trellis code
TAS	transmit antenna selection
V2V	vehicle-to-vehicle
V2I	vehicle-to-infrastructure
WAVE	wireless access of vehicular environments
ZF	zero-forcing

Notations

In this thesis, scalar variables are written as plain lower-case letters, vectors as bold-face lower-case letters, and matrices as bold-face upper-case letters. Some further used notations and commonly used acronyms are listed in the following:

a	plain lower-case to denote scalars
$\boldsymbol{a}$	boldface lower-case to denote column vectors
$\boldsymbol{A}$	boldface upper-case to denote matrices
$(\cdot)^*$	the conjugate operation
$(\cdot)^T$	the transpose operation
$(\cdot)^H$	the conjugate transpose operation
$\det(\cdot)$	the determinant of a matrix
$\mathrm{tr}(\cdot)$	the trace of a matrix
$\Re(\cdot)$	the real part of the argument
$\Im(\cdot)$	the imaginary part of the argument
$\|\cdot\|_F^2$	the Frobenius norm square
$\mathrm{erfc}(\cdot)$	the complementary error function
$\Gamma(\cdot)$	the Gamma function
$\Gamma(\cdot,\cdot)$	the upper incomplete Gamma function

Chapter 1

Introduction

Wireless communication has suffered from the fading problem ever since its first appearance in 1897, when Guglielmo Marconi transmitted a wireless signal to a ship in the English Channel. The following century witnessed the remarkable development of wireless communication, especially in the last decade. Consequently, the demand for bandwidth and capacity becomes more and more urgent, and the fading problem has never been so critical.

The capacity of communication systems with a single antenna can be very low, due to the multi-path propagations in wireless channels. The multi-path signals add up constructively or destructively at the receiver antenna to give a fluctuating signal, which can vary widely in amplitude and phase. When the amplitude of the signal experiences a low value it is termed fading and the capability of the wireless channel is severely limited.

Research efforts have focused on ways to make more efficient use of this limited capacity and have accomplished remarkable progress. Efficient techniques, such as frequency reuse and OFDM [1], have been invented to increase the bandwidth efficiency; on the other hand, advances in coding techniques, such as turbo codes [2] and low parity check codes [3,4] make it possible to almost reach Shannon capacity [5],

the theoretical performance limit of the channel. However, the development of the techniques for a single channel has yet to catch up with the increasing demand for the capacity.

While transmitting over one 'bad' wireless channel cannot meet the requirement, it is intuitive to transmit over several 'bad' channels, in order to hedge against the possibility that all the channels are bad simultaneously. The technique of using multiple channels is called *diversity*. Most generally used diversity techniques include *time diversity*, *frequency diversity* and *space diversity* [6, 7]. In the time diversity technique, replicas of the information are transmitted at different times that exceed the coherence time of the channel, so that multiple repetitions of the signal will be received with independent fading conditions, thus providing the diversity. In the frequency diversity technique, replicas of the information are sent on different frequencies, which are separated by more than the coherence bandwidth of the channel, so that diversity is also archived. Space diversity, however, is different from the above two diversity techniques. It exploits the independence of different antennas, which are spatially separated or differently polarized. Since we need not send the replicas of the same information over different times or different frequencies, the diversity is obtained without loss of bandwidth efficiency and data rate.

If the system has one antenna at both the transmitter and the receiver, it is called a SISO (single-input single-output) system. Multiple antennas were first deployed at the receiver end, which form a single-input multiple-output (SIMO) system. The multiple copies of the signal which arrive at the different receive antennas are combined according to certain combination rules, such as selection combining (SC), equal gain combining, (EGC) and maximum ratio combining (MRC). All of these combining schemes show great improvement, compared with SISO system.

However, SIMO systems, which only utilize one side of the diversity in

communication systems, are still not efficient enough. In the last two decades, researchers started to apply multiple antennas at both the transmitter and the receiver ends, which form multiple-input multiple-output (MIMO) systems. MIMO systems greatly increase the capacity of a wireless channel [8–10], and have attracted great research interests. Different kinds of MIMO systems have been invented ever since. Among these systems, the space-time block coding (STBC) system is frequently used now, due to its simple design and good performance.

In the rest of the chapter, we will first review different MIMO systems and then focus on space-time coding (STC). The performance and the design of STBC over various fading channels will be discussed. The discussion will lead to the objectives and the contribution of this thesis.

1.1 MIMO Systems and Space-Time Coding

1.1.1 Background of MIMO Systems

The rudiment of the first MIMO system appeared in 1987, when two communication systems, communicating between multiple mobiles and a base station with multiple antennas, and communicating between two mobiles each with multiple antennas, were proposed in [11]. This is the first paper that discusses the use of multiple antennas at both the receiver and the transmitter. The capacity expression is given in terms of the eigenvalues of the channel matrix. Later on, a communication system which simultaneously transmits the same message with several adjacent base stations is proposed in [12, 13]. In [14], a similar system, which transmits the same symbol through multiple antennas at different times, is suggested.

Different from the earlier works which consider simulcasting the same symbol, Foschini presented the analytical basis of MIMO systems in [8, 15], where different

data streams are transmitted at the same time. Reference [15] is the first paper in which Bell Labs proposed BLAST (Bell Labs Layered Architecture of Space-Time) as the communication architecture for the transmission of high data rates, using multiple antennas at both the transmitter and receiver. In the proposed BLAST system the data stream is divided into blocks which are distributed among the transmit antennas. In vertical BLAST sequential data blocks are distributed among consecutive antenna elements, whereas in diagonal BLAST, they are circularly rotated among the antenna elements. The core technologies of the BLAST systems are the signal processing algorithms used at the receiver. At the bank of receiving antennas, high-speed signal processors look at the signals from all the receive antennas simultaneously. The strongest substreams are sequentially detected and extracted from the received signals. The remaining weaker signals are then easier to recover since the stronger signals have been removed as sources of interference. The ability to separate the substreams depends on the slight differences in the way the different substreams propagate through the environment.

Under the rich scattering environments with independent transmission paths, the theoretical capacity of the BLAST architecture with M_T transmit and N_R receive antennas grows linearly proportional to $\min(N_R, M_T)$ [8], even when the total transmitted power is held constant. Thus, the capacity is increased by a factor of $\min(N_R, M_T)$ compared to a SISO system. The laboratory prototype [16] has already demonstrated spectral efficiencies of 20 - 40 bits per second per Hertz of bandwidth, numbers which are simply unattainable using standard SISO techniques.

If the channel state information (CSI) is known at the transmitter, the full capacity of the MIMO system can be reached by transmitting the signal along the eigen-channels and applying 'water filling' principle [9] to allocate the transmitting power to each eigen-channel. This scheme gives the theoretical limit of the channel

capacity which can be attained by MIMO systems. However it is difficult to realize in practice, due to the complexity and the restriction on the feedback channel. Lo [17] proposed the maximum ratio transmission with MRC in 1999, which is also known as MIMO beamforming. Beamforming schemes use the strongest eigen-channel for transmission, and therefore reduce the complexity of a MIMO system in the sense that they only require scalar decoding and feedback of the largest eigenvalue. It has been proved that in certain scenarios, the capacity of beamforming is close to the channel capacity [18]. Based on practical considerations, some modified versions of beamforming are proposed. In order to reduce the feedback overhead, the receiver can quantize the channel information and send back the label of the best beamforming vector in a predetermined code-book to the transmitter [19, 20]. In the slow fading channel, the statistics of the channel, such as the channel covariance matrix is fed back [18, 21]. In order to further reduce the complexity, sub-optimum MIMO schemes are proposed with transmit antenna selection (TAS) and receive antenna selection (RAS) [22]. MIMO systems with TAS, RAS or both can also achieve full diversity, but with much simpler structure. As an example, a MIMO system, using TAS with M_T transmit antennas, only needs $\log_2 M_T$ bits to be fed back to indicate which transmit antenna should be chosen. Moreover, it requires only one radio frequency chain at the transmitter, thus reducing the complexity of equipment.

The advantage of MIMO systems is due to two effects. One is diversity gain since it reduces the chances that several channels are in a deep fade simultaneously. The other is the beamforming gain obtained by combining the signals from different antennas to achieve a higher signal-to-noise ratio (SNR). Since multiple antennas introduce a new dimension of space on top of the conventional time dimension at the transmitter, this triggers tremendous research interests on multi-dimensional coding procedures for MIMO systems, which are generally referred to as space-time coding

schemes. More detailed literature reviews on space-time coding schemes will be given in the next section.

1.1.2 Introduction to Space-Time Coding

Although [14] has attempted to jointly encode multiple transmit antennas, Tarokh *et al.* [23] are the first to introduce the concept of space-time coding by designing codes over both time and space dimensions. The original work in [23] proposes the well known rank-determinant and product distance code design criteria of space-time codes for quasi-static fading and rapid fading channels, respectively. For the quasi-static fading case, the fading coefficients remain constant over an entire transmission frame, whereas the coefficients vary independently from symbol to symbol for the rapid fading case. Following Tarokh's work, much research efforts have been made to develop powerful space-time codes based on different design criteria or improved search algorithms [24–37]. The family of space-time codes includes space-time trellis codes (STTC) [24, 25, 27, 28] and space-time block codes (STBC) [26, 29–37].

It is shown in [23] that space-time coding achieves a pairwise error probability (PEP) that is inversely proportional to $\text{SNR}^{M_T N_R}$, so $M_T N_R$ is called the *diversity gain* of the code. Comparing with the PEP of SISO systems, which is inversely proportional to the SNR, the error rate of MIMO systems is reduced dramatically. Besides the diversity gain, the STTC also provides a coding gain which depends on the complexity of the code, i.e., number of states in the trellis, without any loss in the bandwidth efficiency. The STTC encodes on one input symbol at a time and produces a sequence of vector symbols whose length represents the number of antennas. In order to decode the STTC, it requires a multidimensional Viterbi algorithm at the receiver, so the coding gain of STTC is achieved at the expense of a complex receiver.

In contrast to STTC, STBC encodes the whole block of input symbols together,

and can offer full diversity with relatively simpler design. The first practical space-time block code is proposed by Alamouti in [29], which works for systems with two transmit antennas. It is one of the most successful space-time block codes because of its good performance and simple decoding. Therefore, it has been included in several IEEE standards, e.g. IEEE 802.11n. The STBC was later generalized to the cases for an arbitrary number of transmit antennas in [30]. It was also pointed out in [30] that the full-rate complex orthogonal designs (COD) only exist for two transmit antennas [29], and COD for more than two transmit antennas must have a rate less than one. Based on the generalized orthogonal code structure defined in [30], the designs of orthogonal STBC were extensively studied in [32–37].

Space-time coding is a promising technology. However its performance in different channel models is still not completely evaluated. Tarokh *et al.* [23] first derived performance criteria for STC based on the PEP, for both slow and fast fading channels. They made use of the Chernoff bound on the Q-function to derive a loose upper bound on the PEP, which depends on the eigenvalues of the code difference matrix. Fitz et. al. [38] proposed an upper bound on PEP, which is tighter than Tarokh's one, but it applies a high SNR approximation, so that it is loose at the lower SNR region. The bounding technique is not unique. In other references, [39] gives both upper and lower bounds on the PEP, [40] proposes a lower bound with a code design criterion, and [41] summarizes several existing bounds in a general form and introduces a new code design criterion as well. A more accurate performance evaluation can be obtained by exactly calculating the PEP, rather than calculating the bounds. This can be done by using residue methods based on the characteristic function technique [42] or on the moment generating function method [43, 44]. Generally, no closed form has been achieved for exact PEP evaluation, thus the results in [42–44] provide limited insight into the structure of STC systems.

Most of the performance analysis for STC systems is in terms of PEP, as it is not easy to obtain an exact bit error result, especially for STTC systems. But for STBC systems, bit error probability (BEP) and symbol error probability (SEP) are preferred over PEP, as they are relatively easier to derive and more accurate in describing the performance of the systems. Some performance analysis results for STBC can be found in [45–51]. Gao *et al.* assumed that the CSI was perfectly known at the receiver in [45], and obtained exact BEP expressions for both BPSK and QPSK with Alamouti's code [29] and one receive antenna. In [46], the author obtained a PEP expression based on perfect CSI knowledge using the moment generating function method, and the result is not in explicit form. SEP expressions for MPSK and MQAM constellations over the keyhole Nakagami-m channel were presented in [47] assuming perfect CSI at the receiver. More recently in [48], an accurate BEP upper bound is proposed for a symbol-by-symbol (SBS) detector, but again, the result in [48] requires perfect CSI for decoding. Channel estimation error was first taken into account in [49], but the complex computation of the eigen-values for a correlation matrix made it difficult to analyze the PEP in [49]. Alternatively, Cheon *et al.* used Alamouti's code [29] and pilot-symbol assisted modulation (PSAM) [52] for channel estimation, but the BEP result obtained in [50] was given in an unsolved integral form that must be evaluated by a numerical approach. In [51] Shan *et al.* extended the BEP analysis to general STBC's, where the channel was estimated by decision-feedback or PSAM method. Exact BEP results are obtained in [51].

All the above works on STBC, however, are based on assumptions of STC systems, which are inherited from the very first work [23]. These assumptions, on the one hand, simplify the analysis and design of STBC, but on the other hand lose the generality. Consequently, the results of STBC obtained might not be readily applied in a more practical and more general case in the real world. Therefore, this thesis begins

by relaxing these ideal assumptions and determines the performance of STBC under more realistic channel assumptions. In the next section, we will consider some of the ideal assumptions that have been made for the STBC systems in the existing works.

1.2 Space-Time Block Codes over General Fading Channels

1.2.1 Non-identical Channels

The first ideal assumption of STBC system is the 'identical channels' assumption. In most of the previous works on STBC, e.g. [23, 29, 45–51], we can explicitly or implicitly find the preliminary condition that the channel gains of the links between different transmit and receive antennas are independent and identically distributed (i.i.d.). However, this assumption is somewhat contradictory to the nature of MIMO systems in the first place. In MIMO systems, in order to enjoy the spatial diversity, the antenna spacing needs to be sufficiently large to minimize the correlation between channels. However, this large spatial channel separation implies that the channels would encounter very different propagation environments. If we consider the cooperative diversity scenario, where the antennas are not even co-located and distributed STBC's [53] are used, then we can expect that the channels are always non-identically distributed. Thus, it is of great interest to examine STBC over non-identical channels.

MIMO systems are not the first cases where the non-identical channel assumption becomes an issue. Earlier in the SIMO systems, the effect of non-identical channels was investigated in [54–56]. These works analyze the performance of SIMO systems with diversity reception over independent, non-identical, Rayleigh fading channels.

In MIMO systems, the non-identical channels first appeared in distributed STBC systems [57–59], and then in the point-to-point MIMO systems [60, 61]. The performance of STBC over non-identical channels was also implicitly discussed in [62–64], as the issue correlated channels can be view as special case of non-identical channels.

However, the existing works on STBC over non-identical channels are far from complete. Since the non-identical channels not only change the performance of STBC, but also affect the receiver structure, many questions remain unsolved.

1.2.2 Time-Selective Channels

In [23], design criteria are derived for STC, namely, rank-determinant criteria for quasi-static channels, and product distance criteria for rapid fading channels. This work divides the fading channels into two typical classes, either they remain constant during one frame, or they change independently from symbol to symbol. STBC are then designed on the base of the first class. As STBC assume that the channel remains constant within one code block, the channels are also referred to as block-wise constant. Based on this assumption, STBC shows its advantage that full diversity is achieved with a simple maximum likelihood (ML) decoding structure [30].

Obviously, the 'block-wise constant channels' is an ideal assumption, as we cannot make the channels change only when one block ends. The channels must change continuously from symbol to symbol, more or less, and, therefore, it is more natural to assume a time-selective channel model.

For a system with two transmit antennas, one STBC code block extends over two symbols and the channels can change significantly within one block in some cases [65–67] (and references therein). Systems with three or more transmit antennas are even more vulnerable to channel variations than the systems with two transmit antennas, due

to the longer code block length of STBC [68, 69]. If the channels vary from symbol to symbol, the orthogonality will be corrupted and (inter-symbol interference) ISI is introduced, so the linear ML decoder [30] is no longer optimum.

Consequently, the performance analysis of STBC's over time-selective channels differs from the conventional one when channels are block-wise constant. In the existing references, however, only a few works [70, 71] obtained the exact error performance, when the special case of Alamouti's code [29] is applied. Other works either presented conditional error performance based on one channel realization, or simply obtained the error performance through simulations, especially for the STBC's with higher numbers of transmit antennas. More importantly, due to the lack of theoretical analysis, little insight can be gained and it remains unclear how the code structures affect the performance of STBC when the channels are time-selective.

1.2.3 Relay Channels

For conventional MIMO systems, the transmitters and the receivers are assumed to have multiple antennas. However, if the communication systems involve small mobile terminals, it is usually difficult to implement multiple antennas, due to the limited size. In such scenarios, spatial diversity may be exploited through the cooperation of neighboring nodes [72–74], such that multiple single-antenna nodes forms a virtual MIMO system, on which the STBC can be applied in a distributed fashion.

In these cooperative scenarios, the STBC's are first broadcast to the neighboring nodes, which act as relays. And then the relays forward the information to the destination nodes. Since the STBC's experience two hops of transmission, it can be viewed as the STBC's being transmitted over two-hop relay channels.

A relay node can work either in full-duplex mode or half-duplex mode. Full-duplex mode means the relay node receives and transmits at the same time on

the same frequency band. The interference from its transmit antenna needs to be cancelled from the received signals at its receive antenna. Therefore, the full-duplex mode achieves high spectral efficiency, at the expense of high complexity. Half-duplex mode, as the name suggests, does not allow the relay node to transmit and receive at the same time on the same frequency band, so the transmitter and the receiver either share the bandwidth, or work alternately. Because of its simplicity, half-duplex mode is often used in cooperative scenarios.

Several strategies can be used to process and forward the received signals at the relay. The most common strategies are amplify-and-forward (AF) and decode-and-forward (DF). Other strategies include compress-and-forward (CF) and selection relay (SR). Among these strategies, AF is sometimes preferred due to its simpler requirements on the relay nodes.

In cooperative STBC systems, the relay node using AF strategy simply forwards the received signals in analog form [59, 75–77], so the additive noise at the relay is forwarded to the destination as well. As a result, the end-to-end performance is difficult to analyze and existing works, e.g. [59, 75–77], have not obtained the exact performance result.

1.3 Research Objectives and Contributions

As discussed in Section 1.2, the existing works on the STBC are based on certain restrictions and ideal assumptions, which are not always true in the real world. There are large gaps between the real applications of STBC and the theoretical results derived from the ideal models. The purpose of this thesis is to investigate STBC in more realistic models, over more general fading channels.

For the sake of illustration, the topic will be addressed in three aspects. This thesis

will investigate STBC over

1. non-identically distributed fading channels: STBC's over non-identical channels with perfect CSI and estimated CSI are analyzed respectively. In the case of perfect CSI, we analyze the BEP of orthogonal STBC over independent, non-identically distributed, block Rayleigh and Ricean channels. Both an upper bound and the exact BEP results are derived. The results are applicable to both point-to-point and distributed STBC, with any number of transmit and receive antennas for which orthogonal STBCs are defined. With the analytical performance results, we also examine different effects of non-identical channel statistics on the performance of STBC. The results show that the non-identical channel distributions degrade the performance in Rayleigh channels. But in Ricean channels, the non-identical distributions can have different effects on the performance. Based on the BEP results, we propose optimum power allocation schemes (OPAS) for STBC over non-identical channels. The performance of OPAS is compared with the one of conventional equal power allocation scheme (EPAS).

   In the case of estimated channels, we show that the conventional SBS decoder [30] for orthogonal STBC is no longer optimum in this situation. The whole STBC system is re-examined, and a new optimum decoder is proposed. This decoder can be simplified to a new SBS decoder under certain conditions. Performance analysis is provided, and the analytical and simulation results show that our new decoder provides a much better performance compared to the conventional SBS decoder in this situation.

2. time-selective fading channels: We first introduce an approach to analyze the performance of STBC's over time-selective channels, with arbitrary numbers of

antennas for which orthogonal STBC's are defined. Exact error performances are obtained in closed forms. Through the analysis, the relationship between the ISI and the STBC code structure is revealed.

Considering $\mathcal{G}_i$ systems [30], one proposition and two design criteria are then introduced. Applying the criteria, it is easy to design modified code matrices which have less ISI, compared with the original code matrix. Alternatively, we show how to use the proposition to search for an optimum code matrix with minimized ISI.

3. relay fading channels: We analyze the exact bit error performance of cooperative STBC with AF strategy. Three existing transmission protocols are considered, and exact BEP results are obtained in closed form for all of these protocols. Based on the exact BEP, we compare our results with the existing asymptotic BEP in [59]. Then, we compare the performances of the protocols in different situations and examine the robustness of these protocols.

   For cooperative STBC over relay channels with AF strategy, we also address the key question of when the relay should stop forwarding signals. We first examine the effect of the forwarded noise on the received SNR and find a critical condition, under which the forwarded signal from the relay will be deleterious. According to this condition, we propose adaptive forwarding schemes for cooperative STBC with full CSI, partial CSI and no CSI available at the relay. The exact BEP's of these adaptive cooperative STBC schemes, which are much better than that of the conventional cooperative STBC, are also obtained in closed form. Finally, the energy efficiencies of these adaptive schemes are discussed.

Viewed another way, this thesis has two major contributions. On the one hand,

the mathematical method used for the performance analysis in this thesis is insightful. It provides a way to investigate physical meaning of the theoretical results. Therefore, it leads to better code design, receiver structures and transmission strategies. On the other hand, the simple analytical performance results obtained in this thesis are based on more realistic channel models, so they should be directly applicable to the practical implementation of STBC in the real environments, providing a clear guide to telecommunication engineers.

1.4 Organization of the Thesis

The rest of the thesis is organized as follows

Chapter 2 analyzes the BEP of orthogonal STBC over independent, non-identically distributed, block Rayleigh/Ricean fading channels with perfect CSI. With symbol-by-symbol detection, exact BEP results are derived in both Rayleigh and Ricean fading channels. A simple but insightful upper bound on the BEP is also obtained. Using the BEP expressions, the effects of non-identical channel statistics on the performance of STBC are investigated. Based on these results, an optimum power allocation strategy is also proposed.

Chapter 3 extends the results in Chapter 2 by assuming estimated channels. It is shown that the non-identical channel statistics lead to non-identical channel estimation error variances, which consequently affect the structure and the performance of orthogonal STBC. A new optimum decoder is derived, which can be simplified to a new SBS decoder under certain conditions. Performance analysis and simulations are also provided.

Chapter 4 analyzes the performance of STBC over time-selective channels. Exact error performances are obtained in closed form. The analysis reveals the relationship

between the ISI and the structure of STBC matrices, such that one proposition and two design criteria are proposed accordingly. STBC's, which have less ISI compared with the original code matrix, are obtained using these criteria and proposition.

Chapter 5 analyzes the performance of cooperative STBC with AF strategy. Exact BEP results are derived in closed form for three existing protocols. The effect of the forwarded noise is examined and a critical condition, which indicates when the relay should forward and when it should not, is proposed. Based on this condition, adaptive forwarding schemes for cooperative STBC are proposed. The performances of these schemes are also obtained in closed form. The energy efficiencies of these adaptive schemes are discussed.

Finally Chapter 6 summarizes our work, and points out a number of future research directions.

Chapter 2

Space-Time Block Codes over Non-identical Channels with Perfect CSI

In this chapter, we analyze the bit error performance of orthogonal STBC over independent, non-identically distributed, block Rayleigh/Ricean fading channels with perfect CSI. With symbol-by-symbol detection, we derive the expressions of the exact BEP in both Rayleigh and Ricean fading channels. The results are applicable to any number of transmit and receive antennas, for which orthogonal STBC's are defined. A simple but insightful upper bound on the BEP is also obtained. Using the BEP expressions, we investigate the effects of non-identical channel statistics on the performance of STBC. Based on these results, we also propose an optimum power allocation strategy, which provides better BEP performance compared with the original equal power allocation strategy.

2.1 Introduction

It is well known that STC [23] can greatly improve the performance of wireless communication systems equipped with multiple transmit and receive antennas. In practice, STBC [29, 30] are commonly used due to their simple decoder structures. The decoding rules and the performance of STBC have been extensively studied in many works, e.g. [45, 48, 51] and the references therein. Most of the previous works, however, assume that the channels between different transmit and receive antennas are i.i.d.. The assumption of identical channel statistics may simplify the design and the analysis of STBC, but it does not always hold in real environments, especially in MIMO systems.

Several factors may introduce a statistical imbalance between channels. For example, in a MIMO system, the antenna spacing needs to be sufficiently large to reduce the correlation between channels. Therefore, the channels may involve very different propagation environments. In some cases, directional antennas are used at a base station. The different pointing directions of the transmit antennas will also cause non-identical channel statistics. (Here, we consider the down-links from the base station to users.) As a third example, one may consider the cooperative diversity scenario, where the antennas are not co-located and some distributed STBC [53] may be used. Then, it is natural to expect that the channels are always non-identically distributed. Therefore, it is of great practical and theoretical interest to examine the effects of non-identical channels on the performance of STBC.

The effect of non-identical channels was first investigated in SIMO systems. References [54–56] analyze the performance of SIMO systems with diversity reception over independent, non-identical, Rayleigh fading channels. In point-to-point MIMO systems, non-identical channels have only been addressed by [60] and [61] recently.

In [60], Tao and Kam considered the optimal detection and the error performance of differential STBC over independent and semi-identically distributed, block Rayleigh fading channels, where the semi-identically distributed channels refer to the case that the channel gains associated with a common receive antenna are identically distributed, but the ones associated with a common transmit antenna are not. In [61], Li and Kam examined the pair-wise error probability of space-time trellis codes (STTC) over independent, non-identically distributed, rapid Rayleigh fading channels. A new pilot power allocation scheme is also proposed based on the performance result. In a cooperative diversity scenario, [57–59] have considered the performance of STBC over non-identical channels to some extent, where they assume the STBC works in a distributed manner. However, these last three works either approximate the average BEP, or consider a system with only two transmit antennas, and all of them only consider the case of non-identical Rayleigh channels.

In this chapter, we first analyze the BEP of orthogonal STBC over independent, non-identically distributed, block Rayleigh and Ricean channels. Both an upper bound and the exact BEP results are obtained in closed form. The results are applicable to both point-to-point and distributed STBC, with any number of transmit and receive antennas for which orthogonal STBC's are defined. With the analytical performance results, we examine the different effects of non-identical channel statistics on the performance of STBC. The results show that the non-identical channel distributions degrade the performance in Rayleigh channels, which is similar to the observation in SIMO systems over non-identical Rayleigh fading channels [54–56]. But in Ricean channels, the non-identical distributions can have different effects on the performance.

From the analytical BEP results, it can be seen that the original equal power allocation strategy at the transmit antennas may not be an optimum way to apply STBC over non-identical channels. Therefore, designing an optimum power allocation

strategy is another goal of this chapter. Some existing works [78–82] also considered unequal transmit power allocation for STBC, but they assume the transmitter has the instantaneous CSI, which causes high overhead in the feedback channel, especially in time-varying channels. Therefore, it may not be realistic to apply these techniques in practice. If the feedback channel is not error-free, [78] and [82] propose some error-tolerant algorithms to optimize the transmit weight. However, these error-tolerant algorithms are not explicitly related to the BEP, and cannot guarantee an optimum performance. Our analytical BEP results, on the other hand, give a simple and direct way to optimize the transmit power allocation, in order to achive the minimum BEP. Moreover, our scheme only requires the knowledge of channel statistics at the transmitter. Therefore, it greatly reduces the feedback overhead. In the case of the Rayleigh channels with two transmit and one receiver antenna, our OPAS tends to allocate more power to the (statistically) stronger channel in the low SNR region. The performance improvement is up to $2\ dB$ in SNR, compared with the equal power allocation scheme. In the high SNR region, however, the OPAS converges to the EPAS. In Ricean channels, on the other hand, our OPAS may need to put more power in the statistically weaker channels for a better performance. (We will explain the meaning of *statistically weaker channels* in the following part of this chapter)

The rest of the chapter is organized as follows. Section 2.2 describes the system model and the SBS detector structure. In section 2.3, the exact BEP together with a simple, upper bound are derived for both Rayleigh and Ricean channels. Section 2.4 examines the effects of non-identical channel statistics on the BEP of STBC, with different unbalanced channel parameters. Section 2.5 studies the optimal transmit power allocation strategy. A summary is given in section 2.6.

2.2 System Model and Receiver Structure

We consider a communication system with M_T transmit and N_R receive antennas. The transmit/receive antennas can be co-located in one communication unit, or distributed in several units. If the antennas are not co-located, we assume the synchronization is perfect. The space-time block code **S** is a $P \times M_T$ matrix, where each row of **S** is transmitted through N_T transmit antennas at one time, and the transmission covers P symbol periods. It has a linear complex orthogonal design, and can be represented as [32]

$$\mathbf{S} = \sum_{k=1}^{K} (s_k \mathbf{A}_k + s_k^* \mathbf{B}_k). \tag{2.1}$$

Here, $\mathbf{A}_k$ and $\mathbf{B}_k$ are $P \times M_T$ matrices with constant complex entries, and K is the number of symbols transmitted in one block. Therefore, each entry of **S** is a linear combination of the data symbols $s_k, k = 1, 2, \cdots, K$, and their conjugates s_k^*, where each s_k is from a certain complex signal constellation. The rate of the orthogonal STBC is defined as K/P.

For orthogonal STBC, we have [30]

$$\mathbf{S}^H \mathbf{S} = \text{diag}\left[\sum_{k=1}^{K} \lambda_{1,k} |s_k|^2, \ldots, \sum_{k=1}^{K} \lambda_{M_T,k} |s_k|^2\right] = \mathbf{D} \tag{2.2}$$

where **D** is a diagonal matrix and $\{\lambda_{i,k}\}_{i=1}^{M_T}$ are positive numbers. For an arbitrary signal constellation, it requires that

$$\mathbf{A}_k^H \mathbf{A}_l + \mathbf{B}_l^H \mathbf{B}_k = \delta_{k,l} \text{diag}[\lambda_{1,k}, \cdots, \lambda_{M_T,k}], \tag{2.3}$$

$$\mathbf{A}_k^H \mathbf{B}_l + \mathbf{A}_l^H \mathbf{B}_k = \mathbf{0}, \tag{2.4}$$

We assume here M-ary phase-shift keying (MPSK) modulation and a constant transmitted energy per information bit E_b. Therefore, the total energy assigned to one block is $E_b K \log_2 M$. From the orthogonality condition (2.2), it can be seen that

the total energy for one block is given by $\sum_m^{M_T} \sum_k^K \lambda_{m,k} |s_k|^2$. Thus, the transmitted energy per MPSK symbol is given by

$$E_s = \frac{E_b K \log_2 M}{\sum_m^{M_T} \sum_k^K \lambda_{m,k}}. \tag{2.5}$$

The received signal **R** is a $P \times N_R$ matrix, which is given by

$$\mathbf{R} = \mathbf{SH} + \mathbf{N}. \tag{2.6}$$

Here, **N** is a $P \times N_R$ noise matrix, whose entries are i.i.d., complex, Gaussian random variables with mean zero and variance $N_o/2$ per dimension. $\mathbf{H} = [h_{mn}]$ is a $M_T \times N_R$ channel matrix, where each entry h_{mn} is the channel gain of the link from m-th transmit antenna to n-th receive antenna. We assume $\{h_{mn}\}$ are independent, complex, Gaussian random variables, each with a deterministic mean M_{mn} and variance $2\sigma_{mn}^2$. Since the channels are non-identical, each channel can have a different mean and a different variance. We assume the channel matrix **H** is perfectly known at the receiver, therefore, the ML decoding rule is given by

$$\hat{\mathbf{S}} = \arg\max_{\mathbf{S}} p(\mathbf{R}|\ \mathbf{S}, \mathbf{H}) \tag{2.7}$$

Now, the conditional probability density function (PDF) of the received signal is given by

$$p(\mathbf{R}|\ \mathbf{S}, \mathbf{H}) = \det{}^{N_R}(\pi N_o \mathbf{I}_{p\times p}) \exp\left(-\mathrm{Tr}\left[(\mathbf{R}-\mathbf{SH})^H (N_o \mathbf{I}_{p\times p})^{-1} (\mathbf{R}-\mathbf{SH})\right]\right). \tag{2.8}$$

Thus, the ML decoding rule (2.7) simplifies to

$$\hat{\mathbf{S}} = \arg\min_{\mathbf{S}} \|\mathbf{R} - \mathbf{SH}\|^2. \tag{2.9}$$

Substituting equation (2.1) into the above equation, the ML decoder can be further simplified to a SBS detector

$$\hat{s}_k = \arg \max_{s \in MPSK} \Re[z_{k'} s^*], \forall k' = 1, \cdots, K \tag{2.10}$$

where

$$z_k = \text{Tr}[\mathbf{R}^H \mathbf{B}_k \mathbf{H} + \mathbf{H}^H \mathbf{A}_k^H \mathbf{R}]. \tag{2.11}$$

The above equations show that, in the case of perfect CSI, the SBS decoder does not depend on the statistics of the channel matrix **H**. Therefore, the SBS decoder can be similarly applied as it is in the identical channel case.

2.3 Bit Error Performance Analysis

With PSK modulation, we have $s_k = \sqrt{E_s} e^{j\phi_k}$, and the detector makes its decision $\hat{s}_k$ on s_k as

$$\hat{s}_k = \arg\max \Re[z_{k'} e^{-j\phi_k}], \forall k' = 1, \cdots, K \tag{2.12}$$

Here, we have

$$z_{k'} = x_{k'} + u_{k'}, \tag{2.13}$$

where

$$\begin{aligned} x_{k'} = \sum_{k=1}^{K} \big[& s_k^* \text{Tr}[\mathbf{H}^H \mathbf{A}_k^H \mathbf{B}_{k'} \mathbf{H} + \mathbf{H}^H \mathbf{A}_{k'}^H \mathbf{B}_k \mathbf{H}] \\ & + s_k \text{Tr}[\mathbf{H}^H \mathbf{A}_{k'}^H \mathbf{A}_k \mathbf{H} + \mathbf{H}^H \mathbf{B}_k^H \mathbf{B}_{k'} \mathbf{H}] \big], \end{aligned} \tag{2.14}$$

$$u_{k'} = \text{Tr}[\mathbf{N}^H \mathbf{B}_{k'} \mathbf{H} + \mathbf{H}^H \mathbf{A}_{k'} \mathbf{N}]. \tag{2.15}$$

By applying (2.3) and (2.4) to (2.14), we can see that the expression for $x_{k'}$ reduces to

$$x_{k'} = s_{k'} \sum_{m=1}^{M_T} \sum_{n=1}^{N_R} \lambda_{m,k'} |h_{mn}|^2. \tag{2.16}$$

Conditioned on the transmitted signal $s_{k'}$ and the channel matrix **H**, $x_{k'}$ can be seen from (2.16) to be a deterministic constant. Similarly, u_l can be shown from (2.15) to be a conditional, complex, Gaussian random variable with mean zero and variance

$N_o \sum_{m=1}^{M_T} \sum_{n=1}^{N_R} \lambda_{m,k'} |h_{mn}|^2$. It then follows easily from (2.13) that $z_{k'}$ is a conditional, complex, Gaussian random variable with mean $s_{k'} \sum_{m=1}^{M_T} \sum_{n=1}^{N_R} \lambda_{m,k'} |h_{mn}|^2$ and variance $N_o \sum_{m=1}^{M_T} \sum_{n=1}^{N_R} \lambda_{m,k'} |h_{mn}|^2$.

For equally likely symbols, we can assume $s_{k'} = \sqrt{E_s}$ without loss of generality, and the conditional BEP can be computed from the probability $P(\Re[z_{k'} e^{-j\alpha}] < 0 | s_{k'} = \sqrt{E_s}, \mathbf{H})$ [83], where α is some angle that depends on the modulation scheme. Thus, the conditional BEP for $s_{k'}$ is given by

$$P_{k'}(e|\mathbf{H}) = Q\left(\sqrt{\frac{2E_s}{N_o} \cos^2 \alpha \sum_{m=1}^{M_T} \sum_{n=1}^{N_R} \lambda_{m,k'} |h_{mn}|^2}\right). \tag{2.17}$$

2.3.1 Rayleigh Fading Channels

If all the channels are Rayleigh distributed, the means M_{mn}'s are all zero. We can rewrite the conditional BEP as

$$P_{k'}(e|\mathbf{H}) = Q\left(\sqrt{\sum_{q=1}^{M_T N_R} \gamma_q}\right) \tag{2.18}$$

where

$$\gamma_q = \frac{2E_s \lambda_{m,k'} |h_{mn}|^2 \cos^2 \alpha}{N_o},\ m = 1, \cdots, M_T,\ n = 1, \cdots, N_R. \tag{2.19}$$

Obviously, γ_q has a chi-square distribution, which is given by [7]

$$p_{\gamma_q}(x) = \frac{1}{\bar{\gamma}_q} \exp\left(-\frac{x}{\bar{\gamma}_q}\right) \tag{2.20}$$

where

$$\bar{\gamma}_q = E[\gamma_q]. \tag{2.21}$$

Since, γ_q's are independent of one another, the characteristic function of $\sum_{q=1}^{M_T N_R} \gamma_q$ is given by

$$\psi_{\sum_{q=1}^{M_T N_R} \gamma_q}(jv) = \prod_{q=1}^{M_T N_R} \frac{1}{1 - jv\bar{\gamma}_q}. \tag{2.22}$$

From the characteristic function above, we can obtain the PDF of $\sum_{q=1}^{N_T N_R} \gamma_q$ as

$$p_{\sum_{q=1}^{N_T N_R} \gamma_q}(x) = \sum_{q=1}^{M_T N_R} \frac{\pi_q}{\bar{\gamma}_q} \exp(-\frac{x}{\bar{\gamma}_q}) \tag{2.23}$$

where

$$\pi_q = \sum_{p \neq q,\ p=1}^{M_T N_R} \frac{\bar{\gamma}_q}{\bar{\gamma}_q - \bar{\gamma}_p}. \tag{2.24}$$

Averaging the conditional BEP (2.17) over $\sum_{q=1}^{M_T N_R} \gamma_q$ with the PDF (2.23), the average BEP is given by [7]

$$P_{k'}(e) = \frac{1}{2} \sum_{q=1}^{M_T N_R} \pi_q \left[1 - \sqrt{\frac{\bar{\gamma}_q}{2 + \bar{\gamma}_q}} \right]. \tag{2.25}$$

2.3.2 Ricean Fading Channels

The average BEP in (2.25) is exact, however, the closed-form BEP result can only be obtained for Rayleigh channels via the method above. In the more general case where the means of the channel gains are arbitrary, we first apply Craig's alternative form of the Q-function [84] and rewrite the conditional BEP (2.17) as

$$P_{k'}(e|\mathbf{H}) = \frac{1}{\pi} \int_0^{\frac{\pi}{2}} \exp\left(-\frac{\gamma \cos^2 \alpha}{\sin^2 \theta} \sum_{m=1}^{M_T} \sum_{n=1}^{N_R} \lambda_{m,k'} |h_{mn}|^2 \right) d\theta. \tag{2.26}$$

Here, $\gamma = E_s/N_o$ is the input SNR per symbol. To average the above conditional error probability, we take the expectation of the integrand in (2.26) over the entries of $\mathbf{H} = [h_{mn}]$, using the following lemma [85, eqn. 7.76].

Lemma 2.1. *If x is a real Gaussian random variable with mean M_x and variance σ_x^2, we have*

$$E\left[\exp(wx^2)\right] = \frac{\exp\left(\frac{wM_x^2}{1-2w\sigma_x^2}\right)}{\sqrt{1-2w\sigma_x^2}}, \tag{2.27}$$

where w is any complex constant with real part less than $1/2\sigma_x^2$.

Since $|h_{mn}|^2 = |\Re[h_{mn}]|^2 + |\Im[h_{mn}]|^2$, and $\Re[h_{mn}]$ is independent of $\Im[h_{mn}]$, we can apply the above lemma to average the conditional BEP in (2.26). Defining $\mu_m = \gamma\lambda_{m,k'}\cos^2\alpha$, we obtain

$$P_{k'}(e) = \frac{1}{\pi}\int_0^{\frac{\pi}{2}} \prod_{m=1}^{M_T}\prod_{n=1}^{N_R} \frac{\exp\left(-\frac{\mu_m|M_{mn}|^2}{\sin^2\theta+2\sigma_{mn}^2\mu_m}\right)}{1+\frac{2\sigma_{mn}^2\mu_m}{\sin^2\theta}}d\theta. \tag{2.28}$$

The above expression (2.28) for the exact BEP is explicit. However, its evaluation still involves numerical integration. The dependence of the BEP on the system parameters can be shown more explicitly using a bound. A simple upper bound on the BEP can be obtained by setting $\theta = \pi/2$ in equation (2.28), giving

$$P_{k'}(e) < \frac{1}{2}\prod_{m=1}^{M_T}\prod_{n=1}^{N_R} \frac{\exp\left(-\frac{\mu_m|M_{mn}|^2}{1+2\sigma_{mn}^2\mu_m}\right)}{1+2\sigma_{mn}^2\mu_m}. \tag{2.29}$$

The product terms show that the total diversity order of the STBC is $M_T N_R$.

For the special case of Rayleigh fading, we have the means $M_{mn} = 0$ for all m and n. The results (2.28) and (2.29) reduce, respectively, to

$$P_{k'}(e) = \frac{1}{\pi}\int_0^{\frac{\pi}{2}} \prod_{m=1}^{M_T}\prod_{n=1}^{N_R} \left(1+\frac{2\sigma_{mn}^2\mu_m}{\sin^2\theta}\right)^{-1} d\theta \tag{2.30}$$

and

$$P_{k'}(e) < \frac{1}{2}\prod_{m=1}^{M_T}\prod_{n=1}^{N_R}(1+2\sigma_{mn}^2\mu_m)^{-1}. \tag{2.31}$$

Here, the BEP (2.30) is equivalent to the BEP (2.25).

Equations (2.25), (2.28) and (2.30) give the BEP for a single symbol $s_{k'}$. As there are K symbols in one block, the average BEP for one block is obtained from the average probability $\Gamma(\alpha)$, which is given by

$$P_\alpha(e) = \frac{1}{K}\sum_{k'=1}^{K} P_{k'}(e). \tag{2.32}$$

For BPSK, the BEP is given by $P_{\alpha=0}(e)$, and for QPSK with Gray coding, by $P_{\alpha=\frac{\pi}{4}}(e)$ [83].

2.4 Effects of Non-identical Channel Parameters

2.4.1 Rayleigh Channels

We first consider the orthogonal STBC's, which satisfy

$$\lambda_{m,k'} = \lambda_{k'},\ m = 1, \cdots, M_T, \tag{2.33}$$

e.g., Alamouti's design [29], the 4×4 and 8×8 real designs [30], and the 4×4 rate-$3/4$ STBC in [32]. A summary of those known STBC's satisfying condition (2.33) is given in Table 2.1. Therefore, $\mu_m = \gamma\lambda_{k'}\cos^2\alpha$ is a constant, which only depends on the codes and signal constellation. We define the received SNR for each transmit-receive pair as $\gamma_{mn} = E\left[\gamma|h_{mn}|^2\right]$. For Rayleigh channels, the total received SNR γ_{Ray} is given by

$$\gamma_{Ray} = \sum_{m=1}^{M_T}\sum_{n=1}^{N_R}\gamma_{mn} = \sum_{m=1}^{M_T}\sum_{n=1}^{N_R}2\sigma_{mn}^2\gamma. \tag{2.34}$$

Applying the arithmetic mean-geometric mean inequality [86], we can obtain an inequality

$$\prod_{i=1}^{Q}(1+x_i) \le (1+x_{am})^Q \tag{2.35}$$

where $x_i \ge 0$ and x_{am} is the arithmetic mean of all x_i. Using this inequality, the BEP (2.30) can be lower bounded as

$$P_{k'}(e) \ge \frac{1}{\pi}\int_0^{\frac{\pi}{2}}\left(1+\frac{A_1}{\sin^2\theta}\right)^{-M_TN_R}d\theta, \tag{2.36}$$

where

$$A_1 = \frac{\lambda_{k'}\cos^2\alpha}{M_TN_R}\sum_{m=1}^{M_T}\sum_{n=1}^{N_R}2\sigma_{mn}^2\gamma = \frac{\lambda_{k'}\cos^2\alpha}{M_TN_R}\gamma_{Ray}. \tag{2.37}$$

The equality sign holds when all channel variances $2\sigma_{mn}^2$'s are equal. Therefore, for a fixed total received SNR γ_{Ray}, the non-identical channel distributions can be seen to degrade the bit error performance.

	STBC in	Size $(P \times M_T)$	Rate	$\lambda_{k'}$
Real orthogonal designs satisfying condition (2.33)	[30]	2×2	1	1
		$4 \times 4, 3$	1	1
		$8 \times 8, 7, 6, 5$	1	1
Complex orthogonal designs satisfying condition (2.33)	[29]	2×2	1	1
	[30] [32]	$4 \times 4, 3$	$3/4$	1
	[35]	30×6	$2/3$	1
		56×7	$5/8$	1
	[30]	4×2	$1/2$	2
		$8 \times 4, 3$	$1/2$	2
		$16 \times 8, 7, 6, 5$	$1/2$	2
	[34]	7×4	$4/7$	1
	[36] [37]	15×5	$5/8$	1
Designs which do not satisfy condition (2.33)	[34]	11×5	$5/8$	$\{1, 2\}_{k'=1,2,3}$
		30×6	$3/5$	$\{1, 2\}_{k'=1,\cdots,11}$

Table 2.1: List of STBC's which satisfy, or do not satisfy the condition (2.33)

2.4.2 Ricean Channels

In Ricean channels, the total received SNR γ_{Ric} consists of the direct line-of-sight (LOS) component and the scattered component, and is given by

$$\gamma_{Ric} = \sum_{m=1}^{M_T}\sum_{n=1}^{N_R}\gamma\left(2\sigma_{mn}^2 + |M_{mn}|^2\right) = \sum_{M=1}^{M_T}\sum_{n=1}^{N_R} 2\sigma_{mn}^2\gamma\left(1+K_{mn}\right). \tag{2.38}$$

where $K_{mn} = \frac{|M_{mn}|^2}{2\sigma_{mn}^2}$ is the Ricean K-factor of the channel from the m-th transmit antenna to the n-th receive antenna. There are three cases of interest.

Non-identical Channel Variances, Identical Ricean K-factors

First, we assume all channels have the same Ricean K-factors, i.e., $K_{mn} = K_o$ for all channels, where K_o is a constant. Since the channels are non-identical, these channels can be seen as scaled versions of one another, in that the LOS component $|M_{mn}|^2$ has to bear a fixed relationship with the scattered component $2\sigma_{mn}^2$. We can obtain a lower bound from (2.28) as

$$P_{k'}(e) \geq \frac{1}{\pi}\int_0^{\frac{\pi}{2}} \frac{\exp\left(-\frac{M_T N_R K_o A_1}{\sin^2\theta + A_1}\right)}{\left(1+\frac{A_1}{\sin^2\theta}\right)^{M_T N_R}} d\theta, \tag{2.39}$$

where, again, the equality sign holds when all channel variances $2\sigma_{mn}^2$'s are equal. The proof of the inequality (2.39) is given in Appendix A. Therefore, the result is similar to the Rayleigh channel case in that for a fixed total received SNR γ_{Ric} and identical Ricean K-factors, the non-identical channel distributions degrade the bit error performance. For the special case of $K_o = 0$, it reduces to the Rayleigh channel case (2.36). This result also shows that for STBC over identical channels, the transmit powers should be equally assigned to the transmit antennas, in order to obtain the best performance.

Non-identical Ricean K-factors, Identical Channel Variances

In this case, we assume all channels have the same channel variances, i.e., $2\sigma_{mn}^2 = 2\sigma^2$ for all channels, where $2\sigma^2$ is a constant. However, the Ricean K-factors are different for different channels. Now, equation (2.28) reduces to

$$P_{k'}(e) = \frac{1}{\pi}\int_0^{\frac{\pi}{2}} \frac{\exp\left(-\frac{A_2\sum_{m=1}^{M_T}\sum_{n=1}^{N_R}K_{mn}}{\sin^2\theta+A_2}\right)}{\left(1+\frac{A_2}{\sin^2\theta}\right)^{M_T N_R}}d\theta, \tag{2.40}$$

where $A_2 = 2\sigma^2\gamma\lambda_{k'}\cos^2\alpha$. From (2.40), it is obvious that the BEP only depends on $\sum_{m=1}^{M_T}\sum_{n=1}^{N_R}K_{mn}$ and not on each K_{mn} individually. Therefore, for a fixed total received SNR γ_{Ric} and identical channel variances, the non-identical Ricean K-factors do not affect the bit error performance. For the special case of $2\sigma^2 = 0$, all channels become Gaussian channels, and the same results hold that the non-identical distribution of Gaussian channels will not affect the performance.

Non-identical Channel Variances, Identical Channel Means

Now, we assume all channels have the same channel means, i.e., $M_{mn} = M$ for all channels, where M is a constant. The channel variances are different for each channel. In Rayleigh channels, the unbalanced channel variances always degrade the performance. However, this is not true in the Ricean case. If the channel means are identical and nonzero, the unbalanced channel variances can either degrade or enhance the performance. It may be difficult to see this observation from the analytical BEP expression (2.28) directly, so we will illustrate this result in detail with numerical examples in the next section.

The three cases above show that the imbalance of different channel parameters can have different effects on the performance of STBC, and our analytical BEP results (2.28) and (2.30) can easily be applied in practice. For the orthogonal STBC's which do not satisfy the condition (2.33), we can group the terms with the same value of

$\lambda_{m,k'}$ together, and the same analytical technique can be applied to each group. Similar results can be easily obtained. A summary of those STBC's is also given in Table 2.1.

2.4.3 Case Study I

For the purpose of illustration, we consider a MIMO system with two transmit and one receive antenna. We use Alamouti's code [29] with QPSK modulation. The code matrix is given by

$$\mathbf{S} = \begin{bmatrix} s_1 & s_2 \\ -s_2^* & s_1^* \end{bmatrix} \tag{2.41}$$

and

$$\mathbf{A}_1 = \begin{bmatrix} 1 & 0 \\ 0 & 0 \end{bmatrix}, \mathbf{A}_2 = \begin{bmatrix} 0 & 1 \\ 0 & 0 \end{bmatrix}, \mathbf{B}_1 = \begin{bmatrix} 0 & 0 \\ 0 & 1 \end{bmatrix}, \mathbf{B}_2 = \begin{bmatrix} 0 & 0 \\ -1 & 0 \end{bmatrix}, \tag{2.42}$$

respectively. For this case, it is easy to see that $\lambda_{m,k'} = 1$, for all m and k'. We define here the following parameters:

$$\eta = \frac{2\sigma_{1,1}^2}{2\sigma_{1,1}^2 + 2\sigma_{2,1}^2}, \tag{2.43}$$

$$\theta = \frac{|M_{1,1}|^2}{|M_{1,1}|^2 + |M_{2,1}|^2}, \tag{2.44}$$

$$\zeta = \frac{|M_{1,1}|^2 + |M_{2,1}|^2}{2\sigma_{1,1}^2 + |M_{1,1}|^2 + 2\sigma_{2,1}^2 + |M_{2,1}|^2}. \tag{2.45}$$

Here, η is the fraction of the scattered component received at the first channel, θ is the fraction of the LOS component received at the first channel, and ζ is the ratio of the total LOS components to the total received SNR.

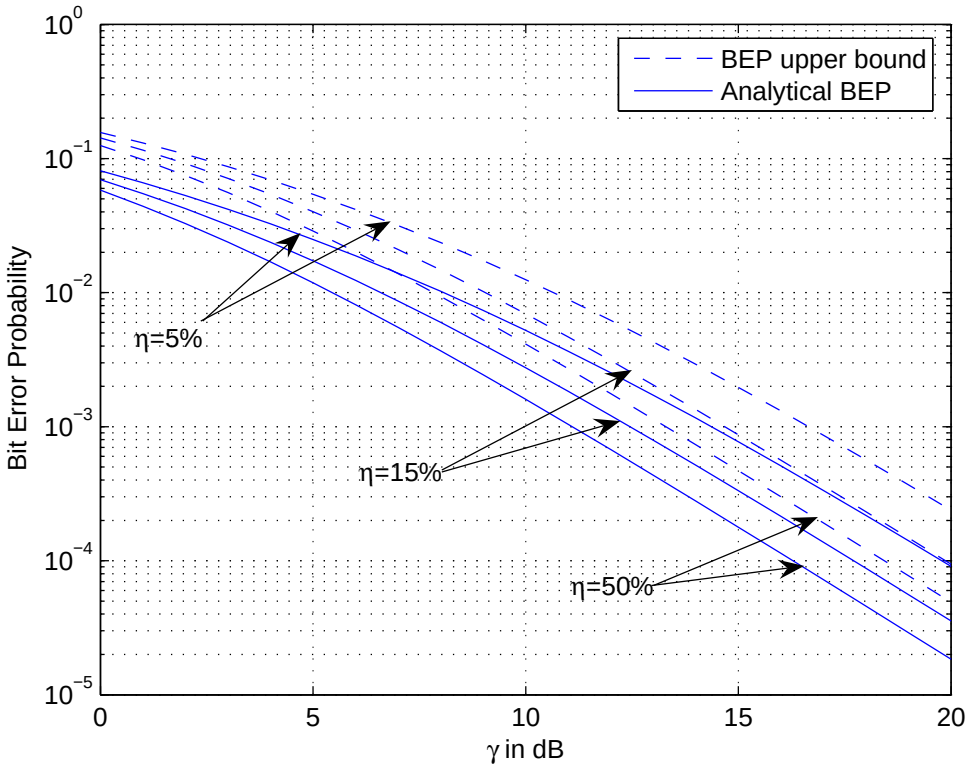

Figure 2.1: Analytical BEP (2.30) and BEP upper bound (2.31) for Rayleigh channels with $\eta = 50\%, 15\%$ and 5%, respectively.

We first consider Rayleigh channels with $M_{mn} = 0$ for all m and n, and the total received SNR, $\gamma \sum_{m=1}^{M_T} \sum_{n=1}^{N_R} 2\sigma_{mn}^2$, is set to 4γ for convenience. Fig. 2.1 plots the exact BEP (2.30) and BEP upper bound (2.31) with $\eta = 50\%, 15\%$ and 5%, respectively.

The results show that the upper bound (2.31) on the BEP is tight, and within 2 dB from the exact BEP (2.30). They also show that the non-identical channel distributions degrade the performance of STBC in Rayleigh fading channels. For instance, for a BEP of 10^{-4}, the unbalanced channel variances ($\eta = 5\%$) cause a loss in SNR of about $4\ dB$, compared to the identical channel case ($\eta = 50\%$).

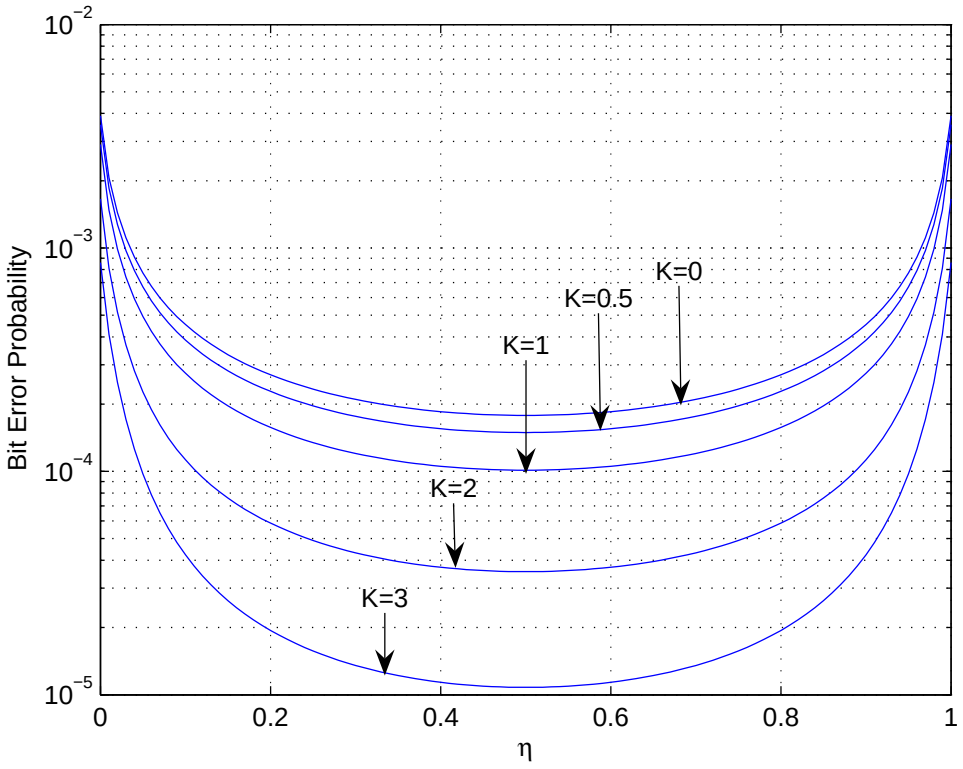

Figure 2.2: Analytical BEP (2.28) for Ricean channels with identical Ricean K-factors and non-identical channel variances. $\gamma = 15\ dB$.

In Fig. 2.2, Ricean channels with identical Ricean K-factors and non-identical channel variances are considered. The total received SNR, $\gamma \sum_{m=1}^{M_T} \sum_{n=1}^{N_R} 2\sigma_{mn}^2 (1+K)$, is also set to 4γ for convenience, where $\gamma = 15\ dB$. We plot the exact BEP (2.28) with Ricean K-factor$= 3, 2, 1, 0.5$ and 0, respectively. Fig. 2.2 shows that for all values of the Ricean K-factor, if the total received SNR is fixed, the best bit error performance is achieved when $\eta = 0.5$. In other words, the unbalanced channel variances degrade the performance of STBC over Ricean channels in this case.

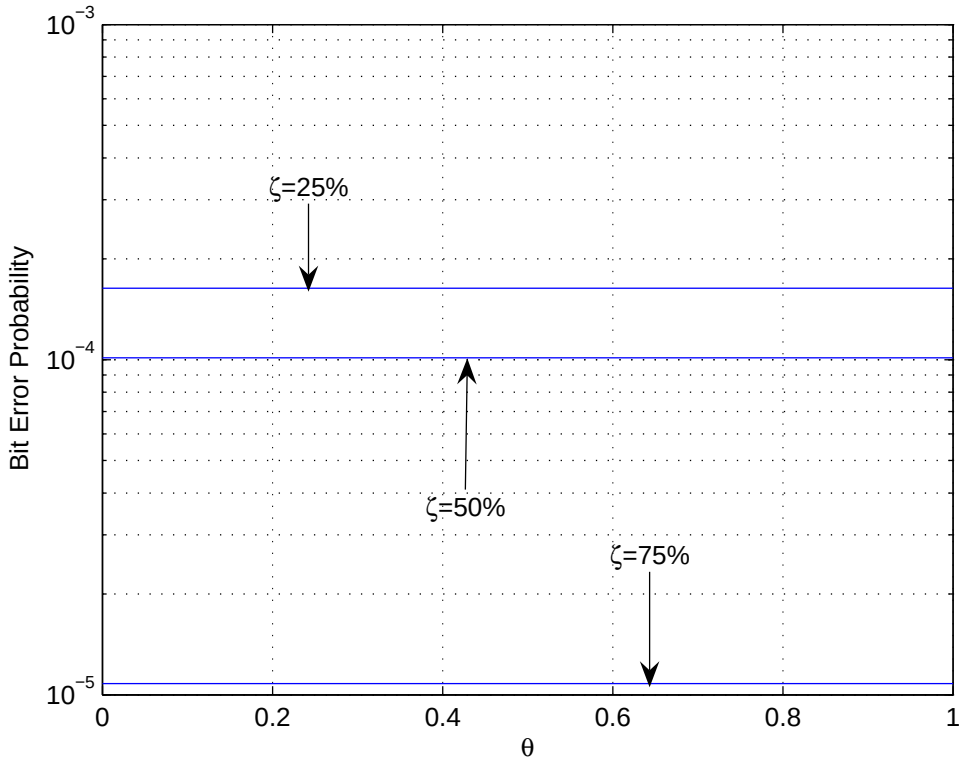

Figure 2.3: Analytical BEP (2.28) for Ricean channels with identical channel variances and non-identical Ricean K-factors. $\gamma = 15\ dB$.

Fig. 2.3 considers Ricean channels with identical channel variances and non-identical Ricean K-factors. With the same fixed, total received SNR given in the last example, we plot the exact BEP (2.28) with $\zeta = 25\%,\ 50\%$ and 75%, respectively. We can see that for identical channel variances, the non-identical channel means (or the non-identical Ricean K-factors) do not affect the bit error performance. When ζ increases from 25% to 75%, we can see from Fig. 2.3 that the bit error performance also increases. This is similar to the single channel case in that the increase of LOS component improves the quality of the channel, thus reducing the BEP.

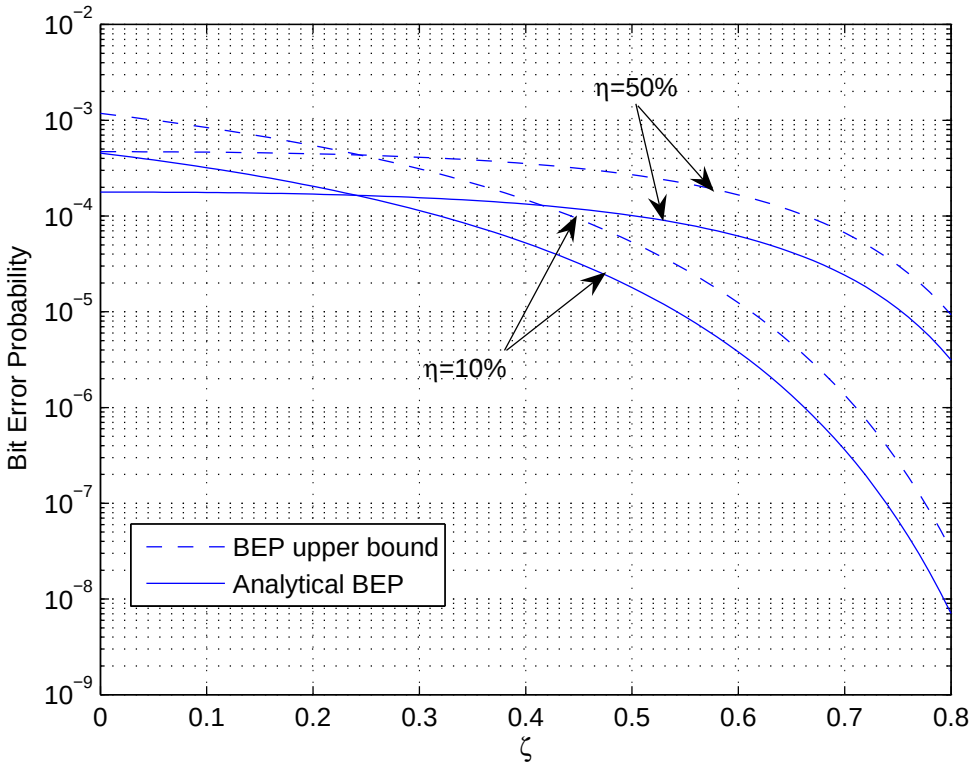

Figure 2.4: Analytical BEP (2.28) and the BEP upper bound (2.29) for Ricean channels with identical channel means and non-identical channel variances. $\gamma = 15\ dB$.

In the last example, we consider Ricean channels with identical channel means and non-identical channel variances. With the same fixed, total received SNR, we compare the BEP for non-identical channel variances ($\eta = 10\%$) and identical channel variances ($\eta = 50\%$) in Fig. 2.4. It shows that, when ζ is small, the bit error performance of the identical channel case is better, But when ζ increases, e.g. $\zeta > 0.25$, the bit error performance of the non-identical channel case is better. Therefore, we can conclude that the bit error performance of the non-identical channel case is not always worse than that of the identical channel case in Ricean channels. If the channel means are identical, the unbalanced channel variances can either degrade

or enhance the performance, depending on the ratio of the total LOS components to the total received SNR.

2.5 Optimal Transmit Power Allocation

2.5.1 The Weighted Transmit Power

In the previous sections, we considered orthogonal space-time block codes with EPAS at transmit antennas. If the channels are identically distributed, EPAS is optimum (which we will show in the following part of this section). However, if the channels are non-identically distributed, we may have to allocate different transmit powers to different transmit antennas, in order to improve the performance with an instantaneous power constraint. Now, we consider that the m-th transmit antenna sends each symbol with power of $w_m\sqrt{E_s}$ for all $m \in 1, 2, \cdots, M_T$, where w_m is a nonnegative scalar and satisfies

$$\sum_{m=1}^{M_T} w_m^2 = M_T. \tag{2.46}$$

Therefore, the total transmit energy remains the same. The received signal matrix $\mathbf{R}$ can be written as

$$\begin{aligned} \mathbf{R} &= \mathbf{SWH} + \mathbf{N} && (2.47) \\ &= \mathbf{S}\tilde{\mathbf{H}} + \mathbf{N} && (2.48) \end{aligned}$$

where $\mathbf{W} = \text{diag}[w_1, w_2, \cdots, w_{M_T}]$ and $\tilde{\mathbf{H}} = [w_m h_{mn}]_{m=1,n=1}^{M_T,N_R}$. Equation (2.48) is similar to (2.6), with $\mathbf{H}$ replaced by the "effective" channel $\tilde{\mathbf{H}}$. In order to keep the orthogonal structure of the space-time codes, the receiver can use $\tilde{\mathbf{H}}$ instead of $\mathbf{H}$, and apply a similar symbol-by-symbol detector, which is given by

$$\hat{s}_k = \arg \max_{k'=1,\cdots,K} \text{Re}[\tilde{z}_{k'} s_{k'}^*], \tag{2.49}$$

where

$$\tilde{z}_{k'} = \mathrm{Tr}[\mathbf{R}^H \mathbf{B}_{k'} \tilde{\mathbf{H}} + \tilde{\mathbf{H}}^H \mathbf{A}_{k'}^H \mathbf{R}]. \tag{2.50}$$

Following the same steps in section 2.3, the bit error probability is now given by

$$P_{k'}(e) = \frac{1}{\pi} \int_0^{\frac{\pi}{2}} \prod_{m=1}^{M_T} \prod_{n=1}^{N_R} \frac{\exp\left(-\frac{\mu_m w_m |M_{mn}|^2}{\sin^2\theta + 2w_m^2 \sigma_{mn}^2 \mu_m}\right)}{1 + \frac{2w_m^2 \sigma_{mn}^2 \mu_m}{\sin^2\theta}} d\theta. \tag{2.51}$$

In the case of identical channels, where $M_{mn} = M$ and $2\sigma_{mn}^2 = 2\sigma^2$ for all m, n, it is easy to see that the bit error probability (2.51) is minimized by setting $w_1 = w_2 = \cdots = w_{M_T} = 1$. Therefore, the EPAS is optimum in identical channels. In the case of non-identical channels, we need to optimize the bit error probability (2.51) subject to the constraints

$$\begin{aligned} &0 \le w_m \le \sqrt{M_T}, \quad \text{for all } m, \\ &\sum_{m=1}^{M_T} w_m^2 = M_T. \end{aligned} \tag{2.52}$$

The constrained optimization problem above is nontrivial, and may require complex computations. Fortunately, the statistics of channels change slowly in practice, so that the computation for the optimum is not required frequently. The optimum w_m's can be calculated for different system conditions in advance and stored in a table. Therefore, the transmitter and receiver need only to look up for the optimum w_m according to the channels condition.

2.5.2 Case Study II

In this case, we first consider the same system as in case study I, with two transmit and one receive antenna. Alamouti's code [29] with QPSK modulation is also applied.

Rayleigh Channels

The channels here are first assumed to be independent non-identical Rayleigh fading channels. The BEP (2.30) is thus reduced to

$$P_{k'}(e) = \frac{1}{\pi}\int_0^{\frac{\pi}{2}} \left(1+\frac{w_1^2\sigma_{1,1}^2\gamma}{\sin^2\theta}\right)^{-1}\left(1+\frac{(2-w_1^2)\sigma_{2,1}^2\gamma}{\sin^2\theta}\right)^{-1} d\theta, \tag{2.53}$$

where we replaced w_2^2 with $2-w_1^2$, since the power constraint is $\sum_{i=1}^{2} w_i^2 = 2$. Before calculating the integration over θ in the BEP (2.53), we first inspect the integrand of (2.53) with the value of θ fixed. Obviously, given a fixed θ, the optimum w_1 is the solution of the following equation

$$\frac{\partial\left(\left(1+\frac{w_1^2\sigma_{1,1}^2\gamma}{\sin^2\theta}\right)\left(1+\frac{(2-w_1^2)\sigma_{2,1}^2\gamma}{\sin^2\theta}\right)\right)}{\partial w_1^2} = 0, \tag{2.54}$$

subject the constraint

$$0 \le w_1^2 \le 2. \tag{2.55}$$

After some manipulations, equation (2.54) has the solution

$$w_1^2 = 1 + \frac{\sin^2\theta}{2\gamma}\left(\frac{\sigma_{1,1}^2-\sigma_{2,1}^2}{\sigma_{1,1}^2\sigma_{2,1}^2}\right). \tag{2.56}$$

From the above equation, it can be seen that the optimum w_1 depends on θ and the channel variances. However, if the SNR increases, $\sin^2\theta/2\gamma$ approaches to zero, and we obtain

$$w_1^2|_{\gamma\to\infty} = 1. \tag{2.57}$$

for any value of θ. This observation means in the high SNR case, the optimum transmit power should be equally allocated among all the antennas, even though the channels are non-identically distributed.

On the other hand, if the SNR approaches zero, we have

$$\frac{\sin^2\theta}{2\gamma}\left(\frac{\sigma_{1,1}^2-\sigma_{2,1}^2}{\sigma_{1,1}^2\sigma_{2,1}^2}\right)\Bigg|_{\gamma\to 0,\ \sin^2\theta\neq 0} = \infty. \tag{2.58}$$

Here, we assume $\sigma_{1,1}^2 > \sigma_{2,1}^2$, without loss of generality. Therefore, the constraint on w_1^2 becomes a hard constraint, and we have $w_1^2 = 2$. In this low SNR case, we can see that the OPAS is to assign all the power to the stronger channel. This result implies that space-time coding is not optimum in the case of low SNR with non-identically distributed, Rayleigh channels. Selecting the (statistically) stronger channel with single channel coding may outperform the space-time code. Note that the channel selection here is different from the conventional transmit antenna selection [78–82].

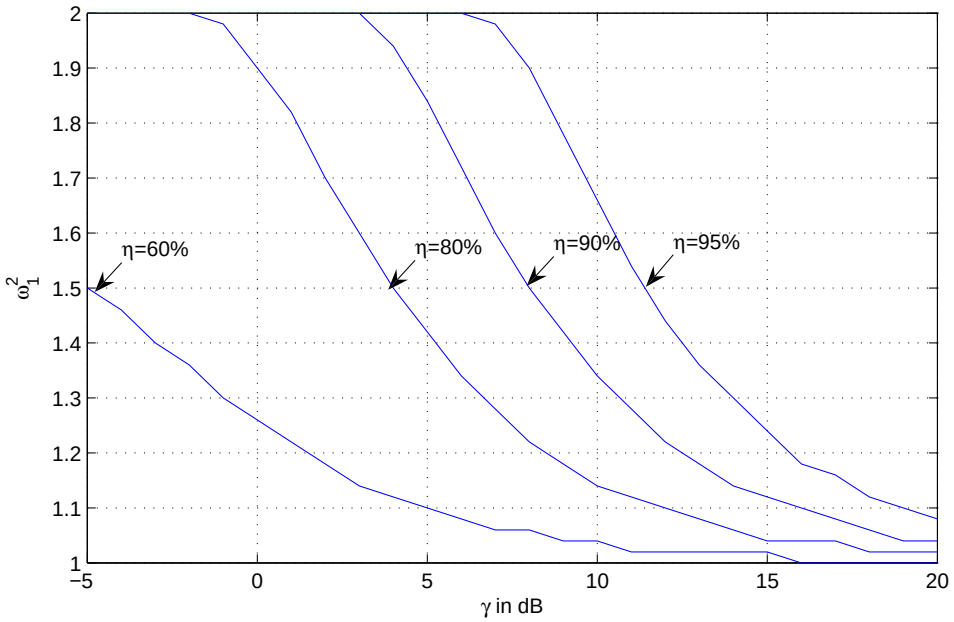

Figure 2.5: Values of w_1^2, with $\eta = 95\%,\ 90\%,\ 80\%$ and 60%, respectively.

The optimum values of w_1^2 are given in Figure 2.5, with $\eta = 95\%,\ 90\%,\ 80\%$, and 60%, respectively, where η is defined in (2.43). Figure 2.5 validates the discussion above that the OPAS tends to allocate more power to the (statistically) stronger channel in the low SNR region ($w_1^2 \to 2$), but converges to the EPAS in the high SNR region ($w_1^2 \to 1$).

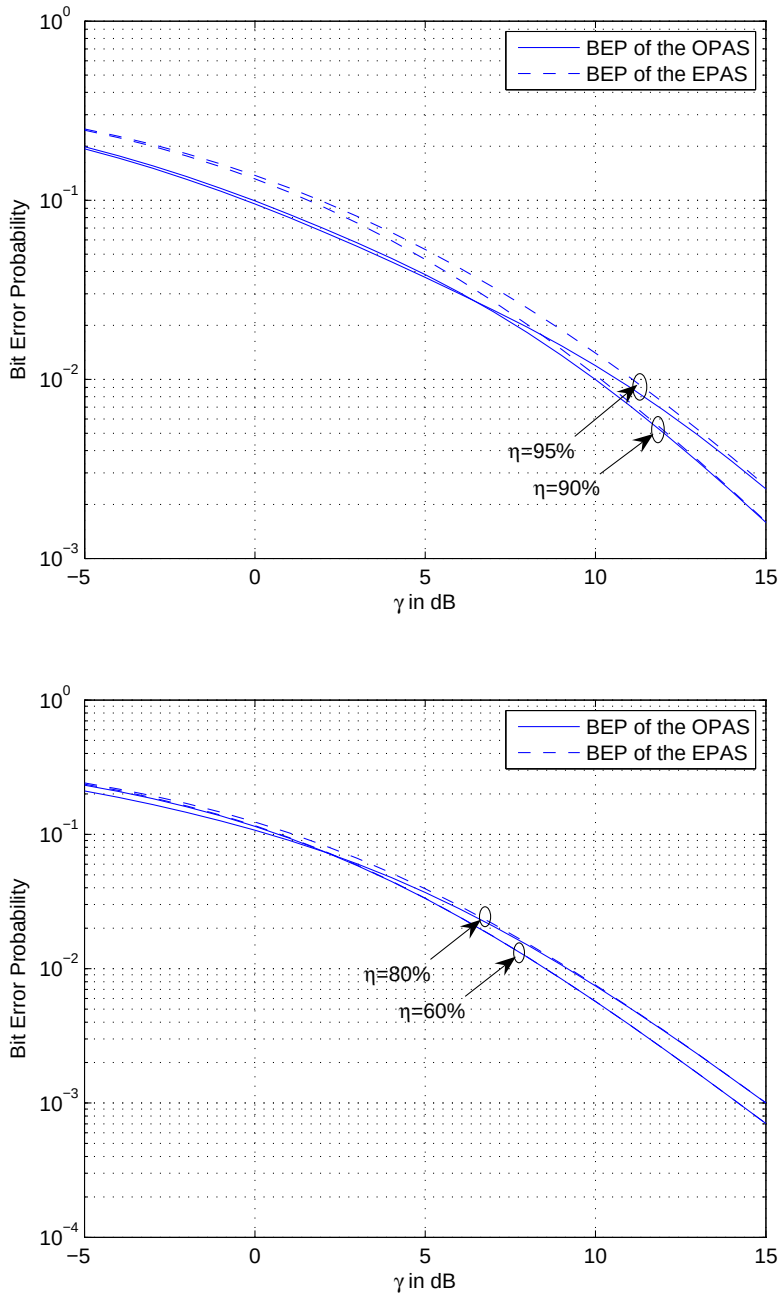

Figure 2.6: BEP for the optimum power allocation and the equal power allocation, with $\eta = 95\%,\ 90\%,\ 80\%$ and 60%, respectively.

The bit error performance of OPAS and EPAS is compared in Figure 2.6. It shows that the performance of the OPAS can have a SNR gain of up to 2 dB, when η is

large and SNR is low. However, the difference becomes negligible if $\eta < 60\%$, or SNR$> 15\ dB$.

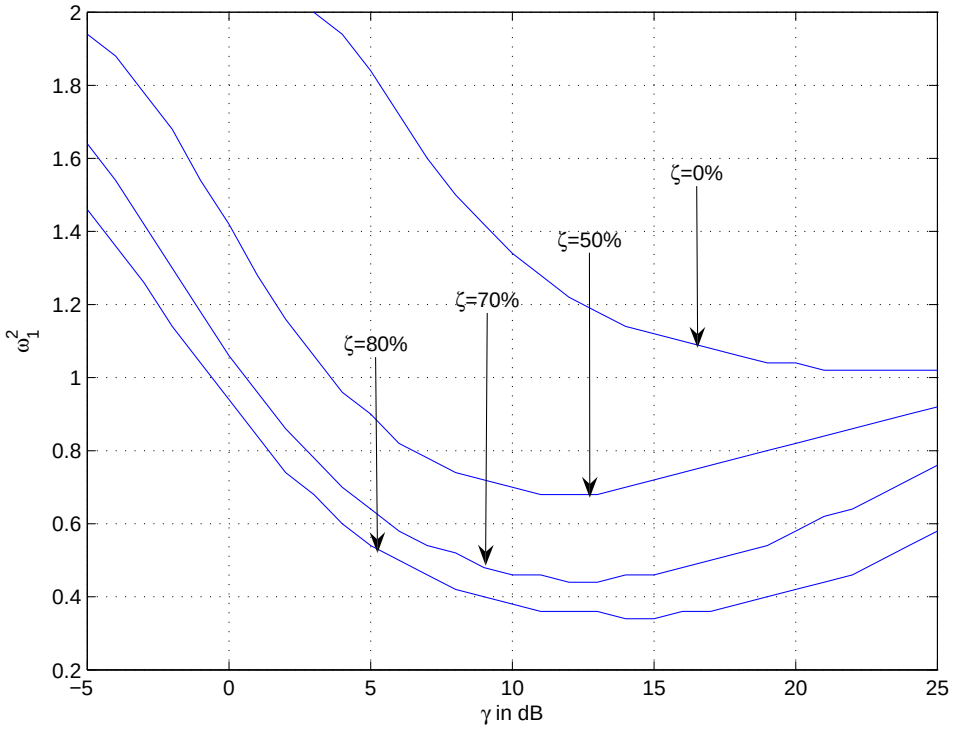

Figure 2.7: Values of w_1^2, with $\eta = 90\%$ and $\zeta = 95\%,\ 90\%,\ 80\%$ and 60%, respectively.

Ricean Channels

Although in Rayleigh channels, the OPAS tends to allocate more power to the stronger channel, this may not be the same in Ricean channels. Now, we assume the channel means are not zero, and $M_{1,1} = M_{2,1}$. Figure 2.7 gives the optimum value of w_1^2 with $\zeta = 80\%,\ 70\%,\ 50\%$, and 0%, respectively. Here, ζ is defined in (2.45) and $\eta = 90\%$. It can be seen that the OPAS allocates more power to the weaker channel ($w_1^2 < 1$) in some situations. The comparison of BEP between OPAS and EPAS is given in Figure

2.8, where the OPAS can achieve a SNR gain of up to 1 dB in the high SNR region.

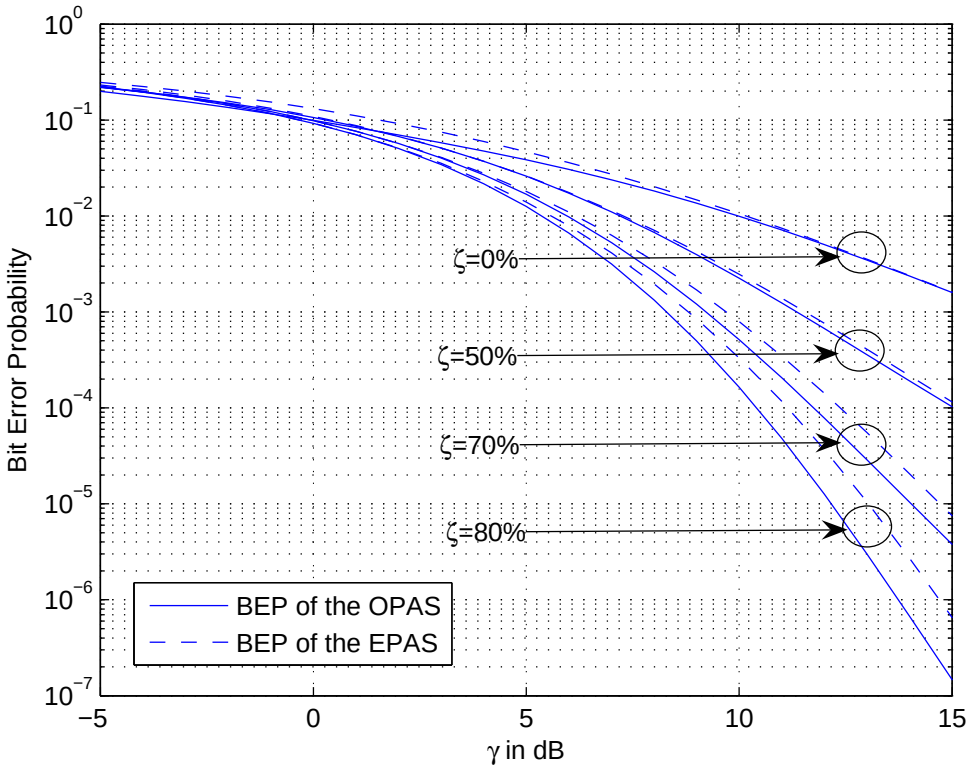

Figure 2.8: BEP for the optimum power allocation and the equal power allocation, with $\eta = 90\%$ and $\zeta = 80\%,\ 70\%,\ 50\%$ and 0%, respectively.

Multiple Receive antennas

In the above two examples, we considered the system with only one receive antenna. If the number of receive antennas increases, the problem becomes more complicated. We cannot guarantee that all the channels linked with the same transmit antenna are stronger or weaker than the ones linked with other transmit antennas, unless one of the transmit antennas is heavily blocked, so that the channels linked with this transmit antenna are all weakened.

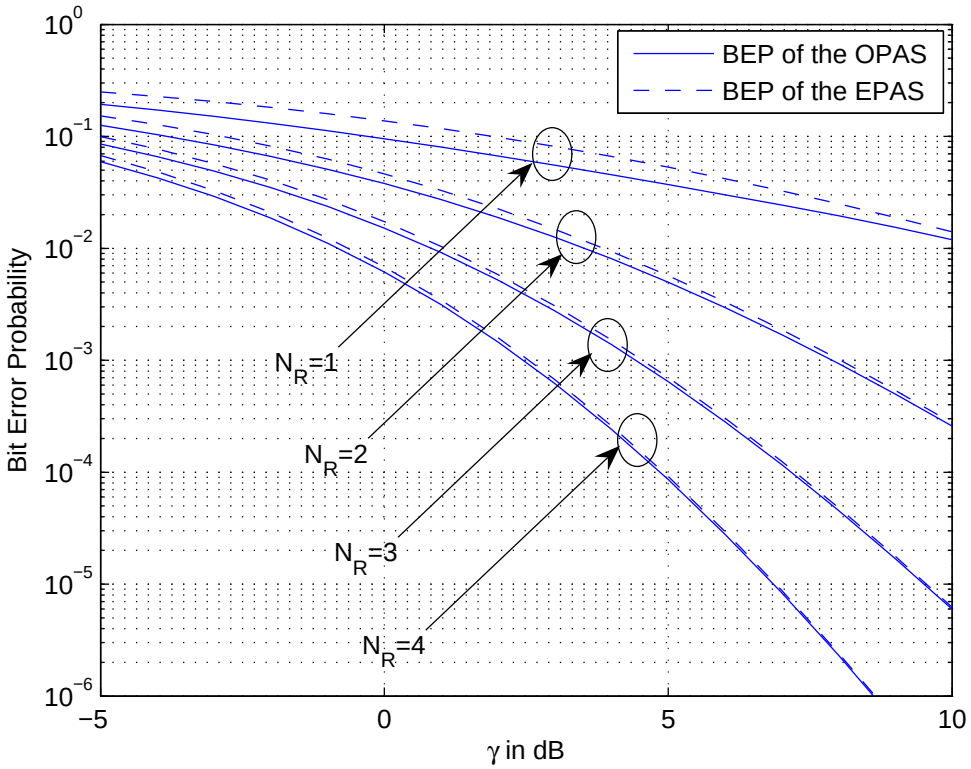

Figure 2.9: BEP for the optimum power allocation and the equal power allocation, with $\eta = 95\%$ and $N_R = 1, 2$ and 3, respectively.

In Figure 2.9, we consider a system with two transmit and multiple receive antennas. The channels linked with the first receive antenna are assumed to be non-identical Rayleigh channels, and η is equal to 95%. For all the other channels, we assume identical channel variances. It can be seen that when we increase the number of receive antennas, the performance gain of the OPAS gradually vanishes. If the number of receive antennas is greater than three, the EPAS can be safely applied without much loss in the performance. In Ricean channels, similar observations can be made.

2.6 Conclusions

We analyze the bit error performance for orthogonal STBC over independent and non-identically distributed channels. The exact BEP and a simple upper bound on the BEP are obtained for BPSK and QPSK modulations. The results show that the non-identical channel distribution degrades the bit error performance of STBC in Rayleigh channels. In Ricean channels, if the channel variances are identical, the unbalanced Ricean K-factors do not affect the bit error performance. If the Ricean K-factors are identical, the unbalanced channel variances can degrade the performance of STBC. However, if the channel means are identical, the unbalanced channel variances can either degrade or enhance the performance of STBC, depending on the ratio of the LOS component to the total received SNR.

Based on the analytical BEP, we also propose the optimum transmit power allocation for STBC over nonidentical channels. In the case of Rayleigh fading channels with two transmit and one receive antenna, our OPAS tends to allocate more power to the (statistically) stronger channel, and provides a performance gain of up to 2 dB in the low SNR region. On the contrary, in the Ricean case, the OPAS may need to allocate more power to the (statistically) weaker channel in some situations. If the number of receiver antennas increases, however, the performance gain of the OPAS gradually vanishes.

Chapter 3

Space-Time Block Codes over Non-identical Channels with Imperfect CSI

In Chapter 2, we have considered the STBC's over non-identical channels. The model used there is more realistic than the ones in most of the existing works. However, it still makes an ideal assumption that the CSI is perfectly known at the receiver. In this chapter, we will relax this assumption and extend our work to a more general model, which involves the channel estimation and, inevitably, the channel estimation error. In such a situation, the non-identical channel statistics lead to non-identical channel estimation errors, which consequently affect the performance and even the existing receiver structure of orthogonal STBC. We show that the conventional SBS decoder of orthogonal STBC is sub-optimum in this situation. A new optimum decoder is derived, which can be simplified to a new SBS decoder under certain conditions. Performance analysis and simulations are provided, which show that our new decoder substantially outperforms the conventional decoder.

STBC	identical channels	non-identical channels
perfect CSI	I	III
imperfect CSI	II	IV

Table 3.1: List of STBC models with two assumptions

3.1 Introduction

At the beginning of this chapter, let us first classify different STBC models with two assumptions: identical/non-identical channels and perfect/imperfect channel state information, which is given in Table 3.1.

Obviously, class I represents the ideal model. The earlier works on STBC belong to this class, which includes [45–48]. A natural extension of class I is to introduce channel estimation, such as [50, 51] which fall into class II. Class III was first addressed in cooperative diversity scenarios [57–59], where the distributed nodes normally experience non-identical channel statistics. The performance of orthogonal STBC over non-identical channels was also implicitly discussed in [62–64], as the issue of non-identical channels can be viewed as a special case of the correlated channels. Chapter 2, as well as our work in [87], has explicitly described the system model for class III, and given a thorough study on the performance and the power allocation schemes. Similar to the extension from class I to class II, the extension of class III is to introduce channel estimation and channel estimation errors, so the entire Chapter 3 here is devoted to class IV.

Before plunging into the technical details of class IV, let us first look at a practical example in the real world, wireless vehicular communication, which fully reflects the importance of the research on this general STBC model. Wireless vehicular communications, e.g. vehicle-to-vehicle (V2V) and vehicle-to-infrastructure (V2I)

communications, have attracted more and more attention [88–92] recently, as they show substantial potential to enhance traffic safety [89], efficiency and information availability [90]. Several standards are being developed for vehicular communications, such as IEEE 802.11p - wireless access of vehicular environments (WAVE), or IEEE 802.20, which is designed for high-speed mobility situations, e.g. for a high-speed train. The high mobility and the variation of the vehicular environment requires a robust communication link. Fortunately, the size of a vehicle allows it to be equipped with several antennas and to make use of MIMO systems. The orthogonal STBC [30] is, therefore, a suitable technique in vehicular communication [88], since it provides robust transmissions with very simple decoding schemes. In a vehicular environment, both the transmit and receive antennas are mounted at heights of 1-3 meters [90]. The surrounding reflectors of the signals consist of nearby vehicles and roadside buildings, which can be very close to one antenna but far from the others. The link distances are also instantly variable from less than 1-2 meters to several tens of meters. Therefore, the channels are more likely to be non-identically distributed. Further more, the rapidly variable environments and the Doppler shift caused by the moving vehicles make the channel estimation problem nontrivial in vehicular environments. Therefore, a model involving both non-identical channels and channel estimation error is needed in such a situation.

Generally, non-identical channels will result in non-identical channel estimation errors. These estimation errors will consequently affect the performance of the current systems, and even the structure of the existing receiver. Therefore, in this chapter we will re-examine the whole STBC system over non-identical channels with imperfect CSI. We show that the conventional SBS decoder [31] for orthogonal STBC is no longer optimum in this situation. The optimum decoder is obtained, which can be simplified to a new SBS decoder under certain conditions. To the best

of our knowledge, our work here is the first to consider the optimum decoder for orthogonal STBC over non-identical channels with channel estimation. Our analytical and simulation results show that our new decoder provides a much better performance compared to the conventional SBS decoder in this situation.

The rest of the chapter is organized as follows. In Section 3.2, we describe the system model. Section 3.3 examines the structure of the optimum and the SBS decoder. Performance analysis is given in Section 3.4. Sections 3.5 and 3.6 are numerical examples and conclusion, respectively.

3.2 System Model

The system considered in this chapter is similar to the one in Chapter 2. For the convenience of the readers, we repeat some of the descriptions here.

We consider a communication system with M_T transmit and N_R receive antennas. The transmit/receive antennas can be co-located in one vehicle/infrastructure, or distributed in several. If the antennas are not co-located, we assume the synchronization is perfect. The space-time block code $\boldsymbol{S}$ is a $P \times M_T$ matrix, where each row of $\boldsymbol{S}$ is transmitted through M_T transmit antennas at one time, and the transmission covers P symbol periods. It has a linear complex orthogonal design, and can be represented as [32]

$$\boldsymbol{S} = \sum_{k=1}^{K} (s_k \boldsymbol{A}_k + s_k^* \boldsymbol{B}_k). \tag{3.1}$$

Here, $\boldsymbol{A}_k$ and $\boldsymbol{B}_k$ are $P \times M_T$ matrices with constant complex entries, and K is the number of information symbols transmitted in one block. Therefore, each entry of $\boldsymbol{S}$ is a linear combination of the symbols $s_k, k = 1, \cdots, K$, and their conjugates s_k^*, where each s_k is from a certain complex signal constellation. The rate of the orthogonal

STBC is defined as K/P. For orthogonal STBC, we have [30]

$$\boldsymbol{S}^H\boldsymbol{S} = diag\left[\sum_{k=1}^{K}\lambda_{1,k}|s_k|^2,\ldots,\sum_{k=1}^{K}\lambda_{M_T,k}|s_k|^2\right] = \boldsymbol{D} \tag{3.2}$$

where $\{\lambda_{i,k}\}_{i=1}^{M_T}$ are non-negative numbers. For an arbitrary signal constellation, it requires that

$$\boldsymbol{A}_k^H\boldsymbol{A}_l + \boldsymbol{B}_l^H\boldsymbol{B}_k = \delta_{k,l}diag[\lambda_{1,k},\cdots,\lambda_{M_T,k}], \tag{3.3}$$

$$\boldsymbol{A}_k^H\boldsymbol{B}_l + \boldsymbol{A}_l^H\boldsymbol{B}_k = \boldsymbol{0}, \tag{3.4}$$

We assume here MPSK modulation and a constant transmitted energy per information bit E_b. Therefore, the total energy assigned to one block is $E_bK\log_2 M$. From the orthogonality condition (3.2), it can be seen that the total energy for one block is given by $\sum_m^{M_T}\sum_k^K\lambda_{m,k}|s_k|^2$. Thus, the transmitted energy per MPSK symbol is given by

$$E_s = \frac{E_bK\log_2 M}{\sum_m^{M_T}\sum_k^K\lambda_{m,k}} \tag{3.5}$$

However, noting that the channels are now estimated and the estimations of channels may vary from block to block, we introduce a parameter t to indicate the t-th block. Thus, the received signal at the t-th block is a $P \times N_R$ matrix, which is given by

$$\mathbf{R}(t) = \mathbf{S}(t)\mathbf{H}(t) + \mathbf{N}(t). \tag{3.6}$$

Here, $\mathbf{N}(t)$ is a $P \times N_R$ noise matrix, whose entries are i.i.d., complex, Gaussian random variables with means zero and variances $N_o/2$ per dimension. $\mathbf{H}(t)$ is a $M_T \times N_R$ channel matrix, where each entry $h_{mn}(t)$ is the channel gain of the link from the m-th transmit antenna to the n-th receive antenna. We assume $h_{mn}(t)$ is a circularly complex Gaussian random variable with mean zero and variance $2\sigma_{mn}^2$.

It is also assumed that the channels are all block-wise constant. The autocorrelation function of each channel is given as $\mathrm{E}[h_{mn}(t)h^*_{mn}(t')] = 2\sigma^2_{mn}R(t-t')$, where

$$R(t-t') = J_o(2\pi f_d T_b(t-t')) \tag{3.7}$$

for Jakes' model [93]. Here, the autocorrelation functions are assumed to be identical for different channels. If the antennas are co-located in one vehicle/infrastructrue, it is easy to see that the assumption is valid. If the antennas are distributed in several units, however, we can also assume identical autocorrelation functions for different channels, considering one moving unit should choose other unit moving with same direction and speed as a cooperative partner, in order to reduce the possibility of hand over.

In order to coherently detect the code matrix $\mathbf{S}(t)$ in (3.6), the channel matrix must be estimated first. In this chapter, we apply pilot-symbol assisted modulation (PASM) [52], such that a pilot block is inserted into the data stream every L_f blocks. During the pilot block, each transmit antenna transmits a known pilot symbol at its own designated time slot. The receiver estimates the channel matrix $\mathbf{H}(t)$ based on the information set $\Lambda(t)$, which contains the $2L_p$ received pilot blocks nearest in time to the t-th block.

Without loss of generality, we consider the component $h_{mn}(t)$ of the channel matrix $\mathbf{H}(t)$ and let $\mathbf{p}_{mn}$ be the column vector storing the $2L_p$ nearest received pilot symbols from the m-th transmit antenna to the n-th receive antenna. Using the result from [52], it can be shown that the minimum mean square error (MMSE) estimate of $h_{mn}(t)$ is given by

$$\hat{h}_{mn}(t) = \mathbf{d}^H_{mn}(t)\mathbf{p}_{mn}, \tag{3.8}$$

where

$$\mathbf{d}_{mn}(t) = \mathbf{G}^{-1}\mathbf{v}_{mn}(t) \tag{3.9}$$

represents a Weiner filter, with $\mathbf{G} = \frac{1}{2}E[\mathbf{p}_{mn}\mathbf{p}_{mn}^H]$ being the autocorrelation matrix of the received pilot samples $\mathbf{p}_{mn}$, and $\mathbf{v}_{mn}(t) = \frac{1}{2}E[h_{mn}^*(t)\mathbf{p}_{mn}]$ being the correlation of $h_{mn}(t)$ and $\mathbf{p}_{mn}$.

The channel estimation error, defined as $e_{mn}(t) = h_{mn}(t) - \hat{h}_{mn}(t)$, is a Gaussian random variable with mean zero and variance $2v_{mn}^2(t) = \sigma_{mn}^2 - \mathbf{v}_{mn}^H(t)\mathbf{G}^{-1}\mathbf{v}_{mn}(t)$ [52]. Note that $e_{mn}(t)$ is independent of $\hat{h}_{mn}(t)$. Therefore, given the information set $\Lambda(t)$, each $h_{mn}(t)$ is a conditional Gaussian random variable with mean $\hat{h}_{mn}(t)$ and variance $2v_{mn}^2(t)$. It is obvious that if the statistics of the channel gains on the different links are different, the variances of the channel estimation errors are different in general.

3.3 Optimum and Symbol-By-Symbol Decoders

One important advantage of orthogonal STBC is that the ML decoder can reduce to a SBS decoder, which greatly reduces the decoding complex. This conventional SBS decoder is optimum when channels are identical with perfect CSI [30] or with imperfect CSI [51]. It is also an optimum receiver in the case of non-identical channels with perfect CSI [87]. However, if the channels are non-identical and the CSI is imperfect, the conventional receiver is no longer optimum. Therefore, we need to investigate the structure of optimum decoder first.

For ML decoding, we compute the likelihood $p(\mathbf{R}(t), \Lambda(t) \mid \mathbf{S}(t))$ for each possible value of the signal block $\mathbf{S}(t)$. Since, we have

$$p(\mathbf{R}(t), \Lambda(t) \mid \mathbf{S}(t)) = p(\mathbf{R}(t) \mid \mathbf{S}(t), \Lambda(t))p(\Lambda(t) \mid \mathbf{S}(t)) \tag{3.10}$$

and the information set $\Lambda(t)$ is independent of $\mathbf{S}(t)$, the ML decoding rule simplifies to

$$\hat{\mathbf{S}}(t) = \arg\max_{\mathbf{S}(t)} p(\mathbf{R}(t) \mid \mathbf{S}(t), \Lambda(t)) \tag{3.11}$$

where $\mathbf{R}(t)$ is conditionally Gaussian with mean $\mathbf{S}(t)\hat{\mathbf{H}}(t)$, given $\mathbf{S}(t)$ and $\Lambda(t)$.

The column vectors of $\mathbf{R}(t)$ are independent of one another and each has covariance matrix of

$$\mathbf{C}_n(t) = \mathbf{S}(t)\mathbf{V}_n(t)\mathbf{S}^H(t) + N_o\mathbf{I}_{p\times p}\ ,\ n = 1, \cdots, N_R, \tag{3.12}$$

where

$$\mathbf{V}_n(t) = \text{diag}[2v_{mn}^2(t)]_{m=1}^{M_T}\ ,\ n = 1, \cdots, N_R. \tag{3.13}$$

The PDF of the received signal is now given by

$$p(\mathbf{R}(t) \mid \mathbf{S}(t), \Lambda(t)) = \left(\prod_{n=1}^{N_R} \det(\pi\mathbf{C}_n(t))\right)^{-1}$$
$$\cdot \exp\left(-\sum_{n=1}^{N_R}(\mathbf{r}_n(t) - \mathbf{S}(t)\hat{\mathbf{h}}_n(t))^H\mathbf{C}_n^{-1}(t)(\mathbf{r}_n(t) - \mathbf{S}(t)\hat{\mathbf{h}}_n(t))\right). \tag{3.14}$$

Therefore, the ML block-by-block receiver becomes

$$\hat{\mathbf{S}}(t) = \arg\min_{\mathbf{S}(t)}\left(\sum_{n=1}^{N_R}\left(\mathbf{r}_n(t) - \mathbf{S}(t)\hat{\mathbf{h}}_n(t)\right)^H\mathbf{C}_n^{-1}(t)\left(\mathbf{r}_n(t) - \mathbf{S}(t)\hat{\mathbf{h}}_n(t)\right)\right). \tag{3.15}$$

As we will show later, depending on whether the non-identical channels are associated with transmit antennas or receiver antennas, there are different effects on the OSTBC. For the sake of illustration, we will consider two typical cases in the following sections.

Case I: Channels gains from different transmit antennas to a common receive antenna are identically distributed, but the gains associated with different receive antennas are non-identically distributed. Therefore, the variance of $h_{mn}(t)$ reduces to $2\sigma_{on}^2$, and the variance of estimation error reduces to $2v_{on}^2(t)$.

Case II: Channels gains from a common transmit antenna to different receive antennas are identically distributed, but the gains associated with different transmit antennas are non-identically distributed. Therefore, the variance of $h_{mn}(t)$ reduces to $2\sigma_{mo}^2$, and the variance of estimation error reduces to $2v_{mo}^2(t)$.

Other more complex cases can be viewed as the combination of these two cases. Here, notice that the variances of channel gains are constant, but the variances of the estimation errors depend on the position of the code block.

3.3.1 Case I: Channels Associated with One Common Receive Antenna are Identically Distributed

In this case, since $2v_{mn}^2 = 2v_{on}^2$ for all m, we have

$$\mathbf{V}_n(t) = 2v_{on}^2 \mathbf{I}_{N_T \times N_T} \ , \ n = 1, \cdots, N_R. \tag{3.16}$$

If the STBC employed satisfies

$$\mathbf{S}(t)\mathbf{S}^H(t) = \beta \mathbf{I}_{P \times P} \tag{3.17}$$

where β is a constant, then the $\mathbf{C}_n(t)'s$ become constants proportional to an identity matrix. Therefore, the ML receiver (3.15) simplifies to

$$\hat{\mathbf{S}}(t) = \arg \min_{\mathbf{S}(t)} \left\| \tilde{\mathbf{R}}(t) - \mathbf{S}(t)\tilde{\hat{\mathbf{H}}}(t) \right\|^2 \tag{3.18}$$

where

$$\tilde{\mathbf{R}}(t) = \left[\sqrt{\frac{1}{2v_{on}^2\beta + N_o}} \mathbf{r}_n(t) \right]_{n=1}^{N_R} = \mathbf{R}(t) \text{diag} \left[\sqrt{\frac{1}{2v_{on}^2\beta + N_o}} \right]_{n=1}^{N_R}, \tag{3.19}$$

$$\tilde{\hat{\mathbf{H}}}(t) = \left[\sqrt{\frac{1}{2v_{on}^2\beta + N_o}} \hat{\mathbf{h}}_n(t) \right]_{n=1}^{N_R} = \hat{\mathbf{H}}(t) \text{diag} \left[\sqrt{\frac{1}{2v_{on}^2\beta + N_o}} \right]_{n=1}^{N_R}. \tag{3.20}$$

Applying equations (3.3) and (3.4) to (3.18), the receiver can be further simplified to a SBS detector, given by

$$\hat{s}_k(t) = \arg \max_{s \in MPSK} \Re[z_{k'}(t)s^*(t)], \forall k' = 1 \cdots K \tag{3.21}$$

where

$$z_{k'}(t) = \text{Tr} \left[\tilde{\mathbf{R}}^H(t)\mathbf{B}_{k'}\tilde{\hat{\mathbf{H}}}(t) + \tilde{\hat{\mathbf{H}}}^H(t)\mathbf{A}_{k'}^H\tilde{\mathbf{R}}(t) \right]. \tag{3.22}$$

Therefore, in case I, the ML decoding can also be achieved by a SBS decoder, under the condition that the received signal matrix $\mathbf{R}(t)$ and the estimated channel matrix $\hat{\mathbf{H}}(t)$ are properly weighted column by column, according to the variances of the channel estimation errors.

3.3.2 Case II: Channels Associated with One Common Transmit Antenna are Identically Distributed

In case II, since the channels are identically distributed with a common transmit antenna, each column vector of $\mathbf{R}(t)$ has the same covariance matrix

$$\mathbf{C}(t) = \mathbf{S}(t)\mathbf{V}(t)\mathbf{S}^H(t) + N_o\mathbf{I}_{p\times p} \ , \tag{3.23}$$

where

$$\mathbf{V}(t) = \text{diag}[2v_{mo}^2]_{m=1}^{N_T} \ . \tag{3.24}$$

It can easily be seen that $\mathbf{C}^{-1}(t)$ is not a diagonal matrix, because of the non-identical $2v_{mo}^2$'s.

Since, the variances of channel estimation errors, $2v_{mo}^2$'s, are different for the channels associated with one common receive antenna, the ML decoder

$$\hat{\mathbf{S}}(t) = \arg\min_{\mathbf{S}(t)} \left(\sum_{n=1}^{N_R} \left(\mathbf{r}_n(t) - \mathbf{S}(t)\hat{\mathbf{h}}_n(t) \right)^H \mathbf{C}^{-1}(t) \left(\mathbf{r}_n(t) - \mathbf{S}(t)\hat{\mathbf{h}}_n(t) \right) \right) \tag{3.25}$$

cannot reduce to a SBS decoder, no matter how the received signals are weighted.

Fortunately, the most practical OSTBC used in actual communication systems is Alamouti's code [29], which only requires two transmit antennas. In such cases, the ML decoder in case II only requires an affordable decoding complexity of M^2, where M is the order of the modulation.

3.4 Performance Analysis

In this section, we will examine the bit error performance of the new optimum SBS decoder proposed for case I. For the sake of simplicity, we drop the block index t hereafter, but note that the results obtained do depend on the positions of blocks.

3.4.1 Conditional Bit Error Probability

With PSK modulation, i.e. $s_k = \sqrt{E_s}e^{j\phi_k}$, the decoding rule (3.21) is equivalent to

$$\hat{s}_k = \arg\max \Re[z_{k'}e^{-j\phi_k}], \forall k' = 1 \cdots K \tag{3.26}$$

where

$$z_{k'} = \text{Tr}\left[\tilde{\mathbf{R}}^H \mathbf{B}_{k'} \tilde{\hat{\mathbf{H}}} + \tilde{\hat{\mathbf{H}}}^H \mathbf{A}_{k'}^H \tilde{\mathbf{R}}\right] = x_{k'} + \mu_{k'}, \tag{3.27}$$

$$\begin{aligned} x_{k'} = \sum_{k=1}^{K} \Big[& s_k^* \text{Tr}[\tilde{\mathbf{H}}^H \mathbf{A}_k^H \mathbf{B}_{k'} \tilde{\hat{\mathbf{H}}} + \tilde{\hat{\mathbf{H}}}^H \mathbf{A}_{k'}^H \mathbf{B}_k \tilde{\mathbf{H}}] \\ & + s_k \text{Tr}[\tilde{\hat{\mathbf{H}}}^H \mathbf{A}_{k'}^H \mathbf{A}_k \tilde{\mathbf{H}} + \tilde{\mathbf{H}}^H \mathbf{B}_k^H \mathbf{B}_{k'} \tilde{\hat{\mathbf{H}}}] \Big], \end{aligned} \tag{3.28}$$

$$\mu_{k'} = \text{Tr}\left[\tilde{\mathbf{N}}^H \mathbf{B}_{k'} \tilde{\hat{\mathbf{H}}} + \tilde{\hat{\mathbf{H}}}^H \mathbf{A}_{k'}^H \tilde{\mathbf{N}}\right]. \tag{3.29}$$

For equally likely symbols, we can assume $s_{k'} = \sqrt{E_s}$ without loss of generality, thus the BEP depends on the probability $P_\alpha(e) = P(\Re[z_{k'}e^{-j\alpha}] < 0 | s_{k'} = \sqrt{E_s})$, where α is some angle depending on modulation order [83]. For BPSK modulation, the BEP is obviously given by $P_b = P_{\alpha=0}(e)$. For QPSK modulation with Gray mapping, the BEP is given by $P_b = P_{\alpha=\frac{\pi}{4}}(e)$ [83].

Conditioning on the information set Λ and $s_{k'}$, and substituting (3.3) and (3.4) into (3.28), we can see that $x_{k'}$ is a Gaussian random variable, which is given by

$$(x_{k'} | s_{k'}, \Lambda) \sim CN\left(s_{k'} \sum_{n=1}^{N_R} \frac{\mathcal{H}}{\mathcal{V}_n}, E_s \sum_{m=1}^{M_T} \sum_{n=1}^{N_R} \frac{2v_{on}^2 |\xi_{mn}|^2}{\mathcal{V}_n^2}\right) \tag{3.30}$$

where

$$\mathcal{H} = \sum_{m=1}^{M_T} \lambda_{m,k'} |\hat{h}_{mn}|^2, \tag{3.31}$$

$$\mathcal{V}_n = 2v_{on}^2 \beta + N_o \tag{3.32}$$

and

$$\xi_{mn} = \sum_{k=1}^{K} \sum_{i=1}^{M_T} \left((\mathbf{a}_{k,m}^H \mathbf{b}_{k',i} + \mathbf{b}_{k,m}^H \mathbf{b}_{k',i}) \hat{h}_{mn} + (\mathbf{a}_{k',i}^H \mathbf{b}_{k,m} + \mathbf{a}_{k',i}^H \mathbf{a}_{k,m}) \hat{h}_{mn}^* \right). \tag{3.33}$$

Here, $\mathbf{a}_{k,i}$ and $\mathbf{b}_{k,i}$ are the i-th column vectors of matrices $\mathbf{A}_k$ and $\mathbf{B}_k$, respectively. Similarly, the noise term $\mu_{k'}$ in (3.29) is also a conditional Gaussian random variable, which is given by

$$(\mu_{k'} | s_{k'}, \Lambda) \sim CN \left(0, \frac{N_o}{2} \sum_{n=1}^{N_R} \frac{\mathcal{H}}{\mathcal{V}_n^2} \right). \tag{3.34}$$

Therefore, conditioning on the information set Λ, the probability $P_\alpha(e)$ is given by

$$P_\alpha(e|\Lambda) = Q \left(\sqrt{ \frac{E_s \left(\sum_{n=1}^{N_R} \frac{\mathcal{H}}{\mathcal{V}_n} \right)^2 \cos^2 \alpha}{E_s \sum_{m=1}^{M_T} \sum_{n=1}^{N_R} \frac{v_{on}^2 |\xi_{mn}|^2}{\mathcal{V}_n^2} + \frac{N_o}{2} \sum_{n=1}^{N_R} \frac{\mathcal{H}}{\mathcal{V}_n^2}} } \right). \tag{3.35}$$

In the conditional probability above, since both the denominator and the numerator contains the estimated channel gains $\{\hat{h}_{mn}\}$, it is difficult to average equation (3.35) over $\{\hat{h}_{mn}\}$ directly and obtain the exact BEP. Therefore, in the following section we will first investigate the exact BEP in a special case, and then introduce the performance bounds and approximations in general situations.

3.4.2 Exact BEP for the Special Case of Perfect CSI

If the CSI is perfect, such that $2v_{mn}^2 = 0$ for all m and n, we have $\hat{h}_{mn} = h_{mn}$. The conditional probabilities (3.35) can be simplified to

$$P_\alpha(e|\Lambda) = \frac{1}{\pi} \int_0^{\frac{\pi}{2}} \exp \left(-\frac{E_s \cos^2 \alpha}{N_o \sin^2 \theta} \sum_{n=1}^{N_R} \sum_{m=1}^{N_T} \lambda_{m,k'} |h_{mn}|^2 \right) d\theta, \tag{3.36}$$

which is the same as the result (2.26), as expected. Applying Lemma 2.1 to the conditional BEP (3.36), we obtain the exact error probability, which is given by

$$P_\alpha(e) = \frac{1}{\pi}\int_0^{\frac{\pi}{2}} \prod_{m=1}^{M_T}\prod_{n=1}^{N_R}\left(1+\frac{2\sigma_{mn}^2 E_s \lambda_{m,k'}\cos^2\alpha}{N_o \sin^2\theta}\right)^{-1} d\theta. \tag{3.37}$$

3.4.3 Bounds and Approximations of BEP with Imperfect CSI

If the channels are estimated, as we mentioned above, the exact average BEP is difficult to obtain. Therefore, performance approximations and bounds need to be applied. In the following section, we will use Alamouti's code [29] as an example to show how to analyze the average BEP. The method used in this paper can similarly be extended to other orthogonal STBC's.

Using Alamouti's code [29], the code matrix and $\mathbf{A}_k$ and $\mathbf{B}_k$ are given by

$$\mathbf{S} = \begin{bmatrix} s_1 & s_2 \\ -s_2^* & s_1^* \end{bmatrix} : \quad \mathbf{A}_1 = \begin{bmatrix} 1 & 0 \\ 0 & 0 \end{bmatrix}, \mathbf{A}_2 = \begin{bmatrix} 0 & 1 \\ 0 & 0 \end{bmatrix},$$
$$\mathbf{B}_1 = \begin{bmatrix} 0 & 0 \\ 0 & 1 \end{bmatrix}, \mathbf{B}_2 = \begin{bmatrix} 0 & 0 \\ -1 & 0 \end{bmatrix} \tag{3.38}$$

respectively. Thus, $\lambda_{i,k} = 1$ for all i and k. Substituting (3.38) into (3.33), we have

$$\begin{aligned} \begin{bmatrix} \xi_{11} & \xi_{12} \\ \xi_{21} & \xi_{22} \end{bmatrix} &= \begin{bmatrix} \hat{h}_{11} & \hat{h}_{12} \\ -\hat{h}_{21} & -\hat{h}_{22} \end{bmatrix} + \begin{bmatrix} \hat{h}_{11}^* & \hat{h}_{12}^* \\ \hat{h}_{21}^* & \hat{h}_{22}^* \end{bmatrix} \\ &= \begin{bmatrix} 2\Re[\hat{h}_{11}] & 2\Re[\hat{h}_{12}] \\ -2\Im[\hat{h}_{21}] & -2\Im[\hat{h}_{22}] \end{bmatrix}. \end{aligned} \tag{3.39}$$

Since the channel gain h_{mn} is circularly Gaussian, it is easy to see that $\hat{h}_{mn}$ is also circularly Gaussian, and thus we make the approximation that

$$E_s \sum_{m=1}^{M_T}\sum_{n=1}^{N_R} \frac{v_{on}^2 |\xi_{mn}|^2}{\mathcal{V}_n^2} \approx 2E_s \sum_{m=1}^{M_T}\sum_{n=1}^{N_R} \frac{v_{on}^2 |\hat{h}_{mn}|^2}{\mathcal{V}_n^2}. \tag{3.40}$$

This approximation is justified on the grounds that the two terms have the same means, which means that it can give a close approximation to the final BEP, when averaging the conditional BEP over all possible values of the estimated channel gains.

Applying the above approximation, we first rewrite (3.35) as

$$P_\alpha(e|\Lambda) = Q\left(\sqrt{\frac{E_s\left(\sum_{n=1}^{N_R}\sum_{m=1}^{M_T}\frac{|\hat{h}_{mn}|^2}{\mathcal{V}_n}\right)^2\cos^2\alpha}{2E_s\mathcal{I}+\frac{N_o}{2}\mathcal{N}}}\right) \tag{3.41}$$

where the terms $\mathcal{I} = \sum_{m=1}^{M_T}\sum_{n=1}^{N_R}\frac{v_{on}^2}{\mathcal{V}_n}\frac{|\hat{h}_{mn}|^2}{\mathcal{V}_n}$ and $\mathcal{N} = \sum_{n=1}^{N_R}\sum_{m=1}^{M_T}\frac{1}{\mathcal{V}_n}\frac{|\hat{h}_{mn}|^2}{\mathcal{V}_n}$.

Upper and Lower Bounds on the BEP

The terms $\mathcal{I}$ and $\mathcal{N}$ can be upper and lower bounded as

$$\begin{aligned}
\sum_{m=1}^{M_T}\sum_{n=1}^{N_R}\frac{|\hat{h}_{mn}|^2}{\mathcal{V}_n}\max_{n=1,\cdots,N_T}\left[\frac{v_{on}^2}{\mathcal{V}_n}\right] &\geq \mathcal{I} \geq \sum_{m=1}^{M_T}\sum_{n=1}^{N_R}\frac{|\hat{h}_{mn}|^2}{\mathcal{V}_n}\min_{n=1,\cdots,N_T}\left[\frac{v_{on}^2}{\mathcal{V}_n}\right], \\
\sum_{n=1}^{N_R}\sum_{m=1}^{M_T}\frac{|\hat{h}_{mn}|^2}{\mathcal{V}_n}\max_{n=1,\cdots,N_T}\left[\frac{1}{\mathcal{V}_n}\right] &\geq \mathcal{N} \geq \sum_{n=1}^{N_R}\sum_{m=1}^{M_T}\frac{|\hat{h}_{mn}|^2}{\mathcal{V}_n}\min_{n=1,\cdots,N_T}\left[\frac{1}{\mathcal{V}_n}\right].
\end{aligned} \tag{3.42}$$

Consequently, the conditional probability can be bounded as

$$P_\alpha(e|\Lambda) \geq Q\left(\sqrt{\frac{E_s\left(\sum_{n=1}^{N_R}\sum_{m=1}^{M_T}\frac{|\hat{h}_{mn}|^2}{\mathcal{V}_n}\right)\cos^2\alpha}{2E_s\min\left[\frac{v_{on}^2}{\mathcal{V}_n}\right]+\frac{N_o}{2}\min\left[\frac{1}{\mathcal{V}_n}\right]}}\right), \tag{3.43}$$

$$P_\alpha(e|\Lambda) \leq Q\left(\sqrt{\frac{E_s\left(\sum_{n=1}^{N_R}\sum_{m=1}^{M_T}\frac{|\hat{h}_{mn}|^2}{\mathcal{V}_n}\right)\cos^2\alpha}{2E_s\max\left[\frac{v_{on}^2}{\mathcal{V}_n}\right]+\frac{N_o}{2}\max\left[\frac{1}{\mathcal{V}_n}\right]}}\right). \tag{3.44}$$

Since the random variables $\{\hat{h}_{mn}\}$ in the denominator have been cancelled with the common terms in the numerator, it is now possible to average over the estimated channels.

Observing that the estimated channel gains $\{\hat{h}_{mn}\}$ are also independent Gaussian random variables with means zero and variances $\{2\sigma_{mn}^2 - 2v_{mn}^2\}$, we can average the

above inequalities following the same steps from (3.36) to (3.37), and obtain

$$P_\alpha(e) \geq \frac{1}{\pi}\int_0^{\frac{\pi}{2}} \prod_{m=1}^{M_T}\prod_{n=1}^{N_R}\left(1+\frac{(2\sigma_{mn}^2-2v_{mn}^2)\mu_l}{\mathcal{V}_n\sin^2\theta}\right)^{-1} d\theta, \tag{3.45}$$

$$P_\alpha(e) \leq \frac{1}{\pi}\int_0^{\frac{\pi}{2}} \prod_{m=1}^{M_T}\prod_{n=1}^{N_R}\left(1+\frac{(2\sigma_{mn}^2-2v_{mn}^2)\mu_u}{\mathcal{V}_n\sin^2\theta}\right)^{-1} d\theta \tag{3.46}$$

where

$$\mu_l = \frac{E_s\cos^2\alpha}{4E_s\min\left[\frac{v_{on}^2}{\mathcal{V}_n}\right]+N_o\min\left[\frac{1}{\mathcal{V}_n}\right]}, \tag{3.47}$$

$$\mu_u = \frac{E_s\cos^2\alpha}{4E_s\max\left[\frac{v_{on}^2}{\mathcal{V}_n}\right]+N_o\max\left[\frac{1}{\mathcal{V}_n}\right]}. \tag{3.48}$$

Approximations on the BEP

In order to obtain more accurate evaluations of the error performance, we propose two close approximations on the BEP, namely, the geometric approximation and the arithmetic approximation. The terms $\mathcal{I}$ and $\mathcal{N}$ can be closely approximated as

$$\mathcal{I} \approx \sum_{m=1}^{M_T}\sum_{n=1}^{N_R}\frac{|\hat{h}_{mn}|^2}{\mathcal{V}_n}\left[\frac{v_{on}^2}{\mathcal{V}_n}\right]_g, \tag{3.49}$$

$$\mathcal{I} \approx \sum_{m=1}^{M_T}\sum_{n=1}^{N_R}\frac{|\hat{h}_{mn}|^2}{\mathcal{V}_n}\left[\frac{v_{on}^2}{\mathcal{V}_n}\right]_a \tag{3.50}$$

and

$$\mathcal{N} \approx \sum_{n=1}^{N_R}\sum_{m=1}^{M_T}\frac{|\hat{h}_{mn}|^2}{\mathcal{V}_n}\left[\frac{1}{\mathcal{V}_n}\right]_g, \tag{3.51}$$

$$\mathcal{N} \approx \sum_{n=1}^{N_R}\sum_{m=1}^{M_T}\frac{|\hat{h}_{mn}|^2}{\mathcal{V}_n}\left[\frac{1}{\mathcal{V}_n}\right]_a \tag{3.52}$$

respectively. Here,

$$\left[\frac{v_{on}^2}{\mathcal{V}_n}\right]_g = \left(\prod_{n=1}^{N_R}\frac{v_{on}^2}{\mathcal{V}_n}\right)^{1/N_R}, \quad \left[\frac{v_{on}^2}{\mathcal{V}_n}\right]_a = \frac{1}{N_R}\sum_{n=1}^{N_R}\frac{v_{on}^2}{\mathcal{V}_n} \tag{3.53}$$

and

$$\left[\frac{1}{\mathcal{V}_n}\right]_g = \left(\prod_{n=1}^{N_R}\frac{1}{\mathcal{V}_n}\right)^{1/N_R}, \quad \left[\frac{1}{\mathcal{V}_n}\right]_a = \frac{1}{N_R}\sum_{n=1}^{N_R}\frac{1}{\mathcal{V}_n} \tag{3.54}$$

denote, respectively, the geometric and arithmetic means of the sequences $\{\frac{v_{on}^2}{\mathcal{V}_n}\}$ and $\{\frac{1}{\mathcal{V}_n}\}$. Following the same steps as above, the approximations of the probabilities are given by

$$P_\alpha(e) \approx \frac{1}{\pi}\int_0^{\frac{\pi}{2}} \prod_{m=1}^{M_T}\prod_{n=1}^{N_R}\left(1+\frac{(2\sigma_{mn}^2-2v_{mn}^2)\mu_g}{\mathcal{V}_n\sin^2\theta}\right)^{-1} d\theta, \tag{3.55}$$

$$P_\alpha(e) \approx \frac{1}{\pi}\int_0^{\frac{\pi}{2}} \prod_{m=1}^{M_T}\prod_{n=1}^{N_R}\left(1+\frac{(2\sigma_{mn}^2-2v_{mn}^2)\mu_a}{\mathcal{V}_n\sin^2\theta}\right)^{-1} d\theta \tag{3.56}$$

where

$$\mu_g = \frac{E_s\cos^2\alpha}{4E_s\left[\frac{v_{on}^2}{\mathcal{V}_n}\right]_g + N_o\left[\frac{1}{\mathcal{V}_n}\right]_g}, \tag{3.57}$$

$$\mu_a = \frac{E_s\cos^2\alpha}{4E_s\left[\frac{v_{on}^2}{\mathcal{V}_n}\right]_a + N_o\left[\frac{1}{\mathcal{V}_n}\right]_a}. \tag{3.58}$$

Note that if the channel estimation error variances approach zero, the two bounds (3.45), (3.46), and the two approximations (3.55), (3.56) all converge to the exact BEP result (3.37) for the special case of perfect CSI. This further validates our derivations.

Note that although we omitted the block index t here, the BEP results obtained above are based on the t-th block. The average BEP for all the blocks can be calculated by averaging over the L_f blocks within two adjacent pilot blocks.

3.5 Numerical Examples

In the numerical examples, we consider a vehicular communication system with 2 transmit and 2 receive antennas. The Alamouti's code is applied with QPSK modulation. As we mentioned in Section 3.2, since the channels are block-wise constant, we use the block fade rate f_dT_b for the BEP computation and simulation. One pilot block is inserted after every 9 data blocks, and the 4 nearest pilot blocks are used to estimate the channel using PSAM.

In Figure 3.1, we consider case I, where the variances of the channel gains related to the first and second receive antennas are 0.5 and 5, respectively. The block fade rate is set to 0.1. The simulation results show that our optimum receiver provides a large performance gain compared to the conventional receiver. The irreducible error floor caused by the channel fading is also greatly reduced by the optimum receiver.

The analytical lower (3.45) and upper (3.46) bounds in Fig 3.1 show the same trend as the exact BEP curve, meaning that they decrease in parallel with the increase of SNR. The three curves converge in the high SNR region. Furthermore, both the geometric (3.55) and arithmetic (3.56) approximations can closely approximate the exact BEP performance in all SNR regions, with the latter being a closer approximation, the difference being no larger than $0.5\ dB$.

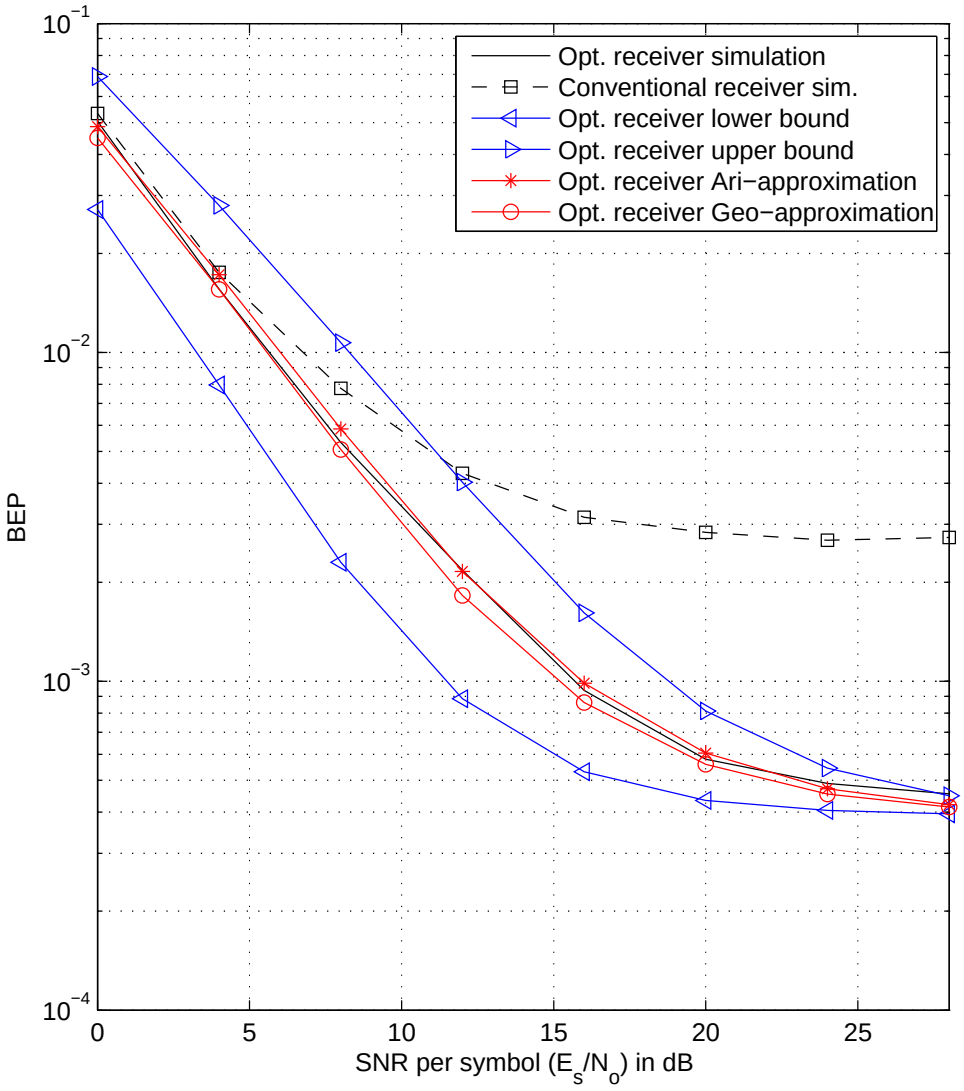

Figure 3.1: Case I: BEP results for the conventional and the optimum SBS receivers, 2Tx and 2Rx Alamouti's code with QPSK modulation, $f_d T_b$=0.1, channels variances of 0.5 and 5, respectively.

In Figures 3.2 and 3.3, we change the channel variances and the block fade rate, and similar observations can be made. Notice that in case I, the performance gain

enjoyed by the optimum SBS receiver comes with little overhead, as it only requires linear processing of the received signal and the estimated channel matrices.

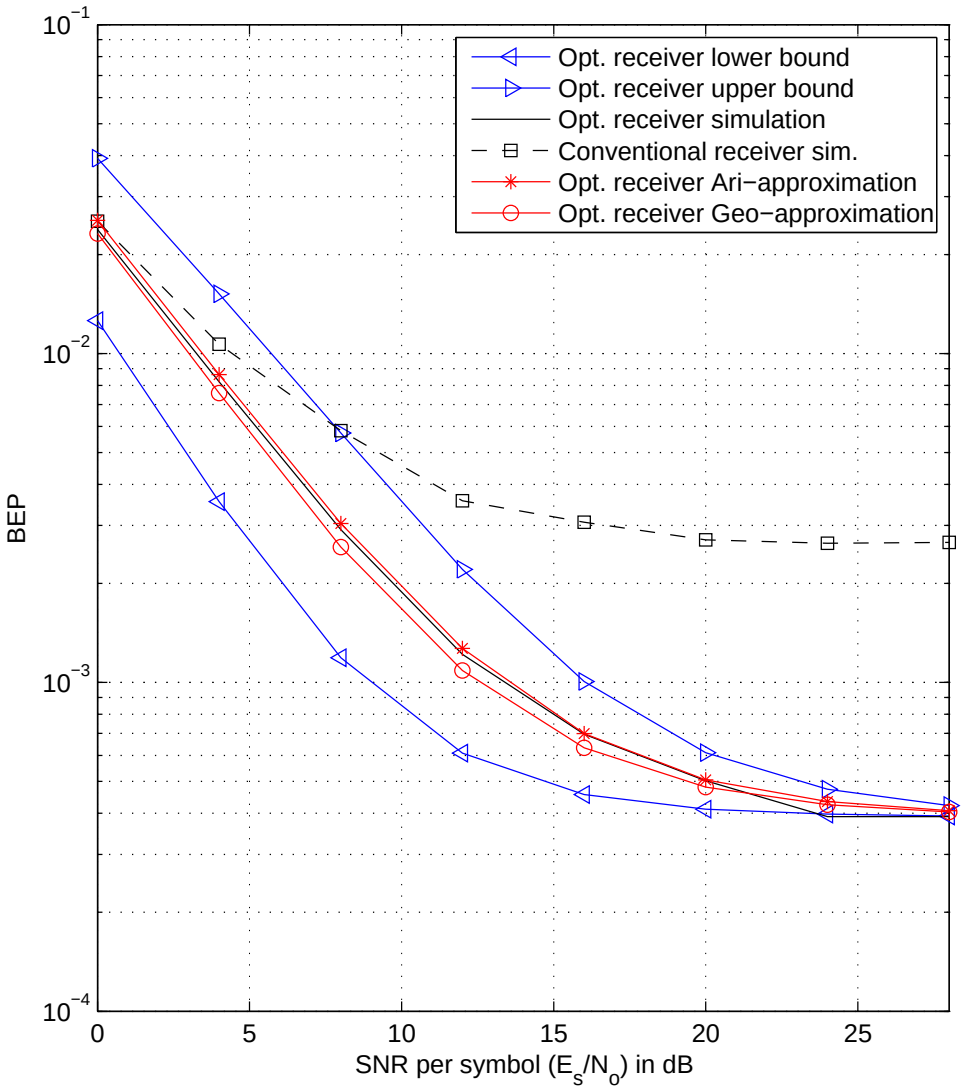

Figure 3.2: Case I: BEP results for the conventional and the optimum SBS receivers, 2Tx and 2Rx Alamouti's code with QPSK modulation, $f_d T_b$=0.1, channel variances are 0.9 and 9, respectively.

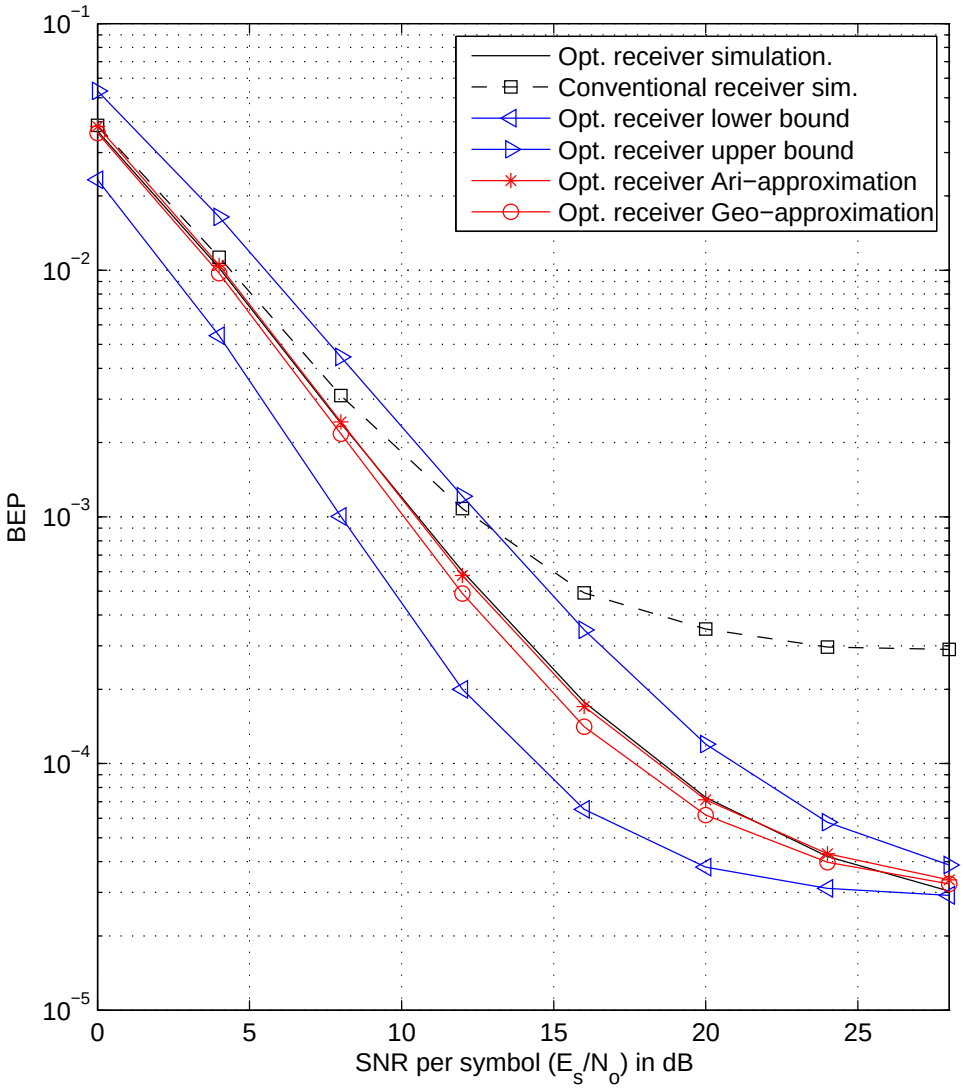

Figure 3.3: Case I: BEP results for the conventional and the optimum SBS receivers, 2Tx and 2Rx Alamouti's code with QPSK modulation, $f_d T_b$=0.06, channel variances are 0.5 and 5, respectively.

Considering case II, we plot the simulation results of the conventional SBS decoder and the proposed optimum decoder (3.25) in Figure 3.4. The block fade rate is

set to 0.1 and the variances of the the channels associated with the first and the second transmit antennas are set to (9, 1), (5, 1) and (2, 1), respectively.

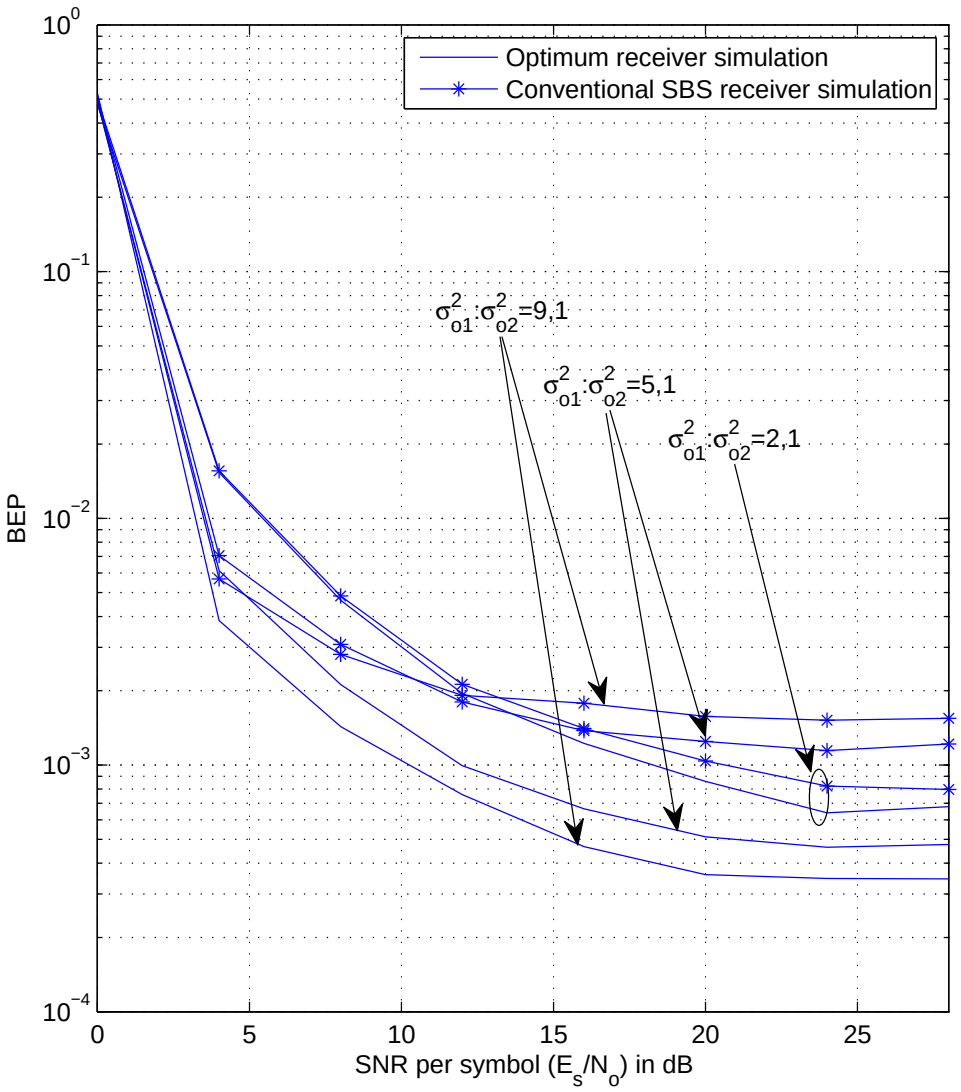

Figure 3.4: Case II: BEP results for the conventional SBS and the optimum receivers, 2Tx and 2Rx Alamouti's code with QPSK modulation, $f_d T_b$=0.1.

All the simulation results show that the optimum decoder can provide a better

performance than the conventional SBS decoder. If the difference between the channel variances is larger, the performance gain is also greater. However, since the optimum decoder has a higher decoding complexity of M^2, compared with the linear decoding complexity of M for the conventional SBS decoder, it is possible to trade off between the performance and the complexity. The simulation results show that if the ratio of the channel variances is smaller than 2 to 1, the conventional SBS decoder can be safely applied.

3.6 Conclusions

This chapter considers orthogonal STBC over non-identical channels with imperfect CSI. It is shown that the conventional SBS decoder is not optimum in this situation. Two typical cases are considered for the case of non-identical channels with channel estimation.

In the first case, where the non-identical channels are associated with one common receive antenna, the optimum decoder is derived. We show that this optimum decoder can be simplified to a SBS decoder, under the condition that the received signal and the estimated channel matrices are properly weighted. In the second case, where the non-identical channels are associated with one common transmit antenna, we also derive the optimum decoder. But it is shown that no matter how the received signals are weighted, the optimum decoder cannot be simplified to a SBS decoder.

The performance of the optimum decoder is also investigated. The upper/lower bounds and close approximations of the BEP performance are obtained for case I. Both the analytical and the simulation results show that our optimum decoder substantially outperforms the conventional SBS decoder.

Chapter 4

Space-Time Block Codes over Time-Selective Channels

Many existing works on STBC assume the channels are block-wise constant, but this assumption does not always hold. In the more general case of time-selective channels, the channel matrix is no longer orthogonal, so inter-symbol interference is generated and the performance can be greatly reduced. Several decoders have been proposed to eliminate the ISI, but it remains unclear how and to what extent the performance is affected by the ISI. In this chapter, we introduce an approach to analyze the performance of STBC over time-selective channels, with arbitrary numbers of antennas for which orthogonal STBC's are defined. Exact error performances are obtained in closed form. Furthermore, the analysis reveals the relationship between the ISI and the structure of STBC matrices. Considering $\mathcal{G}_i$ systems, we then propose one proposition and two design criteria, following which it is easy to design or search for better STBC's that have less ISI compared with the original code matrix.

4.1 Introduction

Orthogonal STBC [30] are commonly used in MIMO systems, due to the simple ML decoding structure. However, this decoding structure is based on the assumption that the channels are block-wise constant, which is not always true in practice. For a system with two transmit antennas, one STBC code block extends over two symbols and the channels can change significantly within one block in some cases [65–67] (and references therein). Systems with three or more transmit antennas are even more vulnerable to channel variations than the systems with two transmit antennas, due to the longer STBC code block [68, 69]. If the channels vary from symbol to symbol, the orthogonality will be corrupted and ISI is introduced, so the linear ML decoder [30] is no longer optimum.

Considering time-selective channels, [65–71, 94–98] proposed different decoders for orthogonal STBC. Assuming the channel variation between two adjacent symbols is negligible, [66] and [67] propose a suboptimum detection scheme, in which they treat the received signal as if the channels are quasi-static, and applied the conventional linear decoder. The suboptimum scheme retains the simple decoding structure, but has an irreducible error floor in the high SNR region. Therefore, it greatly reduces the performance of orthogonal STBC over the time-selective channels. Later, an elegant zero-forcing (ZF) decoder for two transmit antennas is presented in [65], where the ISI is completely removed and full diversity is obtained with the same decoding complexity as the conventional linear decoder for the orthogonal STBC over quasi-static channels. The ZF decoder was extended to three- and four-transmit-antenna cases in [69, 94, 95]. Besides the linear decoders above, there are also non-linear decoders, including the parallel interference cancellation (PIC) decoder [68, 69, 96], ML decoder [70, 96], successive interference cancellation (SIC)

decoder [97] and decision-feedback decoder [70, 71, 98]. Instead of designing a new decoding scheme, a modified orthogonal STBC was developed in [99]. Keeping the full diversity order and the orthogonality, the modified STBC reduces the ISI to a much lower level, compared with the original orthogonal STBC [30].

Obviously, the performance analysis of STBC's over time-selective channels differs from the conventional one where the channels are assumed quasi-static. In the existing references, however, only a few works [70, 71] obtained the exact error performance, when the special case of Alamouti's code [29] is applied. Other works either presented conditional error performance based on one channel realization, or simply obtained the error performance through simulations, especially for the STBC's with higher numbers of transmit antennas. More importantly, due to the lack of analytical results, little insight can be gained and it remains unclear how the code structures affect the performance of STBC when the channels are time-selective. In this chapter, we introduce an approach to analyze the performance of STBC's over time-selective channels, with arbitrary numbers of antennas for which orthogonal STBC's are defined. Exact error performances are obtained in closed form. Through the analysis, the relationship between the ISI and the STBC code structure is revealed. Considering $\mathcal{G}_i$ systems, one proposition and two design criteria are then introduced. Applying the criteria, it is easy to design modified code matrices which have less ISI, compared with the original code matrix. Alternatively, we can use the proposition to search for an optimum code matrix with minimized ISI.

The rest of the chapter is organized as follows. Section 4.2 describes the system model. Section 4.3 first analyzes the BEP for $\mathcal{G}_4$ systems with MPSK modulation, and then extends the approach to other modulation schemes and systems. Code design for $\mathcal{G}_i$ systems is discussed in Section 4.4. Section 4.5 provides numerical examples and a summary is given in Section 4.6.

4.2 System Model

We consider a point-to-point communication system with N_T transmit and N_R receive antennas, transmitting with orthogonal STBC. For the purpose of illustration, we first suppose the system has four transmit ($N_T = 4$) and one receive ($N_R = 1$) antenna, with a modified $\mathcal{G}_4$ encoder [30]. Transmitting four information symbols $\mathbf{s} = [s_1, s_2, s_3, s_4]^T$ in one STBC block, the original $\mathcal{G}_4$ encoder generates an 8×4 code matrix, which is given by [30]

$$\mathcal{G}_4 == \begin{bmatrix} s_1 & s_2 & s_3 & s_4 \\ -s_2 & s_1 & -s_4 & s_3 \\ -s_3 & s_4 & s_1 & -s_2 \\ -s_4 & -s_3 & s_2 & s_1 \\ s_1^* & s_2^* & s_3^* & s_4^* \\ -s_2^* & s_1^* & -s_4^* & s_3^* \\ -s_3^* & s_4^* & s_1^* & -s_2^* \\ -s_4^* & -s_3^* & s_2^* & s_1^* \end{bmatrix}. \tag{4.1}$$

However, the above code matrix generates high ISI over time-selective channels (which we will explain later), and therefore, we use a modified $\mathcal{G}_4$ encoder in this chapter. The modified encoder simply interchanges the rows of the original code

matrix, and is given by

$$\mathcal{G}_4^{op} = \begin{bmatrix} s_1 & s_2 & s_3 & s_4 \\ -s_4^* & -s_3^* & s_2^* & s_1^* \\ -s_2^* & s_1^* & -s_4^* & s_3^* \\ -s_3 & s_4 & s_1 & -s_2 \\ -s_3^* & s_4^* & s_1^* & -s_2^* \\ -s_2 & s_1 & -s_4 & s_3 \\ -s_4 & -s_3 & s_2 & s_1 \\ s_1^* & s_2^* & s_3^* & s_4^* \end{bmatrix}. \tag{4.2}$$

This modified encoder is optimum in the sense that it minimizes the ISI of the $\mathcal{G}_4$ code over time-selective channels. Further explanation will be given in Section 4.4. Defining the manipulated received signal vector as $\mathbf{r} = [r_1, r_2^*, r_3^*, r_4, r_5^*, r_6, r_7, r_8^*]^T$, the received signals can be written as

$$\mathbf{r} = \mathbf{H}\mathbf{s} + \mathbf{n} \tag{4.3}$$

where $\mathbf{n}$ is the noise vector whose elements are i.i.d., complex Gaussian random variables, each with mean zero and variance N_o. The channel matrix $\mathbf{H}$ is given by

$$\mathbf{H} = \begin{bmatrix} h_1(1) & h_2(1) & h_3(1) & h_4(1) \\ h_4^*(2) & h_3^*(2) & -h_2^*(2) & -h_1^*(2) \\ h_2^*(3) & -h_1^*(3) & h_4^*(3) & -h_3^*(3) \\ h_3(4) & -h_4(4) & -h_1(4) & h_2(4) \\ h_3^*(5) & -h_4^*(5) & -h_1^*(5) & h_2^*(5) \\ h_2(6) & -h_1(6) & h_4(6) & -h_3(6) \\ h_4(7) & h_3(7) & -h_2(7) & -h_1(7) \\ h_1^*(8) & h_2^*(8) & h_3^*(8) & h_4^*(8) \end{bmatrix}. \tag{4.4}$$

Here, we assume all the channels undergo frequency-flat, time-selective Rayleigh fading and the channel gains $\{h_i(t)\}_{i=1,t=1}^{4,\ 8}$, are identical complex Gaussian random

variables with means zero and autocorrelation function $\frac{1}{2}E[h_i(t)h_i^*(t+l)] = \sigma_h^2 R(l)$. We normalize the average power of the fading process σ_h^2 to $\frac{1}{2}$ in this chapter. According to Jakes' model [93], we have

$$R(l) = J_o(2\pi f_d T_s l), \tag{4.5}$$

where $J_o(\cdot)$ is the zeroth-order Bessel function of the first kind, f_d is the maximum Doppler shift and T_s is the period of each symbol. Here, we assume the time-selectivity is caused by Doppler shift and the frequency offset is perfectly compensated for. We also assume that the channel fading processes in different transmit-receive links are i.i.d., i.e., the autocorrelation fucntion $R(l)$ is common for all links, and for any $i \neq j$, we have $E[h_i(t)h_j^*(t)] = 0$. Finally, the knowledge of $\mathbf{H}$ and $R(l)$ are assumed to be perfectly known at the receiver end.

4.3 Performance Analysis

4.3.1 The Performance of $\mathcal{G}_4$ System

The beauty of orthogonal STBC is that the optimum decoder can be reduced to a linear decoder, and thus we can use a symbol-by-symbol (SBS) detector. If the same linear decoder is applied in the case of time-selective channels, the decision vector is formed by multiplying the received vector $\mathbf{r}$ by $\mathbf{H}^H$ to give

$$\mathbf{H}^H\mathbf{r} = \mathbf{H}^H\mathbf{H}\mathbf{s} + \mathbf{H}^H\mathbf{n}. \tag{4.6}$$

It is obvious that the off-diagonal elements of

$$\mathbf{H}^H\mathbf{H} = \begin{bmatrix} \|\mathbf{h}_1\|^2 & \beta_{12} & \beta_{13} & \beta_{14} \\ \beta_{21} & \|\mathbf{h}_2\|^2 & \beta_{23} & \beta_{24} \\ \beta_{31} & \beta_{32} & \|\mathbf{h}_3\|^2 & \beta_{34} \\ \beta_{41} & \beta_{42} & \beta_{43} & \|\mathbf{h}_4\|^2 \end{bmatrix} \tag{4.7}$$

are non-zero, i.e., $\beta_{ij} \neq 0$, $i, j = 1, \cdots, 4$. Therefore, they cause ISI. Due to symmetry, each s_i, $i = 1 \cdots 4$, has the same BEP, so we can focus on s_1 and the decision metric is given by

$$z_1 = \underbrace{\|\mathbf{h}_1\|^2 s_1}_{\text{effective signal}} + \underbrace{\beta_{12}s_2 + \beta_{13}s_3 + \beta_{14}s_4}_{\text{inter-symbol-interferences}} + \tilde{n}, \tag{4.8}$$

where $\mathbf{h}_1$ is the first column of the code matrix $\mathbf{H}$ and

$$\begin{aligned}
\beta_{12} &= (h_1^*(1)h_2(1) - h_2(3)h_1^*(3)) + (h_4(2)h_3^*(2) - h_3^*(4)h_4(4)) \\
&\quad + (-h_3(5)h_4^*(5) + h_4(7)h_3^*(7)) + (-h_2^*(6)h_1(6) + h_1(8)h_2(8)), \quad (4.9) \\
\beta_{13} &= (h_1^*(1)h_3(1) - h_3(5)h_1^*(5)) + (h_2(3)h_4^*(3) - h_4^*(7)h_2(7)) \\
&\quad + (-h_4(2)h_2^*(2) + h_2^*(6)h_4(6)) + (-h_3^*(4)h_1(4) + h_1(8)h_3^*(8)), \quad (4.10) \\
\beta_{14} &= (h_1^*(1)h_4(1) - h_4(2)h_1^*(2)) + (-h_2(3)h_3^*(3) + h_3^*(4)h_2(4)) \\
&\quad + (h_3(5)h_2^*(5) - h_2^*(6)h_3(6)) + (-h_4^*(7)h_1(7) + h_1(8)h_4^*(8)). \quad (4.11)
\end{aligned}$$

Here, $\tilde{n}$ is a complex Gaussian random variable with mean zero and variance $\|\mathbf{h}_1\|^2 N_o$.

Since the channel gains $h_i(t)$ and $h_i(t+l)$ are jointly Gaussian for any $i = 1, \cdots, 4$, conditioning on $h_i(t)$, $h_i(t+l)$ is a complex Gaussian random variable with mean $m_i(t+l)$ and variance $1 - E\left[m_i(t+l)\right]^2$ [7]. Here, the mean $m_i(t+l)$ is proportional to the channel gain $h_i(t)$, and is given by $m_i(t+l) = R(l)h_i(t)$. Therefore, conditioning on the channel gain $h_i(t)$, we have

$$h_i(t+l)|_{h_i(t)} \sim CN\left(R(l)h_i(t), 1 - |R(l)|^2\right). \tag{4.12}$$

Similarly, conditioning on the channel gain $h_i(t+l)$, $h_i(t)$ is also a complex Gaussian random variable given by

$$h_i(t)|_{h_i(t+l)} \sim CN\left(R(l)h_i(t+l), 1 - |R(l)|^2\right). \tag{4.13}$$

In (4.9)-(4.11), we have expressed each of the interference parameters $\beta_{1i},\ i = 2, 3, 4$, as the sum of four terms. Applying (4.12) and (4.13) to each of these terms, we find

that they are conditional Gaussian random variables. Therefore, conditioning on $\mathbf{h}_1$, i.e.

$$[h_1(1), h_4^*(2), h_2^*(3), h_3(4), h_3^*(5), h_2(6), h_4(7), h_1^*(8)]^T, \tag{4.14}$$

β_{1i}, $i = 2, 3, 4$, are given by

$$\beta_{12}|_{\mathbf{h}_1} \sim CN(0, \|\mathbf{h}_1\|^2(1 - |R(2)|^2)), \tag{4.15}$$

$$\beta_{13}|_{\mathbf{h}_1} \sim CN(0, \|\mathbf{h}_1\|^2(1 - |R(4)|^2)), \tag{4.16}$$

$$\beta_{14}|_{\mathbf{h}_1} \sim CN(0, \|\mathbf{h}_1\|^2(1 - |R(1)|^2)). \tag{4.17}$$

MPSK Modulations

For MPSK modulation with equal symbol probabilities, we can let $s_1 = \sqrt{E_s}$ without loss of generality. The BEP of s_1 can be computed from the probability $P_\alpha(e) = P\left(\Re[z_1 e^{-j\alpha}] < 0|_{s_1=\sqrt{E_s}}\right)$ [83], where α is an angle that depends on the modulation scheme. For BPSK modulation, the BEP is obviously given by $P_b = P_{\alpha=0}(e)$. For QPSK modulation with Gray mapping, the BEP is given by $P_b = P_{\alpha=\frac{\pi}{4}}(e)$. And for 8-PSK with Gray mapping, the BEP can be closely approximated by $P_b = P_{\alpha=\frac{3\pi}{8}}(e)\left(1 - P_{\alpha=\frac{\pi}{8}}(e)\right)$ [83].

Conditioning on $\mathbf{h}_1$, the total interference term, $\beta_{12}s_2 + \beta_{13}s_3 + \beta_{14}s_4$, is a zero-mean, complex Gaussian random variable, whose variance is independent of s_i, $i = 2, 3, 4$, as the s_i's have the same amplitude. Since $\beta_{12}s_2 + \beta_{13}s_3 + \beta_{14}s_4$ is also independent of the effective signal $\|\mathbf{h}_1\|^2 s_1$ and the noise $\tilde{n}$, we can treat the interference as additional noise. The probability $P_\alpha(e)$ conditioning on $\mathbf{h}_1$ is thus given by

$$\begin{aligned} &P_\alpha(e|\mathbf{h}_1) \\ &= \frac{1}{\pi}\int_0^{\frac{\pi}{2}} \exp\left(\frac{-E_s\|\mathbf{h}_1\|^2\cos^2\alpha}{((3 - |R(1)|^2 - |R(2)|^2 - |R(4)|^2)E_s + N_o)\sin^2\theta}\right) d\theta, \end{aligned} \tag{4.18}$$

where we use the Craig's alternative form of the Q-function [84] and cancel the common term $\|\mathbf{h}_1\|^2$ in the denominator and the numerator.

In order to take the average of the conditional BEP above, $\|\mathbf{h}_1\|^2$ can be split into two parts as

$$\begin{aligned}\|\mathbf{h}_1\|^2 &= \underbrace{|h_1(1)|^2+|h_4(2)|^2+|h_2(3)|^2+|h_3(4)|^2}_{\text{first part}} \\ &\quad + \underbrace{|h_3(5)|^2+|h_2(6)|^2+|h_4(7)|^2+|h_1(8)|^2}_{\text{second part}}. \end{aligned} \tag{4.19}$$

Conditioning on the first part, i.e. $h_1(1)$, $h_2(3)$, $h_3(4)$ and $h_4(2)$, the second part contains four complex Gaussian random variables, whose conditional means and variances can be calculated as in (4.12) and (4.13). Since these four random variables are independent of one another, we can average over them one by one with the help of Lemma 2.1, and obtain

$$\begin{aligned}&P_\alpha(e|\ h_1(1),\ h_2(3),\ h_3(4),\ h_4(2)) \\ &= \frac{1}{\pi}\int_0^{\frac{\pi}{2}} \frac{\exp\left(\frac{-\gamma|h_1(1)|^2}{\sin^2\theta} - \frac{\gamma|R(7)|^2|h_1(1)|^2}{\sin^2\theta+(1-|R(7)|^2)\gamma}\right)}{1+\frac{\gamma(1-|R(7)|^2)}{\sin^2\theta}} \frac{\exp\left(\frac{-\gamma|h_2(3)|^2}{\sin^2\theta} - \frac{\gamma|R(3)|^2|h_2(3)|^2}{\sin^2\theta+(1-|R(3)|^2)\gamma}\right)}{1+\frac{\gamma(1-|R(3)|^2)}{\sin^2\theta}} \\ &\cdot \frac{\exp\left(\frac{-\gamma|h_3(4)|^2}{\sin^2\theta} - \frac{\gamma|R(1)|^2|h_3(4)|^2}{\sin^2\theta+(1-|R(1)|^2)\gamma}\right)}{1+\frac{\gamma(1-|R(1)|^2)}{\sin^2\theta}} \frac{\exp\left(\frac{-\gamma|h_4(2)|^2}{\sin^2\theta} - \frac{\gamma|R(5)|^2|h_4(2)|^2}{\sin^2\theta+(1-|R(5)|^2)\gamma}\right)}{1+\frac{\gamma(1-|R(5)|^2)}{\sin^2\theta}} d\theta \end{aligned} \tag{4.20}$$

where we have

$$\gamma = \frac{E_s\cos^2\alpha}{(3-|R(1)|^2-|R(2)|^2-|R(4)|^2)E_s+N_o}. \tag{4.21}$$

Noting that $|h_1(1)|^2$, $|h_2(3)|^2$, $|h_3(4)|^2$ and $|h_4(2)|^2$ are independent, central chi-square distributed random variables, whose probability density functions are given by [7]

$$p_{|h_i(t)|^2}(x) = \exp\left(-\frac{x}{2\sigma_h^2}\right),\ i=1,\cdots,4, \tag{4.22}$$

we average over $|h_i(t)|^2$, $i=1,\cdots,4$, and finally obtain

$$\begin{aligned}P_\alpha(e) &= \frac{1}{\pi}\int_0^{\frac{\pi}{2}} \sum_{i=0}^{3}\left(\frac{\sin^2\theta}{\sin^2\theta+\gamma\left(1-|R(2i+1)|\right)}\right) \\ &\qquad \left(\frac{\sin^2\theta}{\sin^2\theta+\gamma\left(1+|R(2i+1)|\right)}\right) d\theta. \end{aligned} \tag{4.23}$$

Applying the result in [100, eqn. (5A.75)], the above average BEP can be integrated out, and the closed-form BEP result is given by

$$P_\alpha(e) = \frac{1}{2}\sum_{l=1}^{8}\left(1-\sqrt{\frac{c_l}{1+c_l}}\right)\prod_{n=1,n\neq l}^{8}\left(\frac{c_l}{c_l-c_n}\right) \tag{4.24}$$

where

$$c_l = \begin{cases} \gamma\left(1-|R(l)|\right), & l=1,3,5,7, \\ \gamma\left(1+|R(l-1)|\right), & l=2,4,6,8. \end{cases} \tag{4.25}$$

By setting $\theta = 0$, a simple Chernoff bound is obtained from (4.23), which is given by

$$\begin{aligned} P_a(e) &\leq \sum_{i=0}^{3}\left((1+\gamma)^2-\gamma^2|R(2i+1)|^2\right)^{-1} \\ &= \sum_{i=0}^{3}\left((1+2\gamma+(1-|R(2i+1)|^2)\gamma^2\right)^{-1}. \end{aligned} \tag{4.26}$$

Here, it is interesting to note that the order of diversity is not four, as was in the block fading channels. On one hand, the (modified) $\mathcal{G}_4$ encoder transmits the same symbol (s_i and s_i^*) twice from the same antenna in one block, and the channel varies from one symbol to another, so more degrees of diversity is produced. On the other hand, the performance degrades due to the interferences, which are also caused by the variations of the channels. Since the interferences dominate the overall performance, therefore, the order of diversity is less than four, which will be seen in the numerical examples.

Because of the ISI, an irreducible error floor is expected when SNR is high, i.e. when $E_s \gg N_o$. The analytical result of the irreducible error floor is the same as (4.24), with c_l's replaced by $\hat{c}_l$'s which are given by

$$\hat{c}_l = \begin{cases} \frac{(1-|R(l)|)\cos^2\alpha}{3-|R(1)|^2-|R(2)|^2-|R(4)|^2}, & l=1,3,5,7, \\ \frac{(1+|R(l-1)|)\cos^2\alpha}{3-|R(1)|^2-|R(2)|^2-|R(4)|^2}, & l=2,4,6,8. \end{cases} \tag{4.27}$$

If multiple antennas are applied in the receiver, the performance analysis can be easily carried out in the same way. Since the channel gains of different links are

independent of one another, we can similarly integrate over the channel gains as in (4.20), resulting in more exponential terms. Therefore, the increased number of receive antennas increases the order of diversity.

PAM and MQAM Modulations

For PAM and MQAM modulations, the transmitted symbols have different amplitudes, so the variance of the interference term, $\beta_{12}s_2 + \beta_{13}s_3 + \beta_{14}s_4$, is dependent on the transmitted symbols. The performance analysis of these modulation schemes is similar to the one we introduced for MPSK modulation, except that the BEP is now to be averaged over all the possible combinations of the transmitted symbols.

Considering rectangular MQAM with the Gray mapping of bits, for example, the BEP conditioning on $\mathbf{h}_1$ and $\mathbf{s}$ can be closely approximated by [101, eqn. 18]

$$P(e|\mathbf{h}_1,\ \mathbf{s}) \approx \frac{4}{\log_2 M}\left(1-\frac{1}{\sqrt{M}}\right)\sum_{i=1}^{\sqrt{M}/2} Q\left((2i-1)\sqrt{\frac{3E_b\|\mathbf{h}_1\|^2\log_2 M}{(M-1)(\zeta+N_o)}}\right), \quad (4.28)$$

where $\zeta = (1-|R(2)|^2)|s_2|^2 + (1-|R(4)|^2)|s_3|^2 + (1-|R(1)|^2)|s_4|^2$ is the variance of the interference $\beta_{12}s_2 + \beta_{13}s_3 + \beta_{14}s_4$, depending on the value of $s_i,\ i = 2,3,4$, and $E_b = E_s/\log_2 M$ is the transmit energy per bit. Averaging over $\mathbf{h}_1$ and $\mathbf{s}$, the exact BEP can be expressed as

$$\begin{aligned} P(e) \ \approx\ & \frac{4}{\log_2 M}\left(1-\frac{1}{\sqrt{M}}\right) \\ & \sum_{l\in\phi} p_l \sum_{i=1}^{\sqrt{M}/2} E\left[Q\left((2i-1)\sqrt{\frac{3E_b\|\mathbf{h}_1\|^2\log_2 M}{(M-1)(\zeta_l+N_o)}}\right)\right], \end{aligned} \quad (4.29)$$

where ζ_l is one possible value of the variance belonging to the set of all possible combinations ϕ, and p_l is the probability that the variance takes on the value ζ_l. It it easy to see that the expectation of the Q-functions over the channel gains can be

similarly evaluated as in (4.18)-(4.24), giving

$$P(e) \approx \frac{2}{\log_2 M}\left(1-\frac{1}{\sqrt{M}}\right) \sum_{l\in\phi} p_l \sum_{i=1}^{\sqrt{M}/2}\sum_{t=1}^{8}\left(1-\sqrt{\frac{c_{li}^t}{1+c_{li}^t}}\right)\prod_{n=1,n\neq t}^{8}\left(\frac{c_{li}^t}{c_{li}^t-c_{li}^n}\right), \quad (4.30)$$

where

$$c_{li}^t = \begin{cases} \gamma_{li}\left(1-|R(t)|\right), & t=1,3,5,7 \\ \gamma_{li}\left(1+|R(t-1)|\right), & t=2,4,6,8 \end{cases} \quad (4.31)$$

and

$$\gamma_{li} = \frac{3(2i-1)^2 E_b \log_2 M}{(M-1)(\zeta_l+N_o)}. \quad (4.32)$$

4.3.2 Extension to Other Systems

$\mathcal{G}_3$ system

By setting $h_4(t)$ and $h_4^*(t)$ to zero, for $t = 1,\cdots 8$, in (4.4) and all other related equations, we can similarly derive the BEP performance of s_i, $i = 1,\cdots,4$, in a $\mathcal{G}_3$ system. Since the positions of $h_4(t)$ and $h_4^*(t)$ are different in the four columns of **H**, the BEP results $P_\alpha^i(e)$ of the different symbols $s_i's$ are, therefore, different, so the overall BEP is given by

$$P_\alpha(e) = \frac{1}{4}\sum_{i=1}^{4} P_\alpha^i(e). \quad (4.33)$$

Here, each $P_\alpha^i(e)$ has a similar expression to the one of the $\mathcal{G}_4$ system. The only difference between $P_\alpha^i(e)$ and the BEP in (4.24) is the order of diversity.

$\mathcal{G}_2$ system

If Alamouti's code [29] is used with two transmit antennas, the received signal is given by

$$\begin{bmatrix} r_1 \\ r_2^* \end{bmatrix} = \mathbf{H} \begin{bmatrix} s_1 \\ s_2 \end{bmatrix} + \begin{bmatrix} n_1 \\ n_2^* \end{bmatrix}, \tag{4.34}$$

where the channel matrix is now defined as

$$\mathbf{H} = \begin{bmatrix} h_1(1) & h_2(1) \\ h_2^*(2) & -h_1^*(2) \end{bmatrix}. \tag{4.35}$$

Following the same procedure as given from (4.6) to (4.18), we first obtain the conditional probability for MPSK modulation as

$$P(\alpha)|_{\mathbf{h}_1} = \frac{1}{2}\text{erfc}\left(\sqrt{\frac{E_s\|\mathbf{h}_1\|^2\cos^2\alpha}{(1-|R(1)|^2)E_s+N_o}}\right). \tag{4.36}$$

The result in (4.36) is similar to the one in [66, eqn. (14)]. However, [66] applies an approximation technique by neglecting some fourth order terms, whereas our result here is an exact expression. Since there is only one interference term, $(1-|R(1)|^2)E_s$, in (4.36), the exact average BEP can be obtained for BPSK and QPSK in simple closed form, which is given by

$$P_\alpha(e) = \frac{1}{2} - \frac{1}{2}\sqrt{\frac{E_s\cos^2\alpha}{((1-|R(1)|^2)\,E_s+N_o)\pi}}\cdot\sum_{i=0}^{1}\frac{\Gamma[(2i+1)/2]}{\left(1+\frac{E_s\cos^2\alpha}{(1-|R(1)|^2)E_s+N_o}\right)^{\frac{2i+1}{2}}}. \tag{4.37}$$

Assuming $E_s \gg N_o$, there also exists an irreducible error floor, which is given by

$$P_\alpha^{irr}(e) = \frac{1}{2} - \frac{1}{2}\sqrt{\frac{\cos^2\alpha}{(1-|R(1)|^2)\pi}}\sum_{i=0}^{1}\frac{\Gamma[(2k+1)/2]}{\left(1+\frac{\cos^2\alpha}{(1-|R(1)|^2)}\right)^{\frac{2i+1}{2}}}. \tag{4.38}$$

$\mathcal{H}_i$ Systems

Besides the generalized $\mathcal{G}_i$ design, there is another important generalized design for complex orthogonal STBC, the $\mathcal{H}_i$ design [30, eqn (39-40)]. In order to analyze the

performance of $\mathcal{H}_i$ systems over time-selective channels, the key step is to find the corresponding channel matrix for the manipulated received signals [69, eqn. (3)]. Unlike the channel matrix (4.4) for the $\mathcal{G}_4$ system, it is not straightforward to obtain the channel matrix for $\mathcal{H}_i$ systems, since both s_i and s_i^* appear in the same row of the code matrix. Therefore, the transmitted symbols need to be treated in real and imaginary parts, separately. Consequently, the corresponding channel matrices are also obtained for the real and imaginary parts of the transmitted symbols [69, eqn (4a-4f)]. Having obtained these channel matrices, the performance of $\mathcal{H}_i$ systems can be analyzed with a similar method used for $\mathcal{G}_i$ systems. However, since $\mathcal{H}_i$ code matrices contain more than one information symbol in one entry, so the code structure is more involved and the analysis method is not a direct extension from the one for $\mathcal{G}_i$ systems. Therefore, we are not going to cover the performance analysis for $\mathcal{H}_i$ systems in this chapter.

4.4 Modified orthogonal STBC with Minimized ISI

As mentioned in Section 4.2, the original code matrix (4.1) introduces high ISI. It is important to reduce the ISI, while keeping the orthogonality of the code matrix. One simple but effective method is by changing the positions of the rows in the code matrix [99]. However, the question of how to obtain an optimum code matrix, in the sense that the ISI is minimized is not addressed in [99], where only an intuitive 'every-other-line' scheme is introduced.

One way to find the optimum code is to simulate the performances of all the code matrices, which is difficult, if not impossible. Alternatively, we can evaluate the performance of each code matrix, using the method presented in the previous section. This method is still too complex, since it requires some derivations by hand. For example, there are $16!$ possible code matrices for a $\mathcal{G}_8$ system. Even though we can

reduce this number due to some symmetric equivalent matrices, the derivation burden is still prohibitive. Therefore, it is necessary to investigate the relationship between ISI and the structure of the code matrices, so as to enable the computer search, or simplify the design of the code with better performance. In this chapter, we will focus on the $\mathcal{G}_i$ codes, as they are systematically designed and have similar structures. Since $\mathcal{H}_i$ systems have different and more involved code structures, the issue of code design for $\mathcal{H}_i$ systems over time-selective channels will be covered in future research.

As an illustration, we still use the $\mathcal{G}_4$ code here, but the results obtained can be applied to other $\mathcal{G}_i$ systems, as will be shown later. We first rewrite the original code matrix (4.1) in the form of row vectors, which is given as

$$\mathcal{G}_4 = [\mathbf{s}_1^T, \cdots, \mathbf{s}_4^T, \mathbf{s}_1^H, \cdots, \mathbf{s}_4^H]^T, \tag{4.39}$$

and the corresponding channel matrix is given by

$$\mathbf{H}_o = [\mathbf{h}_1^T(1), \cdots, \mathbf{h}_4^T(4), \mathbf{h}_1^H(5), \cdots, \mathbf{h}_4^H(8)]^T \tag{4.40}$$

where $\mathbf{s}_i^{(*)}$ and $\mathbf{h}_i^{(*)}(t)$ are 1×4 row vectors, and t is the symbol time slot which also can be viewed as the row number of each $\mathbf{h}_i^{(*)}(t)$.

Lemma 4.1. *The sequence of rows in the channel matrix is the same as the one in the code matrix. When we interchange the positions of two rows in the code matrix, the channel matrix changes accordingly.*

Proof. This can be easily seen through the construction of the channel matrix. As an example, the modified code matrix (4.2) we used in the last section can be written as

$$\mathcal{G}_4^{op} = [\mathbf{s}_1^T, \mathbf{s}_4^H, \mathbf{s}_2^H, \mathbf{s}_3^T, \mathbf{s}_3^H, \mathbf{s}_2^T, \mathbf{s}_4^T, \mathbf{s}_1^H]^T, \tag{4.41}$$

while the corresponding channel matrix (4.4) can be rewritten as

$$\mathbf{H} = [\mathbf{h}_1^T(1), \mathbf{h}_4^H(2), \mathbf{h}_2^H(3), \mathbf{h}_3^T(4), \mathbf{h}_3^H(5), \mathbf{h}_2^T(6), \mathbf{h}_4^T(7), \mathbf{h}_1^H(8)]^T. \tag{4.42}$$

Notice that the row vector $\mathbf{h}_i^{(*)}(t)$ here is different from the column vector defined in (4.14). □

For the SBS decoder, since each s_i is decoded independently with similar interferences, we can take s_1 as an example without loss of generality. From (4.6) and (4.8), it can be seen that the effective signal $\|\mathbf{h}_1\|^2 s_1$ and noise $\tilde{n}$ are independent of the row positions in the code matrices. Therefore, no matter how we change the row positions, only the ISI terms will be affected.

For a $\mathcal{G}_4$ system, there are twenty four interference terms (as can be seen from (4.9) to (4.11)), since each row of the channel matrix generates three interference terms from s_2, s_3 and s_4, respectively. For example, the first row of channel matrix **H** in (4.42) is given by

$$\mathbf{h}_1(1) = [h_1(1), h_2(1), h_3(1), h_4(1)] \tag{4.43}$$

and the interferences generated are $h_1^*(1)h_2(1)s_2$, $h_1^*(1)h_3(1)s_3$ and $h_1^*(1)h_4(1)s_4$, respectively. Similar to what we did in (4.9) to (4.11), we can group these twenty four terms into twelve pairs, each of which is a conditional Gaussian random variable. For the same example above, we find three more terms from the rows $\mathbf{h}_2^*(3)$, $\mathbf{h}_3^*(5)$ and $\mathbf{h}_4^*(2)$, and we group them with three terms from the first row, which are given by

$$\left(h_1^*(1)h_2(1) - h_2(3)h_1^*(3)\right) s_2, \tag{4.44}$$

$$\left(h_1^*(1)h_3(1) - h_3(5)h_1^*(5)\right) s_3, \tag{4.45}$$

$$\left(h_1^*(1)h_4(1) - h_4(2)h_1^*(2)\right) s_4, \tag{4.46}$$

respectively. Conditioning on $\mathbf{h}_1$ in (4.14), it is easy to see that these interference terms

are complex Gaussian random variables with means zero and variances

$$(|h_1(1)|^2 + |h_2(3)|^2)(1 - |R(2)|^2)E_s, \tag{4.47}$$

$$(|h_1(1)|^2 + |h_3(5)|^2)(1 - |R(4)|^2)E_s, \tag{4.48}$$

$$(|h_1(1)|^2 + |h_4(2)|^2)(1 - |R(1)|^2)E_s, \tag{4.49}$$

respectively. Since the variances of the channel gains are normalized to 1, the mean values of these ISI's are obtained as $2(1 - |R(1)|^2)E_s$, $2(1 - |R(4)|^2)E_s$ and $2(1 - |R(4)|^2)E_s$, respectively. Notice that these values *depend on and only on* the difference of row numbers between $\mathbf{h}_1(1)$ and each of $\mathbf{h}_2^*(3)$, $\mathbf{h}_3^*(5)$ and $\mathbf{h}_4^*(2)$. The same observation can be made for the rest of the interference terms. Following the discussion above and applying Lemma 4.1, we have Proposition 4.1 below:

Proposition 4.1. *The mean ISI is minimized by minimizing*

$$I = \sum_{i=1}^{P} \sum_{j=1, j\neq i}^{P} \left(1 - \left|R(D[\boldsymbol{s}_i, \boldsymbol{s}_j^*])\right|^2\right) \tag{4.50}$$

where $2P$ is the number of rows and $D[\boldsymbol{s}_i, \boldsymbol{s}_j^*]$ is the distance between rows $\boldsymbol{s}_i$ and $\boldsymbol{s}_j^*$, given by the difference of their row numbers.

Proposition I can be applied to any $\mathcal{G}_i$ system. Now, the design of the modified code matrix is simplified to a $2P$-rows and $2P$-positions problem, i.e., how to arrange $2P$ rows in $2P$ positions in order to minimize the value of I in Proposition 4.1. A computer search can be easily applied to find the optimum code. For the $\mathcal{G}_4$ system, the optimum code matrix we found has been given in (4.2) and (4.41). For a $\mathcal{G}_8$ system, similarly, if we rewrite the original code given by [30] as

$$\mathcal{G}_8 = [\mathbf{s}_1^T, \mathbf{s}_2^T, \mathbf{s}_3^T, \mathbf{s}_4^T, \mathbf{s}_5^T, \mathbf{s}_6^T, \mathbf{s}_7^T, \mathbf{s}_8^T, \mathbf{s}_1^H, \mathbf{s}_2^H, \mathbf{s}_3^H, \mathbf{s}_4^H, \mathbf{s}_5^T, \mathbf{s}_6^H, \mathbf{s}_7^H, \mathbf{s}_8^H]^T, \tag{4.51}$$

the optimum $\mathcal{G}_8$ code we found is given by

$$\mathcal{G}_8^{op} = [\mathbf{s}_1^T, \mathbf{s}_4^H, \mathbf{s}_6^H, \mathbf{s}_7^T, \mathbf{s}_5^H, \mathbf{s}_2^T, \mathbf{s}_3^T, \mathbf{s}_8^T, \mathbf{s}_8^H, \mathbf{s}_3^H, \mathbf{s}_2^H, \mathbf{s}_5^T, \mathbf{s}_7^H, \mathbf{s}_6^T, \mathbf{s}_4^T, \mathbf{s}_1^H]^T. \tag{4.52}$$

As mentioned above, the number of possible code matrices is proportional to $(2N_T)!$. Although the calculation of I in Proposition 4.1 is easy, it is still time consuming to implement an exhaustive search, when the number of transmit antennas is large. From Proposition I, we can observe that only the distance between conjugate rows and non-conjugate rows with different subscripts will affect the ISI, therefore, we propose below two design criteria for the modified code matrix.

Criterion 4.1. *Conjugate rows and non-conjugate rows should be adjacent to one another.*

Criterion 4.2. *Based on criterion I, the rows with the same subscript should be put as far apart as possible.*

Using these two criteria, we can easily design code matrices by hand. In Figure 4.1, we show how to systematically design a $\mathcal{G}_4$ code. The design procedure starts from $\mathbf{s}_1$ and $\mathbf{s}_1^*$. In each of the steps, we put two rows with the same subscript into current vacancies, according to the criteria above. After completing all the rows, the hand-designed $\mathcal{G}_4$ code matrix is given by

$$\mathcal{G}_4^h = [\mathbf{s}_1^T, \mathbf{s}_2^H, \mathbf{s}_3^T, \mathbf{s}_4^H, \mathbf{s}_4^T, \mathbf{s}_3^H, \mathbf{s}_2^T, \mathbf{s}_1^H]^T. \tag{4.53}$$

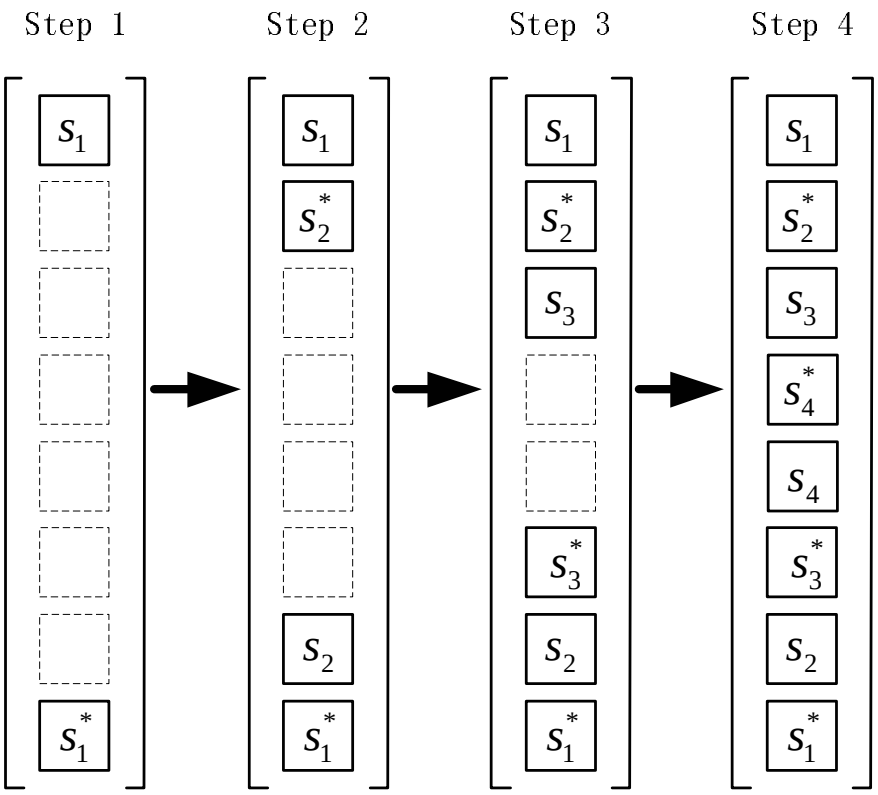

Figure 4.1: Systematical design of $\mathcal{G}_4$ code.

Following the same steps, a hand-designed $\mathcal{G}_8$ code is given by

$$\mathcal{G}_8^h = [\mathbf{s}_1^T, \mathbf{s}_2^H, \mathbf{s}_3^T, \mathbf{s}_4^H, \mathbf{s}_5^T, \mathbf{s}_6^H, \mathbf{s}_7^T, \mathbf{s}_8^H, \mathbf{s}_8^T, \mathbf{s}_7^H, \mathbf{s}_6^T, \mathbf{s}_5^H, \mathbf{s}_4^T, \mathbf{s}_3^H, \mathbf{s}_2^T, \mathbf{s}_1^H]^T. \tag{4.54}$$

As we can see, the design of the code matrix is straightforward. In the next section, we will show that the performances of these hand-designed code matrices are close to optimum.

Notice that although we analyze the ISI with the conventional linear decoder, ISI is independent of the decoding structure. All the other decoders can only mitigate the effect of ISI, but not change the amount of ISI generated. Therefore, with reduced ISI, the modified code matrix not only improves the performance of the conventional linear decoder, but also benefits the PIC, SIC, decision-feedback and other decoders in

existing works.

4.5 Numerical Examples and Discussion

In the numerical examples, we use conventional linear decoders with both BPSK and 16QAM modulations. In order to compare the performances of different systems, we normalize the SNR by the code rate, the number of transmit antennas and the order of modulation, such that the SNR per information bit, E/N_o, is the same. For example, we have the transmit SNR's $E_s/N_o = E/2N_o$, $E_s/N_o = E/6N_o$ and $E_s/N_o = E/8N_o$ for the $\mathcal{G}_2$, $\mathcal{G}_3$ and $\mathcal{G}_4$ systems, respectively, with BPSK modulation, and $E_s/N_o = E/2N_o$ for the $\mathcal{G}_4$ system with 16QAM.

In Figures 4.2-4.4, we compare the analytical BEP results with the simulation results for the optimum $\mathcal{G}_4$ system with BPSK modulation, the optimum $\mathcal{G}_4$ system with 16QAM modulation and the $\mathcal{G}_2$ system with BPSK modulation. The normalized channel fade rate f_dT_s is set to 0.02 0.03 and 0.04, respectively. The analytical results of irreducible error floors are also plotted in these three figures.

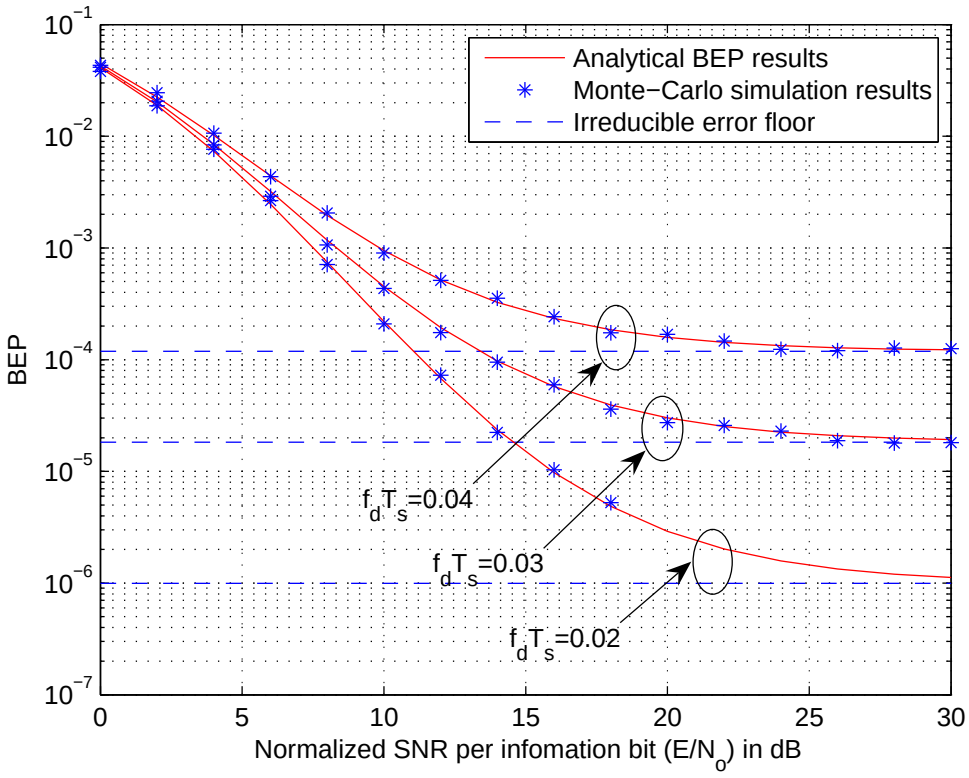

Figure 4.2: The analytical and simulation results for the BEP of the optimum $\mathcal{G}_4$ code matrix against SNR with different channel fade rates and BPSK modulation.

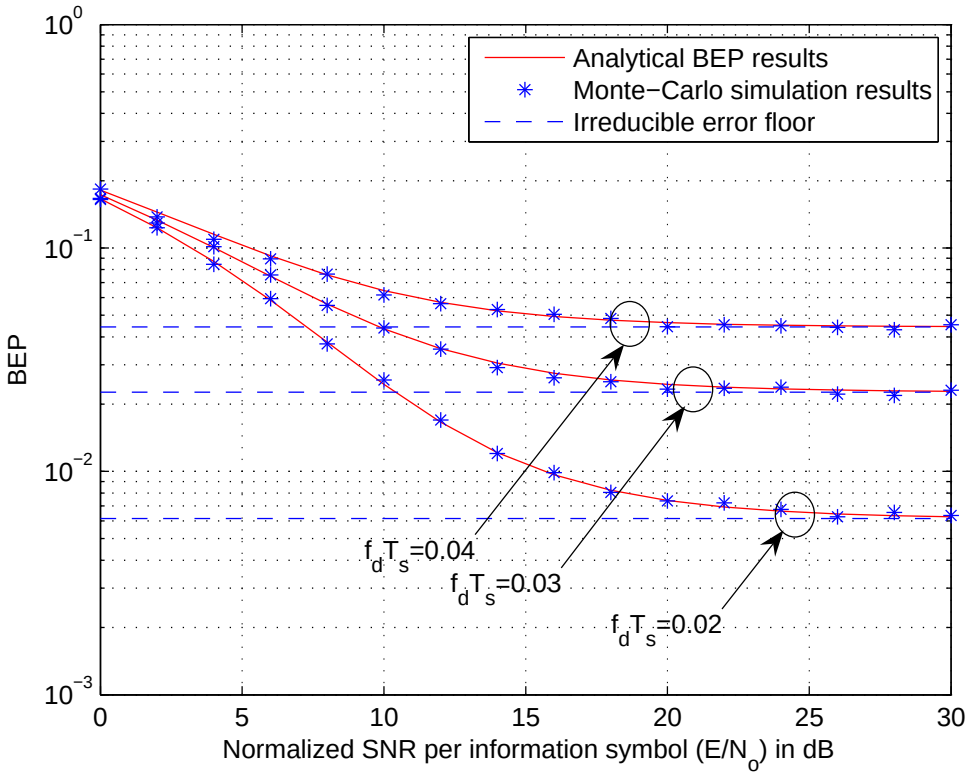

Figure 4.3: The analytical and simulation results for the BEP of the optimum $\mathcal{G}_4$ code matrix against SNR with different channel fade rates and 16QAM modulation.

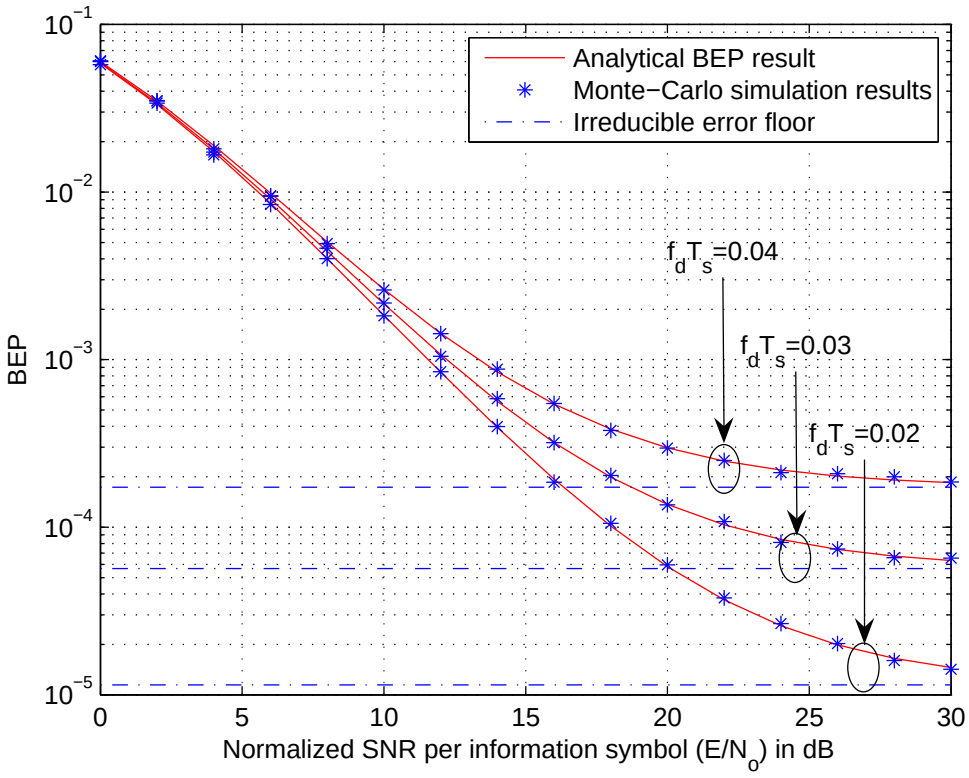

Figure 4.4: The analytical and simulation results for the BEP of $\mathcal{G}_2$ system against SNR with different channel fade rates and BPSK modulation.

As shown in Figures 4.2-4.4, our analytical results agree well with the simulations for both $\mathcal{G}_4$ and $\mathcal{G}_2$ systems, with different modulations and channel fade rates. It also shows that the channel fade rate has a significant effect on the BEP, such that a higher fade rate results in a smaller diversity order and a larger error floor. Comparing Figures 4.2 and 4.3, we can see that the channel fade rate has a greater impact on the system with a higher order of modulation.

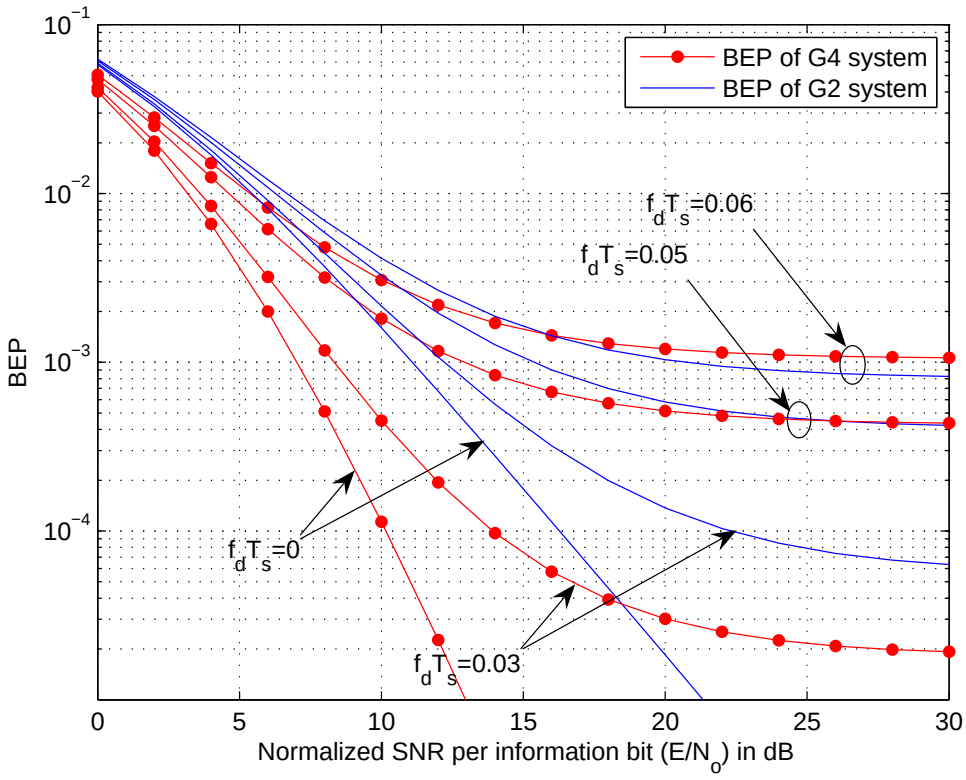

Figure 4.5: BEP comparison of $\mathcal{G}_2$ and the optimum $\mathcal{G}_4$ systems with BPSK modulation.

As we can see from (4.24) and (4.37), the $\mathcal{G}_4$ system generates more ISI than the $\mathcal{G}_2$ system. Therefore, it is obvious that the $\mathcal{G}_4$ system is more sensitive to the channel fade rate. In Figure 4.5, we compare the performances of the two systems with different channel fade rates. When the channel is quasi-static, i.e., $f_dT_s = 0$, the diversity orders of the two systems are four and two, respectively. However, as the channel fade rate increases, the $\mathcal{G}_4$ system loses its transmit diversity advantage faster than the $\mathcal{G}_2$ system. It is interesting to see that the performance of the $\mathcal{G}_4$ system becomes worse than that of the $\mathcal{G}_2$ system in the high SNR region, when the fade rate is greater than 0.05.

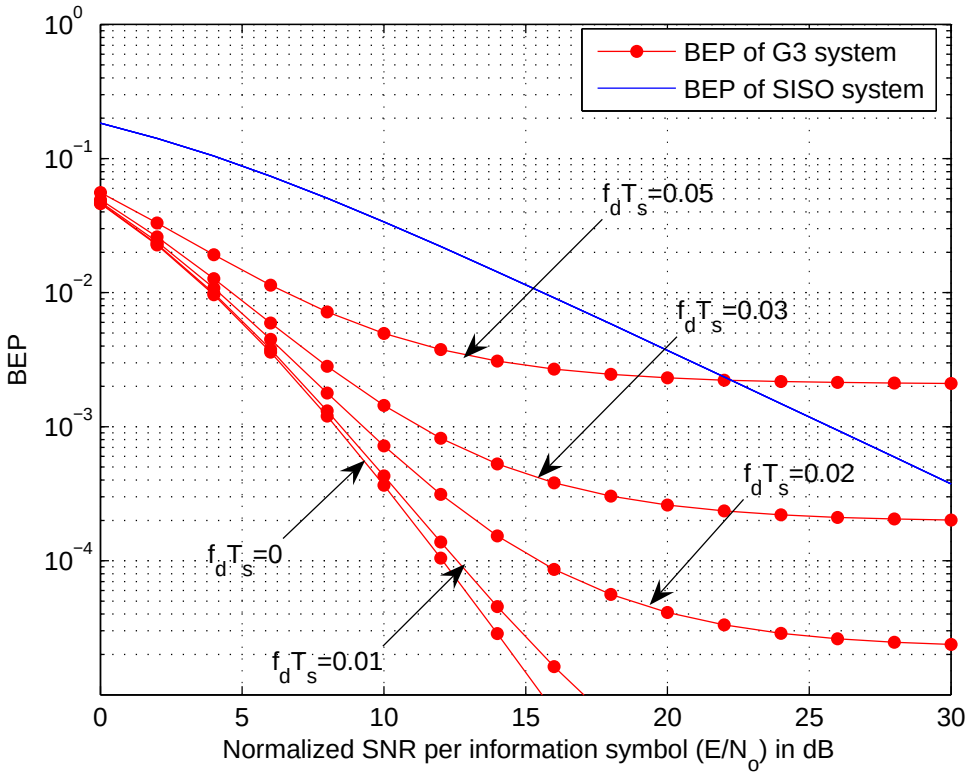

Figure 4.6: BEP comparison of the optimum $\mathcal{G}_3$ and SISO systems with BPSK modulation.

In Figure 4.6, we compare the BEP of the optimum $\mathcal{G}_3$ system (4.33) with that of a SISO system. As the channel fade rate increases, the $\mathcal{G}_3$ system also loses more and more of its transmit diversity advantage. Therefore, in time selective channels, it is not always beneficial to have a large number of transmit antennas.

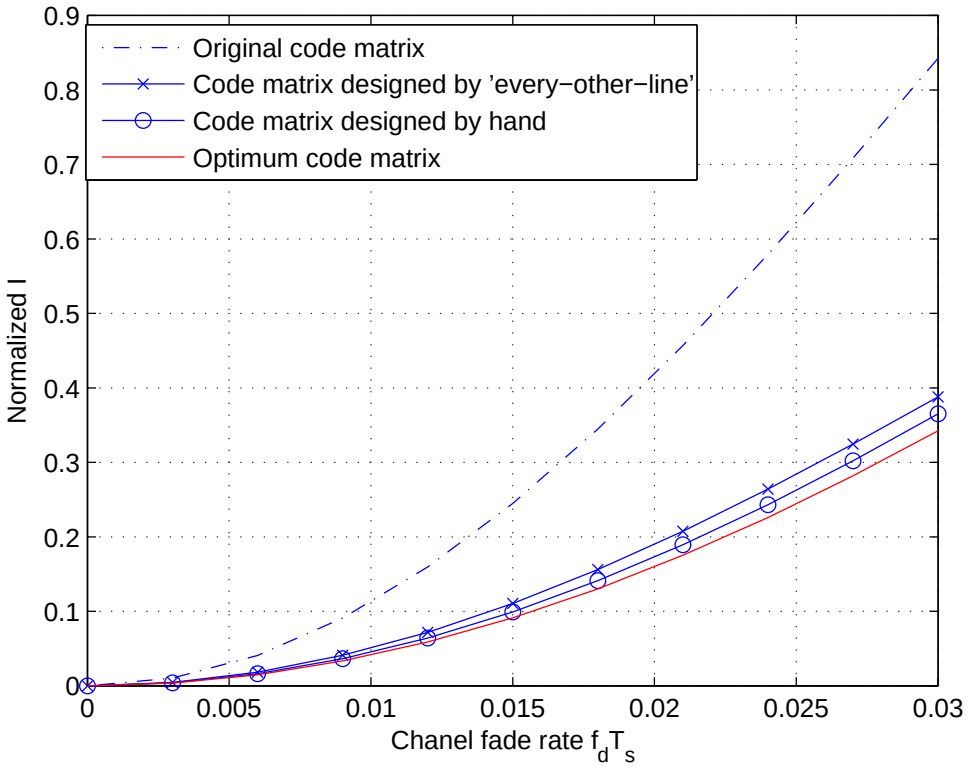

Figure 4.7: The normalized ISI of original $\mathcal{G}_4$ code matrix (4.39), hand-designed code matrix (4.53) and the optimum code matrix (4.41), compared with that of 'every-other-line' code matrix

In Figure 4.7, we compare the normalized ISI of the original $\mathcal{G}_4$ code matrix (4.39), the hand-designed code matrix (4.53) and the optimum code matrix (4.41). As a reference, we also compare with the ISI of the $\mathcal{G}_4$ code designed by the 'every-other-line' scheme, which is given by [99]

$$\mathcal{G}_4^r = [\mathbf{s}_1^T, \mathbf{s}_2^H, \mathbf{s}_3^T, \mathbf{s}_4^H, \mathbf{s}_1^H, \mathbf{s}_2^T, \mathbf{s}_3^H, \mathbf{s}_4^T]^T. \tag{4.55}$$

As shown in Figure 4.7, the original code matrix has a much larger ISI compared with the other three. The optimum code matrix has the smallest ISI, and the hand-designed

code matrix has a near-optimum ISI level. Both our hand-designed and our optimum code matrices perform better than the one from [99].

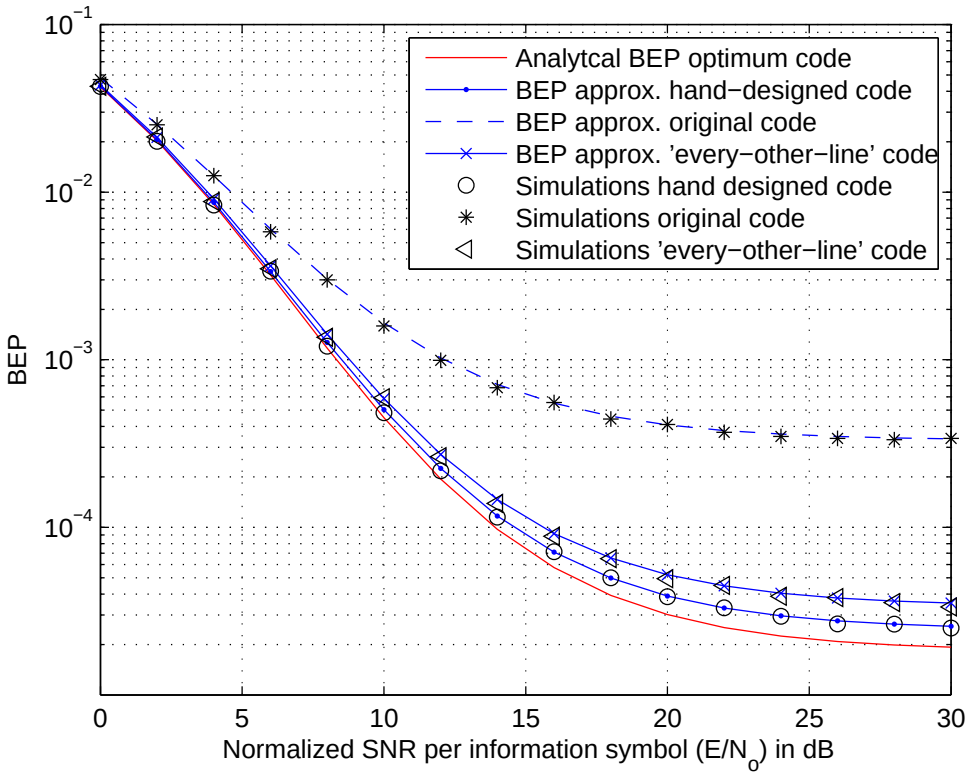

Figure 4.8: The BEP of original $\mathcal{G}_4$ code matrix (4.39), hand-designed code matrix (4.53) and the optimum code matrix (4.41), compared with that of 'every-other-line' code matrix, for $f_d T_s = 0.03$ and BPSK modulation.

In order to further show the effects of reduced ISI of the modified code matrices, we plot the BEP of the optimum code matrix (4.41), the hand-designed code matrix (4.53), the original $\mathcal{G}_4$ code matrix (4.39) and the code matrix from [99] in Figure 4.8. Here, we use the same method to approximate the performances of the latter three code matrices, as introduced in Section 4.3.1 (see also Appendix B). It can be seen that our approximations to the BEP are very close to the simulation results. Figure 4.8 also

shows that the code matrix with less ISI has a better BEP performance.

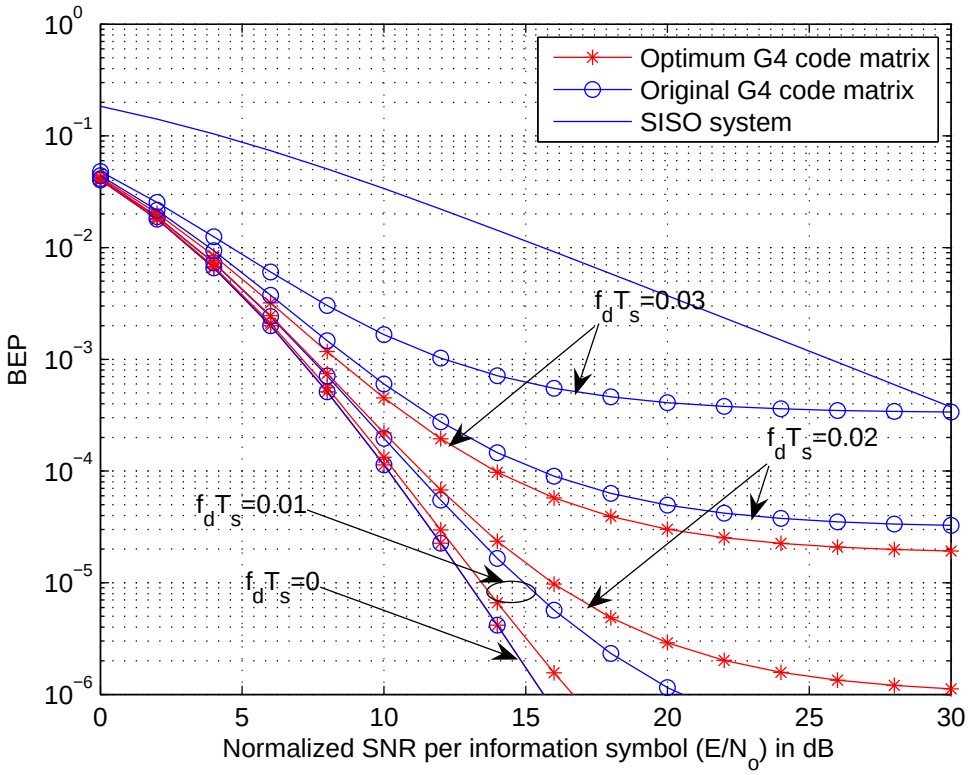

Figure 4.9: BEP comparison of the optimum $\mathcal{G}_4$ code matrix (4.41), the original $\mathcal{G}_4$ code matrix (4.39) and SISO system with BPSK modulation

In Figure 4.9, we compare the BEP's of the optimum $\mathcal{G}_4$ code matrix and the original $\mathcal{G}_4$ code matrix, with different values of the channel fade rate. The BEP of the SISO system is also plotted as a reference. As expected, the performances of the two code matrices are identical to each other when the channel is static, i.e., $f_d T_s = 0$, since there is no ISI introduced in this case. However, if the channel fade rate becomes larger, the performance of the original code matrix degrades much faster than that of the optimum code matrix. And both code matrices lose their transmit diversity advantage compared to the SISO system as fade rate increases.

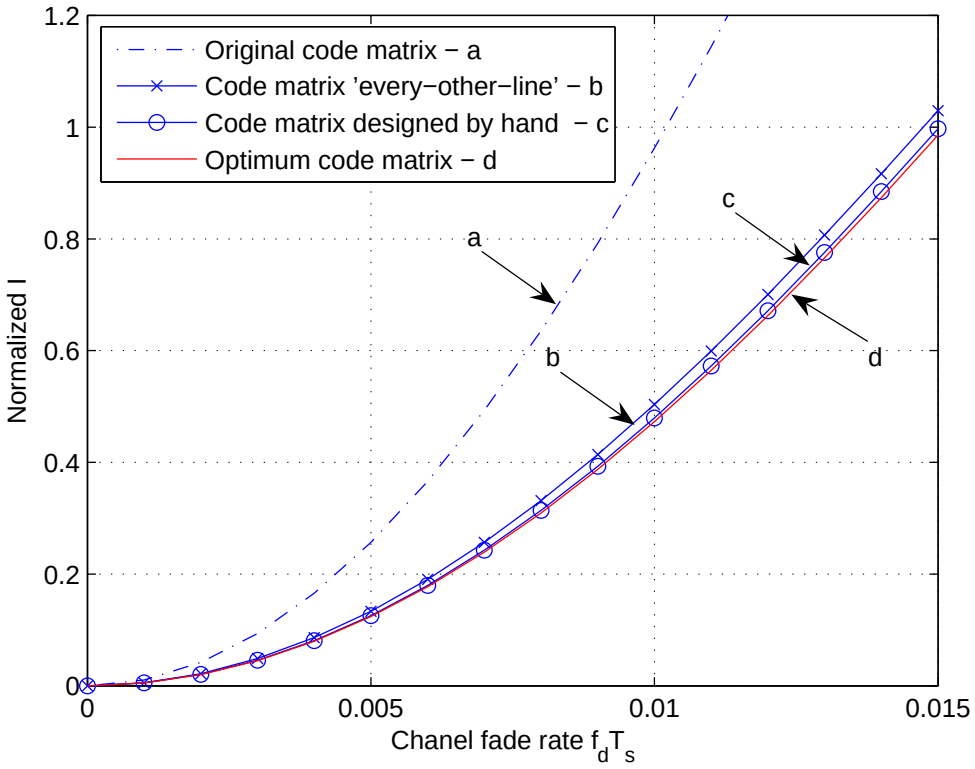

Figure 4.10: The normalized ISI of original $\mathcal{G}_8$ code matrix (4.51), hand-designed code matrix (4.54) and the optimum code matrix (4.52), compared with that of 'every-other-line' code matrix.

In Figure 4.10, we compare the normalized ISI of the modified $\mathcal{G}_8$ code matrices. Here, the one designed by 'every-other-line' scheme is given by [99]

$$\mathcal{G}_8^r = [\mathbf{s}_1^T, \mathbf{s}_2^H, \mathbf{s}_3^T, \mathbf{s}_4^H, \mathbf{s}_5^T, \mathbf{s}_6^H, \mathbf{s}_7^T, \mathbf{s}_8^H, \mathbf{s}_1^H, \mathbf{s}_2^T, \mathbf{s}_3^H, \mathbf{s}_4^T, \mathbf{s}_5^H, \mathbf{s}_6^T, \mathbf{s}_7^H, \mathbf{s}_8^T]^T. \tag{4.56}$$

Similar phenomena can be observed as in Figure 4.7.

Finally, we would like to mention that the decoders for the optimum and the hand-designed code matrices remain the same as the one for the original code matrix, therefore, no extra costs are incurred by using these code matrices.

4.6 Conclusions

We have derived the bit error performance of orthogonal STBC's over time-selective Rayleigh channels with the conventional linear decoder. The exact average BEP results are derived for the $\mathcal{G}_4$, $\mathcal{G}_3$ and $\mathcal{G}_2$ systems in closed form. The analysis of the irreducible error floors is also provided. With the exact BEP result, we can easily compare the performances of different systems. Interesting observations show that the diversity advantage of STBC reduces when the channel fade rate increases, and systems with larger numbers of transmit antennas suffer more performance degradations than the ones with fewer antennas. Therefore, it is important to note that it is not always beneficial to have a large number of transit antennas in real environments. The performance analysis method can be applied to other systems, e.g. $\mathcal{H}_i$ systems, for which orthogonal STBC's are defined.

In the second part of the chapter, we examined the relationship between the ISI and the row positions of the STBC code matrix. In order to minimize the ISI, we have proposed one proposition and two design criteria. Following the criteria, it is easy to design near-optimum code matrices, which have less ISI compared with the original code matrices. Applying the proposition, we also can easily search for an optimum modified code matrix. Finally, numerical examples are provided to verify our results.

Chapter 5

Space-Time Block Codes over Relay Channels

Cooperative STBC is a distributed way to exploit spatial diversity. Because of its simplicity, the amplify-and-forward (AF) strategy is often used at relays. However, the exact performance of this strategy is not available in the existing works. Therefore, in the first part of this chapter, we will analyze the performance of cooperative STBC with the AF strategy. Exact BEP results are derived in closed form for three existing protocols.

Since the AF strategy simply forwards the signals at the relays, the noise at the relay is also forwarded to the destination, and it degrades the received signals from both the relay and the source, due to the receiver structure of STBC. In the second part of this chapter, we examine the effect of the forwarded noise and propose a condition under which the relay should stop forwarding the signals. Based on this condition, adaptive forwarding schemes for cooperative STBC are proposed. The performances of these schemes are studied and the exact BEP's are also obtained in closed form. Finally, the energy efficiencies of these adaptive schemes are discussed.

5.1 Introduction

The MIMO technique is a well known way to exploit spatial diversity and mitigate the fading problem in wireless communication. However, it is sometimes difficult to install multiple antennas in one mobile communication node, due to its limited size. In such scenarios, we can exploit spatial diversity through the cooperation of neighboring nodes [72–74]. Therefore, the information can be cooperatively transmitted by several single antenna users, e.g. [53, 102–104], by creating a "virtual array" of antennas.

If the space-time coding technique is applied with the virtual array, the space-time codes can be viewed as being transmitted over relay channels. More specifically, the transmission is completed in two phases. In the first phase, the source node sends information to relay nodes, and in the second phase, the relay nodes and the source node transmit together using STC. The relay nodes can either amplify and forward, or decode and forward the received signal. The DF strategy can provide a better performance [105] compared with the AF strategy, but it has a higher complexity in decoding the signals. Therefore, the simpler AF strategy is also an attractive choice.

The performance of cooperative STC has been studied in many works. For example, [57, 58, 106] have studied the performance of cooperative STC with DF strategy. At the same time, many works, e.g. [59, 75–77], have investigated cooperative STBC with AF strategy. Under a high SNR assumption, [75] obtained an upper bound on the pair-wise error probability; [59] derived asymptotic BEP results with both perfect and imperfect CSI; [76] generalized the cooperative STBC to the case of an arbitrary number of relays and hops, and presented an asymptotic symbol error probability result. Reference [77] also derived the asymptotic SEP, which was used to optimize the power allocation.

However, none of the above mentioned works has obtained the exact error

performance. Therefore, the first target of this chapter is to analyze the exact bit error performance of cooperative STBC with AF strategy. Three existing transmission protocols are considered, and exact BEP results are obtained in closed form for all of these protocols. Based on the exact BEP, we compare our results with the existing asymptotic BEP in [59]. Then, we compare the performances of the protocols in different situations and examine the robustness of these protocols.

For the cooperative STBC with AF strategy, since the relay simply forwards the received signals, the additive noise at the relay is also forwarded. Due to the decoder structure of STBC, the forwarded noise degrades the received signals from both the relay and the source. If the forwarded noise is too large, then the advantage of cooperative diversity vanishes, and even an error floor can be observed [59, 105]. Therefore, in the second part of this chapter, we address the key question of when the relay should stop forwarding signals. We first examine the effect of the forwarded noise on the received SNR and find a critical condition, under which the forwarded signal from the relay will be deleterious. According to this condition, we propose adaptive forwarding schemes for cooperative STBC with full CSI, partial CSI and no CSI available at the relay. The exact BEP's of these adaptive cooperative STBC schemes, which are much better than that of the conventional cooperative STBC, are also obtained in closed form. Finally, the energy efficiencies of these adaptive schemes are also discussed.

The rest of this chapter is organized as follows: Section 5.2 describes the system model. The exact BEP results of the conventional cooperative STBC are derived in Section 5.3. A comparison of different protocols is also provided in this section. Section 5.4 proposes and analyzes the adaptive cooperative STBC schemes, together with numerical examples and discussion. A summary is given in Section 5.5.

5.2 System Model

5.2.1 Protocols

We consider a cooperative transmission scenario with three nodes, where each node only has one antenna. The source S transmits information to the destination D, with the assistance from the relay R. We assume all the nodes are half duplex, such that they cannot transmit and receive simultaneously. Therefore, we use a time-division multiple-access strategy here, and the transmission is completed in two phases. According to different settings of the source and the destination, three existing protocols are listed in Table 5.1.

Protocol I: The source broadcasts the information to the relay and the destination in the first phase. In the second phase, the source and relay transmit together to the destination using STBC. The destination combines the signals from the first and second phases before decoding.

Protocol II: The source only transmits in the first phase, and the relay transmits in the second phase. The destination listens in both phases and combines the signals.

Protocol III: Similar to protocol I, the source transmits in both phases and relay forwards the signals in the second phase. But, the destination only listens in the second phase.

Notice that the settings of the relay are the same in all of the three protocols, such that it listens in the first phase and forwards in the second phase. However, the source/destination can choose to transmit/listen in one or both phases. These protocols are essentially the same as they all try to exploit spatial diversity through relays. The different settings for the source and the destination can be viewed as adaption to different scenarios. For example, if the channel between the source and the destination varies fast, protocol I should be preferred, since the destination listens

Phase	Protocol I	Protocol II	Protocol III
1	$S \to R,\ D$	$S \to R,\ D$	$S \to R$
2	$S \to D,\ R \to D$	$R \to D$	$S \to D,\ R \to D$

Table 5.1: List of three protocols

to the source in both phases and enjoys greater orders of diversity. Protocols II and III free the source/destination in the second/first phase, so that the latter can be involved in other transmissions, which is an advantage in multi-hop transmission. The further comparison of protocols will be detailed later in Section 5.3.3. In Section 5.3, we will first focus on the performance of protocol III. The results will be extended to protocols I and II later.

We denote the link from A to B as $A \to B$. And the channel gains of $S \to D$, $S \to R$ and $R \to D$ links are denoted as h_{SD}, h_{SR} and h_{RD}, respectively. They are independent, complex, Gaussian random variables with means of zero and variances of $2\sigma_{SD}^2$, $2\sigma_{SR}^2$ and $2\sigma_{RD}^2$, respectively. Here, the channel variances can be different due to the different propagation environments and the distances between nodes. The channels are block fading such that they remain constant for at least one space-time block. The CSI is perfectly known at the receivers of the relay and the destination.

For this scenarios with one relay, we apply Alamouti's code [29] for two transmit antennas, which is given by

$$\begin{bmatrix} s_1 & s_2 \\ -s_2^* & s_1^* \end{bmatrix}, \tag{5.1}$$

where s_1 and s_2 are from a certain complex signal constellation. Here, we assume MPSK modulation such that each $s_i,\ i = 1, 2$, can be written as $s_i = e^{j\phi_i}$, where ϕ_i takes on, with equal probabilities, the values in the set $\{2n\pi/M\}_{n=0}^{M-1}$.

For protocol III, the source transmits the first column of the code matrix to the

relay in the first phase. The received signal, r_{Ri}, is given by

$$r_{Ri} = \sqrt{E_{SR}} h_{SR} x_i + n_{R,i},\ i = 1, 2 \tag{5.2}$$

where $x_1 = s_1$ and $x_2 = -s_2^*$ are transmitted with power $\sqrt{E_{SR}}$, and the noise $n_{R,i}$ is the AWGN with mean zero and variance N_o. In the second phase, the relay amplifies and forwards the received signals to the destination, while the source transmits the second column of the code matrix. Therefore, the received signals at the destination are given by

$$r_1 = \sqrt{E_{RD}}\sqrt{E_{SR}} h_{RD} h_{SR} s_1 + \sqrt{E_{SD}} h_{SD} s_2 + \sqrt{E_{RD}} h_{RD} n_{R,1} + n_{D,1}, \tag{5.3}$$

$$r_2 = -\sqrt{E_{RD}}\sqrt{E_{SR}} h_{RD} h_{SR} s_2^* + \sqrt{E_{SD}} h_{SD} s_1^* + \sqrt{E_{RD}} h_{RD} n_{R,2} + n_{D,2} \tag{5.4}$$

where $\sqrt{E_{RD}}$ and $\sqrt{E_{SD}}$ are the transmission powers of the source and relay in the second phase, and $n_{D,i},\ i = 1, 2$ is the AWGN at the destination, with mean zero and variance N_o.

5.2.2 Signal Normalization at the Relay

After receiving the signals from the source, the relay usually needs to normalize them by some factors before amplifying and forwarding, in order to keep a constant transmit energy or power . We list here two common normalization schemes used in the literature.

Scheme I [59, 75, 107] has been proposed to maintain a long term average energy, so that the transmit energy is normalized by a factor of $E[|r_{Ri}|^2]$, and is given by

$$E_{RD} = \frac{E_{RD}^{avr}}{E[E_{SR}|h_{SD}|^2 + N_o]} = \frac{E_{RD}^{avr}}{2\sigma_{SD}^2 E_{SR} + N_o}, \tag{5.5}$$

where E_{RD}^{avr} is the long term average transmit energy per symbol at the relay.

Scheme II [72, 76, 108] intends to keep a constant transmit power at the relay, and the

normalized transmit energy is given by

$$E_{RD} = \frac{E_{RD}^{avr}}{E_{SR}|h_{SR}|^2 + N_o}. \tag{5.6}$$

However, the denominator of (5.6) consists of the instantaneous energy of the effective signal and the long term average energy of the noise. Due to the noise variation, the transmit power is, actually, *not constant*, especially in the low SNR region. On the other hand, the average transmit energy at the relay is given by

$$E\left[\left|\sqrt{E_{RD}}r_{Ri}\right|^2\right] = E_{RD}^{avr}E\left[\frac{|\sqrt{E_{SR}}h_{SR} + n_{Ri}|^2}{E_{SR}|h_{SR}|^2 + N_o}\right], \tag{5.7}$$

which changes with different values of SNR, E_{SR}/N_o, at the relay. Therefore, scheme II can neither provide a constant transmit power, nor a constant average transmit energy.

In the rest of this chapter, we will normalize the received signal at the relay following scheme I, and keep the average transmit energy as E_{RD}^{avr}. The average transmit energy on the $S \rightarrow D$ and $S \rightarrow R$ links are $E_{SD}^{avr} = E_{SD}$ and $E_{SR}^{avr} = E_{SR}$, respectively. We also assume that all the transmitting nodes, i.e. the source and the relay, only have two status, such that they either transmit with fixed average energies, or keep silent. Therefore, no adaptive power allocation is applied among the nodes, so the structures of the nodes and the network are simple, which is usually the requirement of a wireless senor network with cheap sensors.

5.3 Performance Analysis

5.3.1 Performance of Protocol III

Applying the symbol-by-symbol detector for orthogonal STBC [29, 30], the decision metrics for s_1 and s_2 are given, respectively, as

$$\hat{s}_1 = \sqrt{E_{RD}}\sqrt{E_{SR}}h_{RD}^* h_{SR}^* r_1 + \sqrt{E_{SD}}h_{SD} r_2^*, \tag{5.8}$$

$$\hat{s}_2 = \sqrt{E_{SD}}h_{SD}^* r_1 - \sqrt{E_{RD}}\sqrt{E_{SR}}h_{RD} h_{SR} r_2^*. \tag{5.9}$$

The BEP of s_1 and s_2 are the same, due to symmetry. For equally likely symbols, we can assume $s_1 = 1$ without loss of generality, and the conditional BEP can be computed from the probability $P_\alpha(e) = P(\Re[\hat{s}_1 e^{-j\alpha}] < 0 | s_1 = 1, h_{SR}, h_{SD}, h_{RD})$ [83], where α is some angle that depends on the modulation scheme. Therefore, the conditional BEP for s_1 can be written as

$$P_\alpha(e|h_{SR}, h_{SD}, h_{RD}) = Q\left(\sqrt{\frac{E_{SR}E_{RD}|h_{SR}|^2|h_{RD}|^2 + E_{SD}|h_{SD}|^2}{(E_{RD}|h_{RD}|^2+1)N_o} 2\cos^2\alpha}\right) \tag{5.10}$$

Applying Craig's alternative form of the $Q(\cdot)$ function [84], the above conditional BEP can be rewritten as

$$\begin{aligned} P_\alpha(e|h_{SR}, h_{SD}, h_{RD}) &= \frac{1}{\pi}\int_0^{\frac{\pi}{2}} \exp\left(-\frac{E_{SR}E_{RD}|h_{SR}|^2|h_{RD}|^2\cos^2\alpha}{(E_{RD}|h_{RD}|^2+1)N_o\sin^2\theta}\right) \\ &\quad \cdot \exp\left(-\frac{E_{SD}|h_{SD}|^2\cos^2\alpha}{(E_{RD}|h_{RD}|^2+1)N_o\sin^2\theta}\right) d\theta \end{aligned} \tag{5.11}$$

We notice that the above equation contains two exponential terms, which involve the random variables, h_{SD} and h_{SR}, separately. Conditioning on the channel gain h_{RD}, we first take the expectation over h_{SD} and h_{SR} independently, giving

$$\begin{aligned} P_\alpha(e|h_{RD}) &= \frac{1}{\pi}\int_0^{\frac{\pi}{2}} \left(1 + \frac{2\sigma_{SD}^2 E_{SD}\cos^2\alpha}{(E_{RD}|h_{RD}|^2+1)N_o\sin^2\theta}\right)^{-1} \\ &\quad \cdot \left(1 + \frac{2\sigma_{SR}^2 E_{SR}E_{RD}|h_{RD}|^2\cos^2\alpha}{(E_{RD}|h_{RD}|^2+1)N_o\sin^2\theta}\right)^{-1} d\theta. \end{aligned} \tag{5.12}$$

After some manipulation, the conditional BEP (5.12) can be further written as

$$P_{\alpha}(e|h_{RD}) = \frac{1}{\pi}\int_{0}^{\frac{\pi}{2}} b \cdot \frac{(E_{RD}|h_{RD}|^2+1)^2}{(E_{RD}|h_{RD}|^2+a)\,(E_{RD}|h_{RD}|^2+b)}d\theta, \tag{5.13}$$

where

$$a = 1 + \frac{2\sigma_{SD}^2 E_{SD}\cos^2\alpha}{N_o \sin^2\theta}, \tag{5.14}$$

$$b = \left(1 + \frac{2\sigma_{SR}^2 E_{SR}\cos^2\alpha}{N_o \sin^2\theta}\right)^{-1}. \tag{5.15}$$

Noting that $E_{RD}|h_{RD}|^2$ is a central chi-square random variable with 2 degrees of freedom, its probability density function (PDF) is given by [7]

$$p_{E_{RD}|h_{RD}|^2}(x) = \frac{1}{f}\exp\left(-\frac{x}{f}\right), \tag{5.16}$$

where

$$f = 2\sigma_{RD}^2 E_{RD}. \tag{5.17}$$

Averaging the conditional BEP (5.13) over h_{RD}, we can obtain

$$P_{\alpha}(e) = \int_{0}^{\frac{\pi}{2}} \frac{b}{f\pi(b-a)}\int_{0}^{\infty}(x^2+2x+1)\left(\frac{1}{x+a}-\frac{1}{x+b}\right)\exp\left(-\frac{x}{f}\right)dxd\theta. \tag{5.18}$$

In order to evaluate the above integral, we now introduce Lemma 5.1 [86, eqn. (3.383), (8.356)]

Lemma 5.1.

$$\int_{0}^{\infty}\frac{1}{x+\mu}\exp\left(-\frac{x}{v}\right)dx = e^{\frac{\mu}{v}}\Gamma\left[0,\frac{\mu}{v}\right], \tag{5.19}$$

$$\int_{0}^{\infty}\frac{x}{x+\mu}\exp\left(-\frac{x}{v}\right)dx = v-\mu e^{\frac{\mu}{v}}\Gamma\left[0,\frac{\mu}{v}\right], \tag{5.20}$$

$$\int_{0}^{\infty}\frac{x^2}{x+\mu}\exp\left(-\frac{x}{v}\right)dx = v(v-\mu)+\mu^2 e^{\frac{\mu}{v}}\Gamma\left[0,\frac{\mu}{v}\right] \tag{5.21}$$

where $\Re[v] > 0$, $\Re[\mu] > 0$ *and* $\Gamma\left[0,\frac{\mu}{v}\right]$ *is the incomplete Gamma function, which is given by*

$$\Gamma\left[0,\frac{\mu}{v}\right] = \int_{\frac{\mu}{v}}^{\infty}\exp(-t)t^{-1}dt. \tag{5.22}$$

Applying Lemma 5.1 to (5.18), the average BEP is now given by

$$P_\alpha(e) = \int_0^{\frac{\pi}{2}} \frac{b}{f\pi}\left(f + \frac{(a-1)^2}{b-a}\exp\left(\frac{a}{f}\right)\Gamma\left[0,\frac{a}{f}\right] - \frac{(b-1)^2}{b-a}\exp\left(\frac{b}{f}\right)\Gamma\left[0,\frac{b}{f}\right]\right)d\theta. \quad (5.23)$$

5.3.2 Extensions to Protocols I and II

Protocol I allows the destination to listen in both phases and combine the received signals with maximal-ratio combining. We consider here two cases, where the channel gain h_{SD} changes independently between phases (fast block fading channel), or remains the same in the two adjacent phases (slow block fading channel). These two cases can serve as the lower and upper bounds for the case with an arbitrary channel fade rate. Similar to (5.10), the conditional BEP of protocol I is given by

$$P_\alpha(e|h_{SR},h_{SD},h_{RD}) = Q\left(\sqrt{\left(\frac{E_{SD}|h_{SD}^1|^2}{N_o} + \frac{E_{SR}E_{RD}|h_{SR}|^2|h_{RD}|^2 + E_{SD}|h_{SD}|^2}{(E_{RD}|h_{RD}|^2+1)N_o}\right)2\cos^2\alpha}\right), \quad (5.24)$$

where h_{SD}^1 is the channel gain in the first phase which can be the same as, or independent of h_{SD}, according to different cases. Following the same procedure from (5.11) to (5.23), the average BEP results of protocol I are given by

Case one, fast block fading channel:

$$P_\alpha(e) = \int_0^{\frac{\pi}{2}} \frac{b}{af\pi}\left(f + \frac{(a-1)^2}{b-a}\exp\left(\frac{a}{f}\right)\Gamma\left[0,\frac{a}{f}\right] - \frac{(b-1)^2}{b-a}\exp\left(\frac{b}{f}\right)\Gamma\left[0,\frac{b}{f}\right]\right)d\theta, \quad (5.25)$$

(5.26)

Case two, slow block fading channel:

$$P_\alpha(e) = \int_0^{\frac{\pi}{2}} \frac{b}{af\pi}\left(f + \frac{(\hat{a}-1)^2}{b-\hat{a}}\exp\left(\frac{\hat{a}}{f}\right)\Gamma\left[0,\frac{\hat{a}}{f}\right] - \frac{(b-1)^2}{b-\hat{a}}\exp\left(\frac{b}{f}\right)\Gamma\left[0,\frac{b}{f}\right]\right)d\theta, \quad (5.27)$$

respectively. Here,

$$\hat{a} = 2 - \frac{1}{a}. \tag{5.28}$$

For protocol II, the source only transmits in the first phase, so the conditional BEP is given by

$$\begin{aligned} &P_\alpha(e|h_{SR}, h_{SD}, h_{RD}) \\ &= Q\left(\sqrt{\left(\frac{E_{SR}E_{RD}|h_{SR}|^2|h_{RD}|^2}{(E_{RD}|h_{RD}|^2+1)N_o} + \frac{E_{SD}|h_{SD}^1|^2}{N_o}\right)2\cos^2\alpha}\right). \end{aligned} \tag{5.29}$$

Therefore, the average BEP of protocol II is given by

$$P_\alpha(e) = \int_0^{\frac{\pi}{2}} \frac{b}{af\pi}\left(f + (1-b)\exp\left(\frac{b}{f}\right)\Gamma\left[0, \frac{b}{f}\right]\right)d\theta. \tag{5.30}$$

For all the exact BEP results in (5.23), (5.25), (5.27) and (5.30), we set $\alpha = 0$ for BPSK modulation and $\alpha = \frac{\pi}{4}$ for QPSK modulation with Gray coding [83].

5.3.3 Comparisons of Protocols and Discussion

Comparison with Existing Results

In this section, we first compare our exact BEP result (5.23) with the one in [59], where protocol III is applied. Under a high SNR assumption[1], the asymptotic BEP results for protocol III is obtained in [59, eqn. (15)]. The channel variances $2\sigma_{SD}^2 = 2\sigma_{SR}^2 = 2\sigma_{RD}^2$ are normalized to one, therefore, the values of SNR's E_{SR}^{avr}/N_o, E_{SD}^{avr}/N_o and

[1]In [59], the SNR's defined in equations (7) and (8) are the effective SNR's of two arrival branches at the destination, which is given by

$$\bar{\gamma}_1 = \frac{E_{SR}^{avr}/N_o \cdot E_{RD}^{avr}/N_o}{1 + E_{SR}^{avr}/N_o + E_{RD}^{avr}/N_o}|h_{RD}|^2, \tag{5.31}$$

$$\bar{\gamma}_2 = \frac{(1 + E_{SR}^{avr}/N_o)\cdot E_{SD/N_o}^{avr}}{1 + E_{SR}^{avr}/N_o + E_{RD}^{avr}/N_o}, \tag{5.32}$$

and it is not the same SNR definition we use in this chapter.

E_{RD}^{avr}/N_o will reflect the environmental differences, such as distance, shadowing, etc. Here, BPSK modulation is applied.

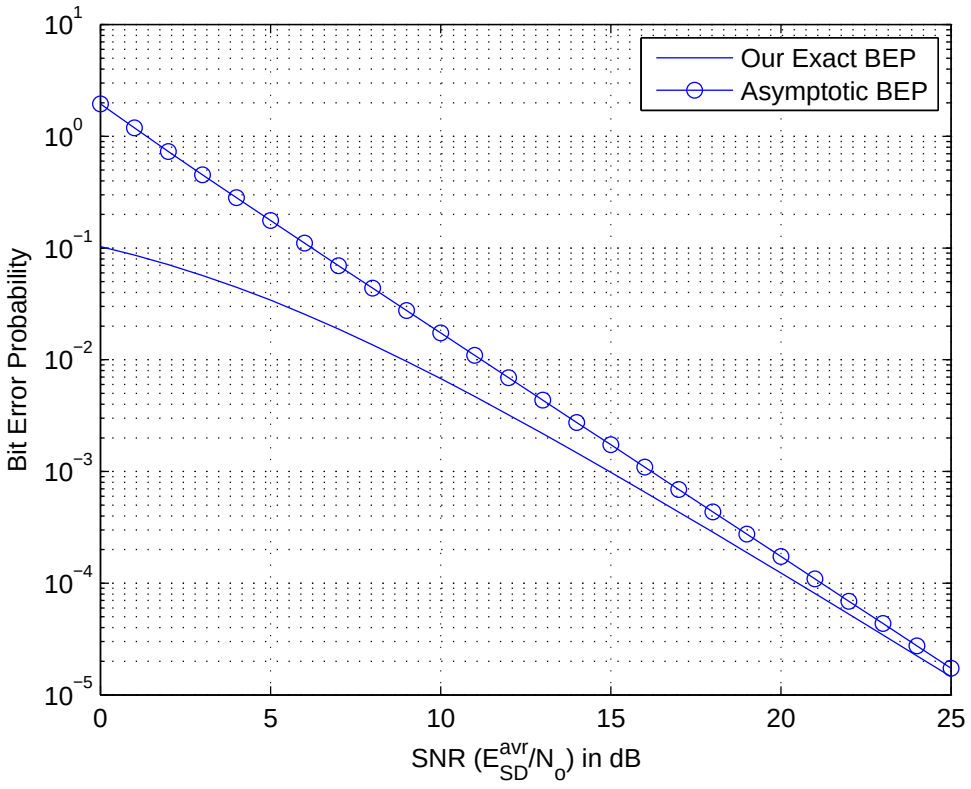

Figure 5.1: Exact BEP result (5.23) and asymptotic BEP, with $E_{SR}^{avr} = E_{RD}^{avr} = E_{SD}^{avr}$.

In Figure 5.1, we first assume the same average energy per symbol, such that $E_{SR}^{avr} = E_{SD}^{avr} = E_{RD}^{avr}$. It is shown that the asymptotic BEP results are not very tight, especially in the low to moderate SNR (E_{SD}^{avr}/N_o) region. Next, we assume E_{SR}^{avr} is fixed and $E_{RD}^{avr} = E_{SD}^{avr}$. In Figure 5.2, we plot the asymptotic and exact BEP results for $E_{SR}^{avr}/N_o = 10\ dB$. In this situation, we can see that the asymptotic results are neither tight in the low SNR (E_{SD}^{avr}/N_o) region, nor in the high SNR (E_{SD}^{avr}/N_o) region. The reason is that when E_{SR}^{avr} is fixed, we cannot guarantee $\bar{\gamma}_1$ in (5.31) and $\bar{\gamma}_2$ in (5.32) are always much greater than 1, therefore the high SNR assumption in [59] is not valid.

The two cases above clearly show that the asymptotic BEP is not always reliable, and an exact and simple BEP result is of great importance to both theoretical and practical applications.

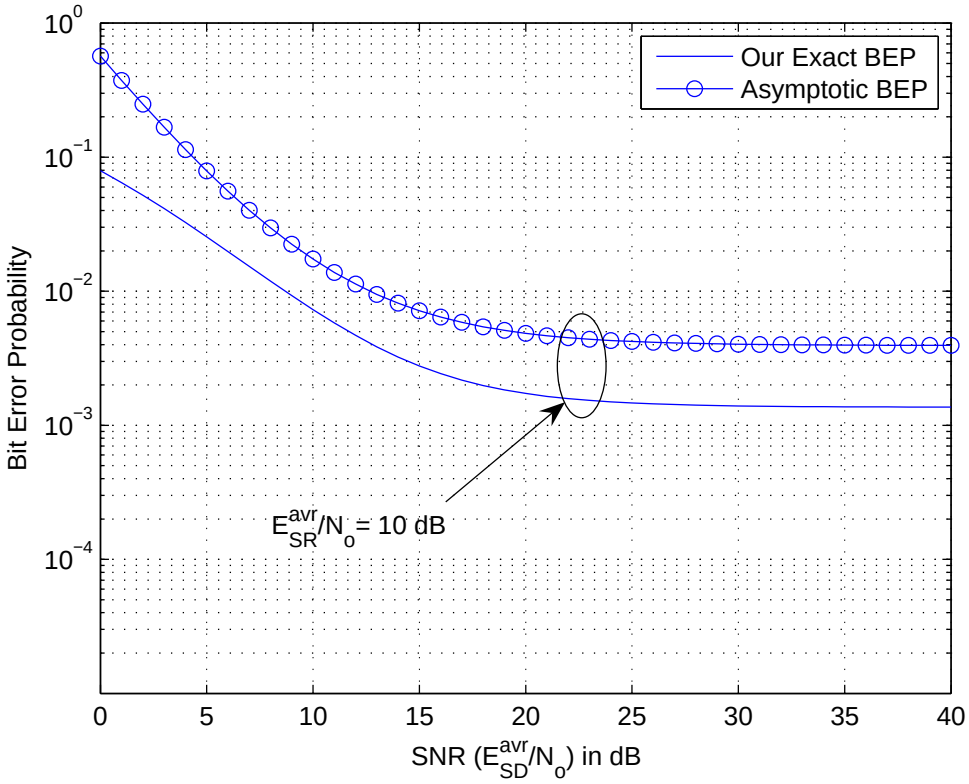

Figure 5.2: Exact BEP result (5.23) and asymptotic BEP, with $E_{RD}^{avr} = E_{SD}^{avr}$, and E_{SR}^{avr}/N_o =10 dB.

Comparison of Protocols

In Section 5.2, we mentioned that the three protocols can be applied in different situations. Now, we will examine their performances based on the exact BEP results. As in the previous section, we assume here all the channel variances are normalized to one, and BPSK modulation is used.

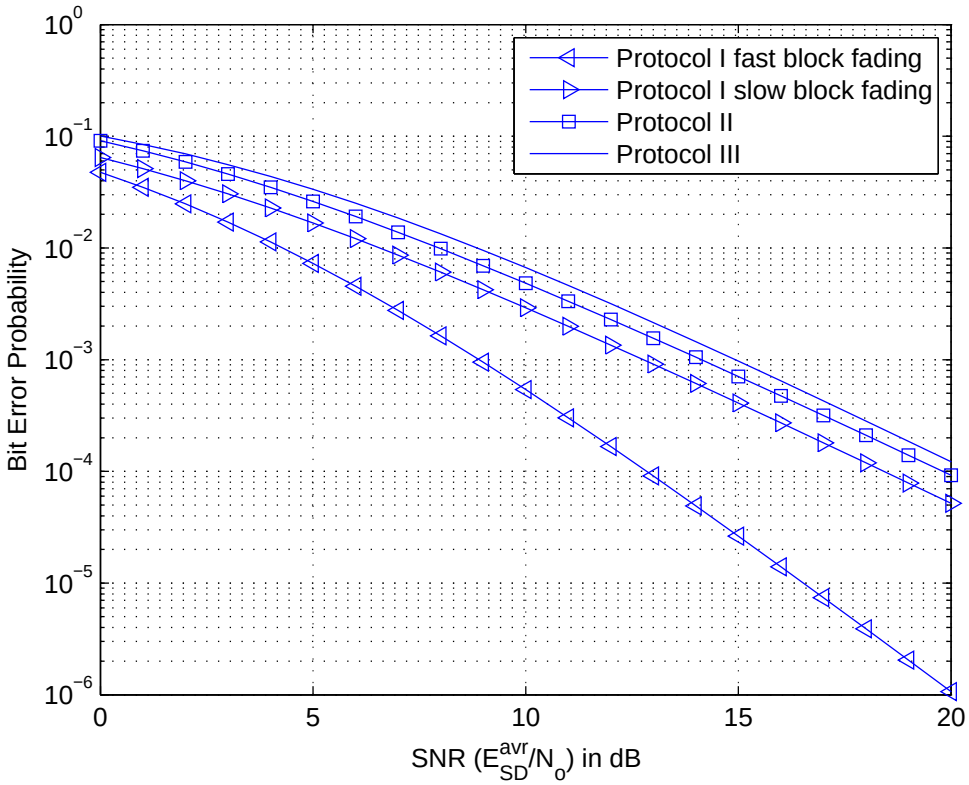

Figure 5.3: Exact BEP for three protocols with $E_{SR}^{avr} = E_{RD}^{avr} = E_{SD}^{avr}$.

We plot the exact BEP of the three protocols in Figure 5.3, with $E_{SR}^{avr} = E_{RD}^{avr} = E_{SD}^{avr}$. In the fast block fading channels, it is shown that protocol I has the best performance, since the diversity order of three is obtained. Protocols II and III both have the diversity order of two. As a matter of fact, the channel fade rate will not affect protocols II and III, since they only receive once from the source. Therefore, in the slow block fading channels, all the three protocols have the same diversity order of two, and their BEP curves have the same slope.

In the slow block fading case, protocol I still has a better performance than the other two, since the destination receives two copies of the same signal from the source. Protocol I is $2\ dB$ better than protocol II, and about $3\ dB$ better than protocol III.

Although protocols II and III both receive once from the source and the relay each, protocol II is slightly better than protocol III. This is because the signals from the source and the relay arrive at the destination separately in protocol II. But in protocol III, both of the signals arrive at the second phase, and the forwarded noise from the relay degrades the signal from the source, as can be seen in (5.10).

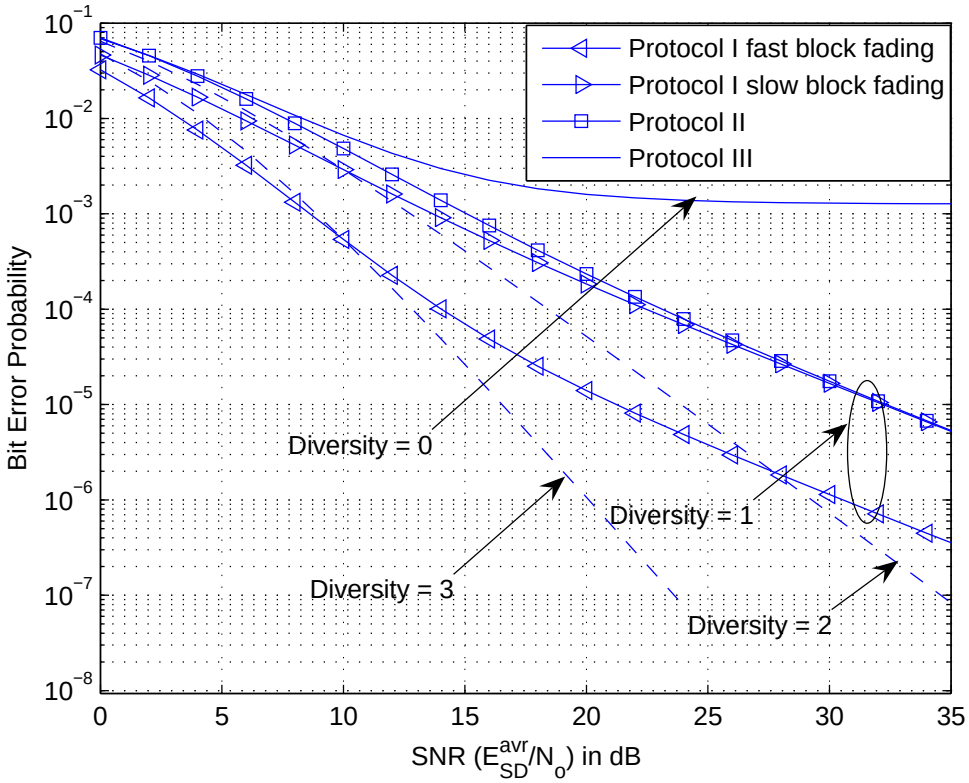

Figure 5.4: Exact BEP for three protocols with $E_{RD}^{avr} = E_{SD}^{avr}$ and $E_{SR}^{avr}/N_o = 10\ dB$.

In Figure 5.4, we set $E_{RD}^{avr} = E_{SD}^{avr}$ and $E_{SR}^{avr}/N_o = 10\ dB$. The BEP of all three protocols are plotted, together with two dashed lines which indicate the diversity orders of two and three, as a comparison. We can see that protocol III shows an error floor when E_{SD}^{avr}/N_o is greater than a certain value. It is easy to understand that when SNR E_{SD}^{avr}/N_o is high, the relatively weaker $S \rightarrow R$ link becomes a bottleneck, and the

forwarded noise from the relay limits the final SNR at the destination. Similarly, the diversity orders of protocols I and II also reduce to one, since both of them have one diversity order from the direct $S \rightarrow D$ link , which is not affected by the relay's noise. Similar phenomena can be observed, when we change E_{SR}^{avr}/N_o to other fixed values.

From the discussion above, we can see that protocol I has the best performance, especially in the fast block fading channel. Protocol II on the other hand, only requires the source to transmit once, which is an advantage when a node's battery lifetime is a concern. And both protocols I and II are quite robust to the deep fading on the $S \rightarrow R$ link. Protocol III appears to be the worst one among the three.

5.4 Adaptive Forwarding Schemes

In the last section, we mentioned that if both the source and the relay transmit in the second phase (Protocol I and III), the forwarded noise from the relay will degrade the total received SNR at the destination. In this section, we first re-examine the received SNR in the second phase. From (5.8) and (5.9), we can see that the received SNR's for s_1 and s_2 are the same, and are given by

$$\gamma_{STBC} = \underbrace{\frac{E_{SR}E_{RD}|h_{SR}|^2|h_{RD}|^2}{(E_{RD}|h_{RD}|^2+1)N_o}}_{\text{SNR from the } R \rightarrow D \text{ link}} + \underbrace{\frac{E_{SD}|h_{SD}|^2}{(E_{RD}|h_{RD}|^2+1)N_o}}_{\text{SNR from the } S \rightarrow D \text{ link}}. \tag{5.33}$$

The above equation shows that the received SNR consists of two parts, which are from the $S \rightarrow D$ and $R \rightarrow D$ links, respectively. We can also see that both parts are degraded by the noise from the relay. On the other hand, if there is only the direct transmission in the second phase, the received SNR is given by

$$\gamma_{Direct} = \frac{E_{SD}|h_{SD}|^2}{N_o}. \tag{5.34}$$

Therefore, the key question we want to address is: *how should the relay decide whether to forward the signals and cooperate to form an STBC?* In the rest of this section, we

will discuss this problem based on different levels of CSI feedback to the relay. More specifically, we consider three cases. (1) Full CSI feedback: the destination feeds back the instantaneous value of the channel gain h_{SD} to the relay. (2) Partial CSI feedback: the destination feeds back the statistics of the channel gain, i.e. the variances of h_{SD} and h_{RD}, to the relay. (3) No CSI feedback: the relay does not require any form of CSI feedback from the destination.

5.4.1 Adaptive Cooperative STBC with Full CSI at the Relay

Based on the received SNR's γ_{STBC} and γ_{Direct}, the BEP results are given by [7]

$$P_b^{STBC} = \frac{1}{2}\text{erfc}\left((\beta\gamma_{STBC})^{\frac{1}{2}}\right) \tag{5.35}$$

and

$$P_b^{Direct} = \frac{1}{2}\text{erfc}\left((\beta\gamma_{Direct})^{\frac{1}{2}}\right), \tag{5.36}$$

respectively. Here, β is some constant that depends on the modulation scheme. Since the erfc$(\cdot)$ function is a monotonically decreasing function, it requires

$$\gamma_{STBC} > \gamma_{Direct} \tag{5.37}$$

to guarantee that the cooperative STBC has a smaller BEP. The above inequality can be rewritten as

$$E_{SR}|h_{SR}|^2 > E_{SD}|h_{SD}|^2. \tag{5.38}$$

In the case when the source transmits with the same energy in the first and second phases, i.e. $E_{SR} = E_{SD}$, the cooperative STBC outperforms the direct transmission simply when the $S \rightarrow R$ link is stronger than the $S \rightarrow D$ link.

Therefore, in an adaptive forwarding scheme, the relay needs to determine whether the condition (5.38) is satisfied before forwarding the signal. If not, the relay

keeps silent in the second phase of transmission and only the source transmits. The BEP of the adaptive forwarding strategy is given as

$$P_\alpha(e) = P_\alpha^{Direct}\left(e|E_{SR}|h_{SR}|^2 \le E_{SD}|h_{SD}|^2\right) + P_\alpha^{STBC}\left(e|E_{SR}|h_{SR}|^2 > E_{SD}|h_{SD}|^2\right). \tag{5.39}$$

Conditioning on the channel gains h_{SR}, h_{SD} and h_{RD}, the second term of (5.39) can be similarly rewritten as (5.11), which is given by

$$\begin{aligned} &P_\alpha^{STBC}\left(e|h_{RD}, h_{SR}, h_{SD}, E_{SR}|h_{SR}|^2 > E_{SD}|h_{SD}|^2\right) \\ &= \frac{1}{\pi}\int_0^{\frac{\pi}{2}} \exp\left(-\frac{E_{SR}E_{RD}|h_{SR}|^2|h_{RD}|^2\cos^2\alpha}{(E_{RD}|h_{RD}|^2+1)N_o\sin^2\theta}\right) \\ &\quad\cdot \exp\left(-\frac{E_{SD}|h_{SD}|^2\cos^2\alpha}{(E_{RD}|h_{RD}|^2+1)N_o\sin^2\theta}\right)d\theta. \end{aligned} \tag{5.40}$$

Averaging over channel gains h_{SR}, h_{RD} and h_{RD}, we obtain (see Appendix C)

$$\begin{aligned} &P_\alpha^{STBC}\left(e|E_{SR}|h_{SR}|^2 > E_{SD}|h_{SD}|^2\right) \\ &= \frac{1}{\pi}\int_0^{\frac{\pi}{2}} \left(\frac{bg}{1+ag} + \frac{bg(1-b)}{f(1+ag)}\exp\left(\frac{b}{f}\right)\Gamma\left[0, \frac{b}{f}\right]\right)d\theta \end{aligned} \tag{5.41}$$

where a, b and f are defined in (5.14), (5.15) and (5.17), respectively, and

$$g = \frac{2\sigma_{SR}^2 E_{SR}}{2\sigma_{SD}^2 E_{SD}}. \tag{5.42}$$

Similarly, the conditional BEP of the direct transmission is given by

$$\begin{aligned} &P_\alpha^{Direct}\left(e|h_{RD}, h_{SR}, h_{SD}, E_{SR}|h_{SR}|^2 \le E_{SD}|h_{SD}|^2\right) \\ &= \frac{1}{\pi}\int_0^{\frac{\pi}{2}} \exp\left(-\frac{E_{SD}|h_{SD}|^2}{N_o\sin^2\theta}\cos^2\alpha\right)d\theta, \end{aligned} \tag{5.43}$$

which is independent of h_{RD}. After averaging over the channel gains h_{SD} and h_{SR}, we have (see Appendix D)

$$P_\alpha^{Direct}\left(e|E_{SR}|h_{SR}|^2 \le E_{SD}|h_{SD}|^2\right) = \frac{1}{\pi}\int_0^{\frac{\pi}{2}} \frac{1}{a}\frac{b}{1+bg}d\theta. \tag{5.44}$$

Substituting (5.41) and (5.44) into (5.39), the BEP of adaptive cooperative STBC is given by

$$P_\alpha(e) = \frac{1}{\pi}\int_0^{\frac{\pi}{2}} \left(\frac{bg}{1+ag} + \frac{1}{a}\frac{b}{1+bg} + \frac{bg(1-b)}{f(1+ag)} \exp\left(\frac{b}{f}\right) \Gamma\left[0, \frac{b}{f}\right] \right) d\theta. \quad (5.45)$$

From the discussion above, it can be seen that the relay requires the instantaneous knowledge of h_{SD}, even if we assume E_{SD} is known previously. Therefore, the destination needs to send h_{SD} to the relay on a feedback channel. If the $S \rightarrow D$ link varies fast, the overhead of the feedback channel will be high.

5.4.2 Adaptive Cooperative STBC with Partial CSI and no CSI at the Relay

Alternatively, the relay can make the decision based on its own CSI of the $S \rightarrow R$ link. If the channel gain h_{SR} is higher than a threshold h_{th}, the relay will forward the signals. Here, the parameter h_{th} can be chosen based on the statistics of the $S \rightarrow R$ link only, e.g. $|h_{th}|^2 = 2\sigma_{SR}^2$, such that no feedback of CSI is required. Or an optimum value of h_{th} can be calculated with the partial knowledge of CSI's, i.e., the variances of h_{SR}, h_{SD} and h_{RD}, using (5.49). Since the statistics of the channels change slowly, the overhead of the feedback channel is low.

With a certain threshold h_{th}, the BEP of the adaptive cooperative STBC is given by

$$P_\alpha(e) = P_\alpha^{Direct}\left(e|\ |h_{SR}|^2 \leq |h_{th}|^2\right) + P_\alpha^{STBC}\left(e|\ |h_{SR}|^2 > |h_{th}|^2\right), \quad (5.46)$$

where the first term is given as

$$P_\alpha^{Direct}\left(e|\ |h_{SR}|^2 \leq |h_{th}|^2\right) = \frac{1-\exp\left(-\frac{|h_{th}|^2}{2\sigma_{SR}^2}\right)}{\pi}\int_0^{\frac{\pi}{2}} \frac{1}{a} d\theta. \quad (5.47)$$

It is difficult to calculate the second term in (5.46) directly. However, under a high SNR assumption that $E_{RD}|h_{RD}|^2 \gg 1$, the asymptotic BEP is given as (see Appendix

E)

$$
\begin{aligned}
&P_{\alpha}^{STBC}\left(e|\ |h_{SR}|^2 > |h_{th}|^2\right) \\
&\approx \frac{\exp\left(-\frac{|h_{th}|^2}{2\sigma_{SR}^2}\right)}{\pi}\int_0^{\frac{\pi}{2}}\left(b+\frac{b(a-1)^2}{f(b-a)}\exp\left(\frac{a}{f}\right)\Gamma\left[0,\frac{a}{f}\right]\right. \\
&\quad\left.-\frac{b(b-1)^2}{f(b-a)}\exp\left(\frac{b}{f}\right)\Gamma\left[0,\frac{b}{f}\right]\right)\exp\left(-\frac{E_{SR}|h_{th}|^2\cos^2\alpha}{N_o\sin^2\theta}\right)d\theta. \quad (5.48)
\end{aligned}
$$

Therefore, the average BEP of cooperative STBC with partial CSI is given by

$$
\begin{aligned}
P_{\alpha}(e) &\approx \left(1-\exp\left(-\frac{|h_{th}|^2}{2\sigma_{SR}^2}\right)\right)\left(\frac{1}{2}-\frac{1}{2}\sqrt{\frac{2\sigma_{SD}^2E_{SD}\cos^2\alpha}{N_o+2\sigma_{SD}^2E_{SD}\cos^2\alpha}}\right) \\
&\quad+\frac{\exp\left(-\frac{|h_{th}|^2}{2\sigma_{SR}^2}\right)}{\pi}\int_0^{\frac{\pi}{2}}\left(b+\frac{b(a-1)^2}{f(b-a)}\exp\left(\frac{a}{f}\right)\Gamma\left[0,\frac{a}{f}\right]\right. \\
&\quad\left.-\frac{b(b-1)^2}{f(b-a)}\exp\left(\frac{b}{f}\right)\Gamma\left[0,\frac{b}{f}\right]\right)\exp\left(-\frac{E_{SR}|h_{th}|^2\cos^2\alpha}{N_o\sin^2\theta}\right)d\theta. \quad (5.49)
\end{aligned}
$$

Here, all the BEP results we obtained for the adaptive forwarding schemes are based on protocol III. It is straightforward to extend the results to protocol I, the only difference is that protocol I has one more direct transmission in the first phase, which will not change the adaptive scheme in the second phase. Therefore, we will omit the detailed results for protocol I here.

5.4.3 Energy Efficiency

In all of the three adaptive forwarding schemes, the relay keeps silent in certain cases. Besides the improvement in the performance, another obvious advantage of the adaptive forwarding schemes is the energy efficiency, which is especially important in wireless sensor networks, or ad hoc networks.

For the adaptive cooperative STBC with full CSI, the relay will stop forwarding the received signal when condition (5.38) is not satisfied. Therefore, normalizing the energy consumption of the conventional cooperative STBC at the relay to one, the

energy consumption of the adaptive cooperative STBC is given by $P(E_{SR}|h_{SR}|^2 > E_{SD}|h_{SD}|^2)$. Averaging over channel gains $|h_{SR}|^2$ and $|h_{SD}|^2$, the energy consumption at the relay is

$$\frac{2\sigma_{SR}^2 E_{SR}}{2\sigma_{SR}^2 E_{SR} + 2\sigma_{SD}^2 E_{SD}} \tag{5.50}$$

for the adaptive cooperative STBC with full CSI. Similarly, the energy consumptions of the schemes with partial and no CSI can be calculated as $P(|h_{SR}|^2 > |h_{th}|^2)$ times the one with conventional cooperative STBC. And the normalized energy consumption at the relay is given as

$$\exp\left(-\frac{|h_{th}|^2}{2\sigma_{SR}^2}\right). \tag{5.51}$$

5.4.4 Numerical Examples and Discussion

As in section 5.3.3, we normalize all the channel variances $2\sigma_{SR}^2$, $2\sigma_{SD}^2$ and $2\sigma_{RD}^2$ to one and apply BPSK modulation. In the first example, we set $E_{SD}^{avr} = E_{RD}^{avr}$. The BEP results of the conventional cooperative STBC (5.23) and the adaptive cooperative STBC with full CSI (5.45) are plotted in Figure 5.5. Here, we consider three cases:

(i) $E_{SR}^{avr}/N_o = E_{SD}^{avr}/N_o$,

(ii) $E_{SR}^{avr}/N_o = E_{SD}^{avr}/N_o - 5dB$,

(iii) $E_{SR}^{avr}/N_o = E_{SD}^{avr}/N_o - 15dB$.

It can be seen that when the $S \rightarrow R$ link is (statistically) as strong as the $S \rightarrow D$ link, the adaptive cooperative STBC provides a small gain. However, when the $S \rightarrow R$ link becomes weaker, our adaptive cooperative STBC can provide about 2 dB gain in case (ii) and 7 dB gain in case (iii). Similar phenomena can be observed when E_{SR}^{avr}/N_o takes on other values, which are smaller than E_{SD}^{avr}/N_o. On the other hand, if $E_{SR}^{avr}/N_o < E_{SD}^{avr}/N_o$, the adaptive cooperative STBC can guarantee that the performance is not worse than that of conventional cooperative STBC. It

can be easily proved by the underlying structure of our adaptive cooperative STBC. Therefore, our adaptive cooperative STBC scheme can be effectively applied to relieve any potential shadowing or deep fading problem in the $S \rightarrow R$ link. Substituting the parameters of cases (i), (ii) and (iii) into (5.50), we can obtain the normalized energy consumptions as 50%, 23.5% and 3.1%, respectively, in comparison with that of conventional cooperative STBC. Therefore, the lifetime of the relay node is greatly extended.

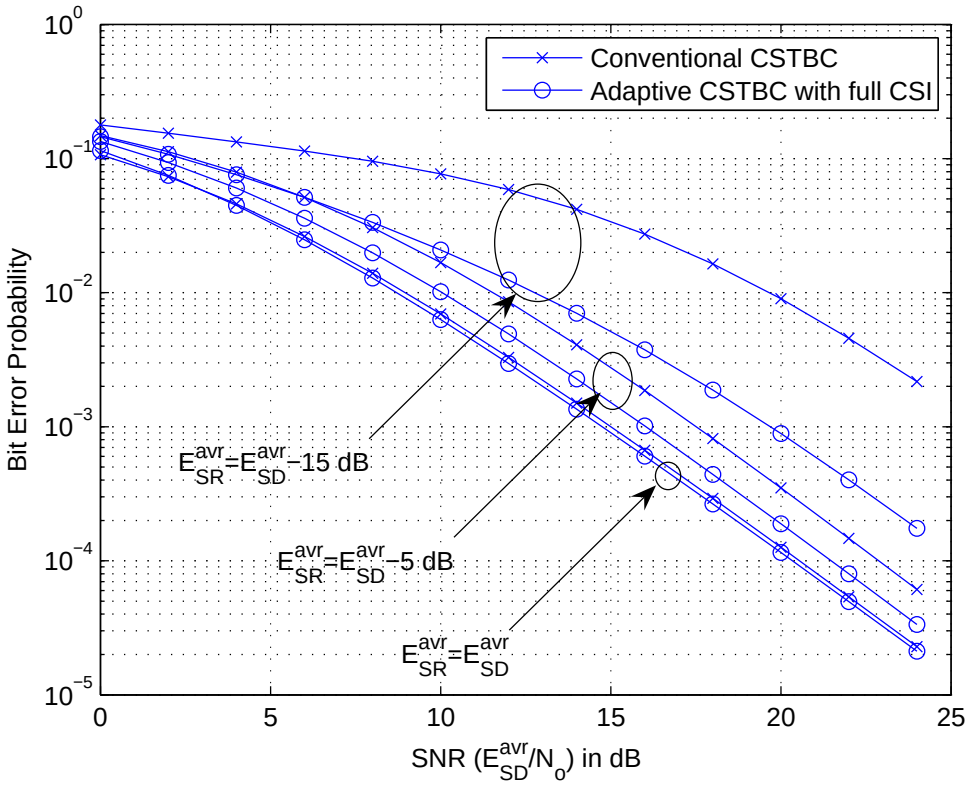

Figure 5.5: Conventional cooperative STBC v.s. adaptive cooperative STBC with full CSI. $E_{SD}^{avr} = E_{RD}^{avr}$, and $E_{SR}^{avr}/N_o = E_{SD}^{avr}/N_o,\ E_{SD}^{avr}/N_o - 5\ dB$ and $E_{SD}^{avr}/N_o - 15\ dB$, respectively.

For the conventional cooperative STBC, we have observed an irreducible error

floor for protocol III in Figure 5.4, when E_{SR}^{avr}/N_o is set to a fixed value. In Figure 5.6, again, we set E_{SR}^{avr}/N_o to fixed values of $5\ dB,\ 10\ dB$ and $20\ dB$, respectively, with all the other parameters remaining the same. It is shown that the BEP of our adaptive cooperative STBC decreases along with the increase of E_{SD}^{avr}/N_o, which shows its superiority over the conventional cooperative STBC.

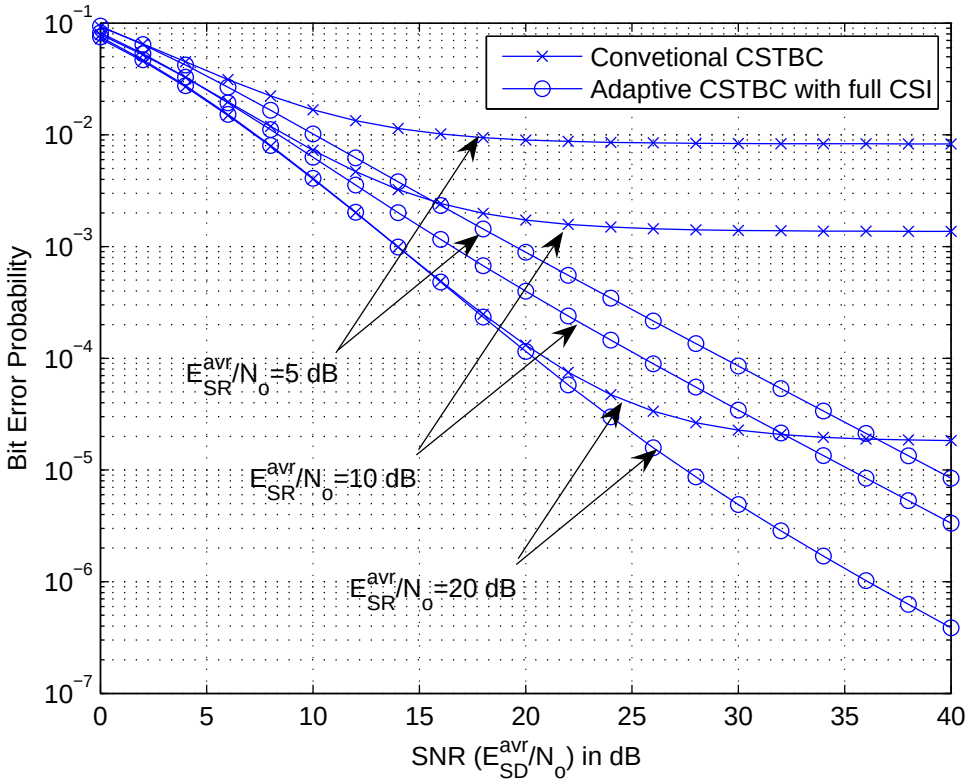

Figure 5.6: Conventional cooperative STBC v.s. adaptive cooperative STBC with full CSI. $E_{SD}^{avr} = E_{RD}^{avr}$ and $E_{SR}^{avr}/N_o = 5\ dB,\ 10\ dB$ and $20\ dB$, respectively.

The normalized energy consumptions at the relay for the adaptive cooperative STBC are plotted in Figure 5.7. For a fixed E_{SR}^{avr}/N_o, as we can see, the energy consumptions decrease, when the SNR E_{SD}^{avr}/N_o increases. This is because the relay is more likely to keep silent, if it cannot provide any help in this situation.

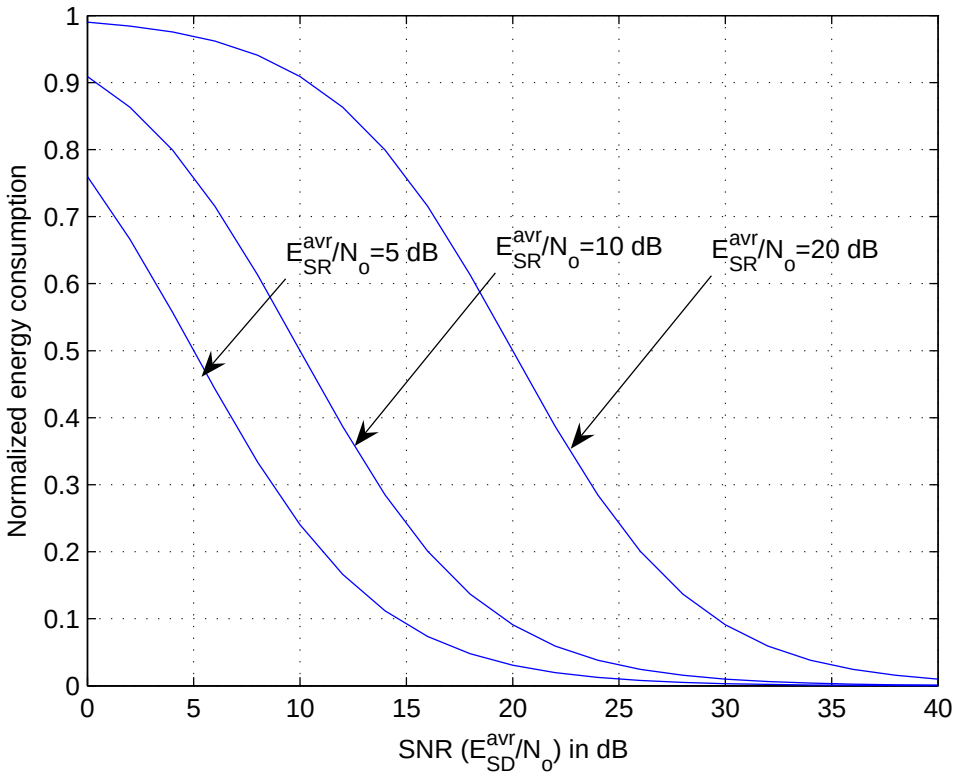

Figure 5.7: The normalized energy consumption at the relay for the adaptive CSTBC with full CSI. $E_{SD}^{avr} = E_{RD}^{avr}$ and $E_{SR}^{avr}/N_o = 5\ dB,\ 10\ dB$ and $20\ dB$, respectively.

In Figure 5.8, we plot the BEP performance of the adaptive cooperative STBC with full, partial and no CSI at the relay. We set $E_{SD}^{avr} = E_{RD}^{avr}$ as above, and $E_{SR}^{avr}/N_o = E_{SD}^{avr}/N_o - 10\ dB$. According to (5.49), we first search for the optimum h_{th} with partial knowledge of CSI. Using the optimum h_{th}, the performance of adaptive cooperative STBC with partial CSI is only about $1\ dB$ less than the one with full CSI. If we do not require any feedback of CSI, we can set $|h_{th}|^2 = 2\sigma_{SR}^2$ as in Figure 5.8. The underlying idea is that if the received SNR $E_{SR}|h_{SR}|^2/N_o$ is less than the average received SNR $2\sigma_{SR}^2 E_{SR}/N_o$, the signal is considered weak and will be discarded. The performance of this scheme is very close to the one with partial CSI in the low to moderate SNR

(E_{SD}^{avr}/N_o) region. However, since this scheme uses a fixed threshold, which does not change according to different situations, it becomes unreliable in some cases (such as in the high SNR region in Figure 5.8).

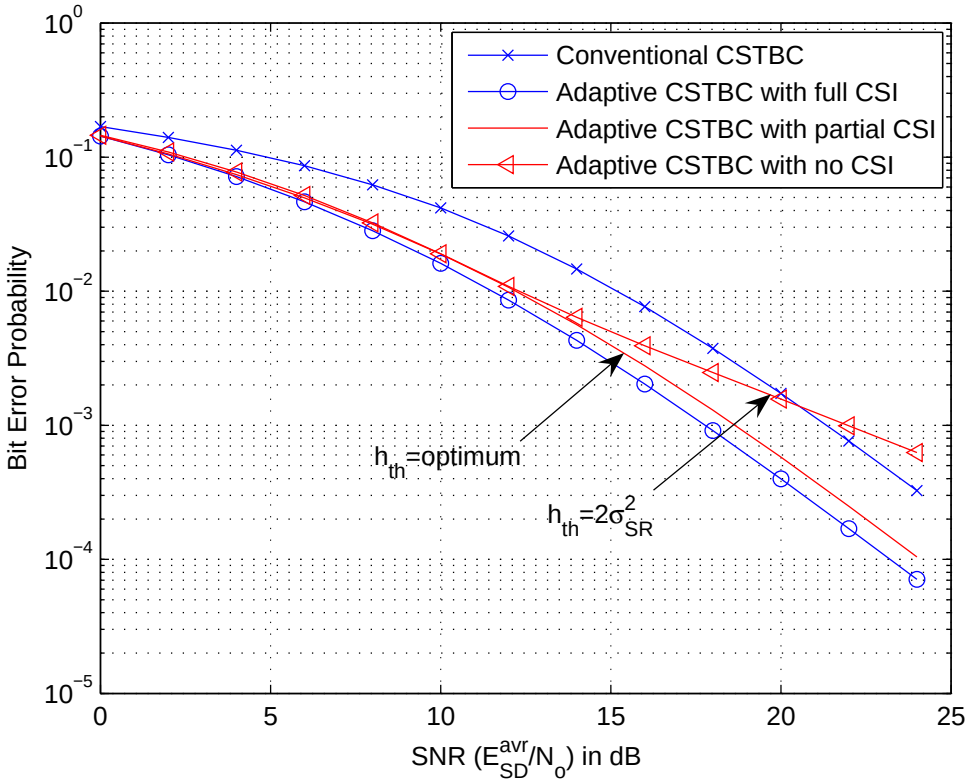

Figure 5.8: BEP of the conventional cooperative STBC and the adaptive cooperative STBC with full/partial CSI. $E_{SD}^{avr} = E_{RD}^{avr}$ and $E_{SR}^{avr}/N_o = E_{SD}^{avr} - 10\ dB$.

The normalized energy consumptions at the relay for the three adaptive cooperative STBC schemes are plotted in Figure 5.9, where we can see all the adaptive schemes are energy efficient, compared with the conventional cooperative STBC.

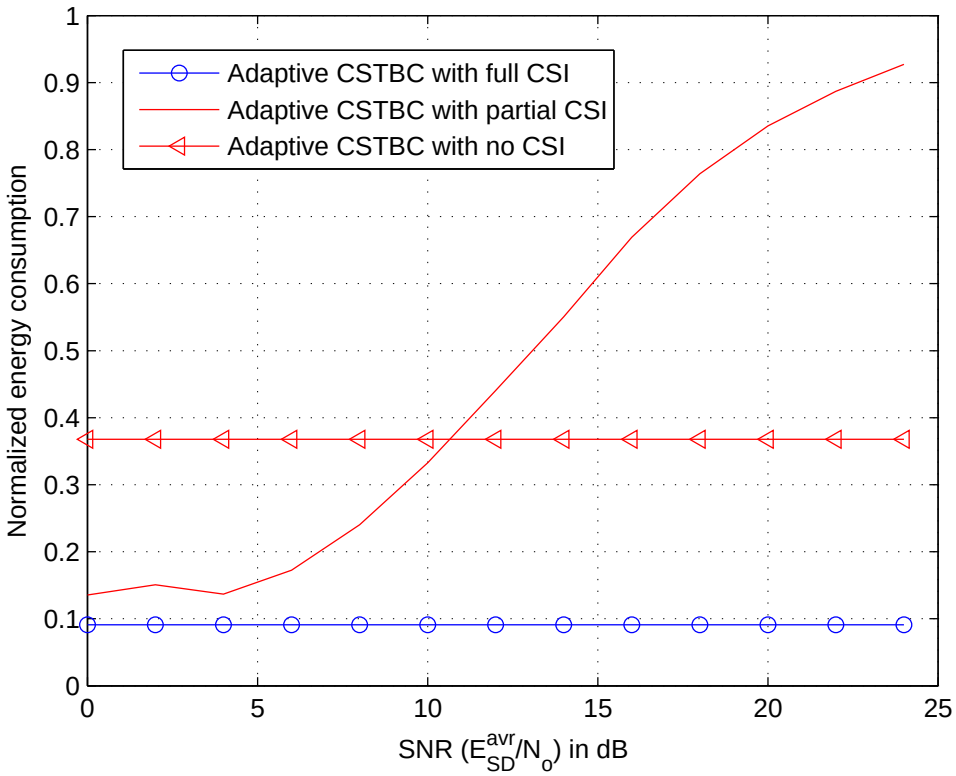

Figure 5.9: Normalized energy consumption of the adaptive cooperative STBC with full, partial and no CSI. $E_{SD}^{avr} = E_{RD}^{avr}$ and $E_{SR}^{avr}/N_o = E_{SD}^{avr} - 10\ dB$.

In summary, we have proposed adaptive cooperative STBC with full CSI, partial CSI and no CSI. The performances of these three schemes are ordered from high to low, but the complexities and the overheads of the feedback channel are also ordered from high to low.

5.5 Conclusions

In this chapter, we have analyzed the performances of cooperative STBC with AF strategy. Three existing protocols are considered and exact BEP results are obtained

in closed forms. Based on the BEP results, we first show that our exact result is more reliable than the existing asymptotic BEP results. We also compare the performances of the three protocols in different situations. It is shown that protocol I has a better performance than the other two; protocols I and II are robust to deep fades on the $S \rightarrow R$ link; and protocol III appears to be the worst one among the three protocols.

In second part of the chapter, we have proposed an adaptive cooperative STBC scheme with full CSI, partial CSI and no CSI available at the relay. The exact BEP results of these adaptive schemes are also obtained in closed form. Through the numerical results, we have shown that our adaptive scheme with full CSI provides significant gain when the $S \rightarrow D$ link is stronger than the $S \rightarrow R$ link. Moreover, the conventional cooperative STBC scheme shows an error floor, when E_{SR}^{avr}/N_o is equal to some fixed value, but our adaptive scheme does not have such a problem. The performance gains of the other two adaptive schemes are relatively small compared with the first one, but they require less/no feedback of the CSI. Finally, we compare the energy consumption of the conventional and the adaptive cooperative STBC schemes, and show that the energy efficiency is another advantage of the adaptive cooperative STBC schemes.

Chapter 6

Conclusions and Future Work

6.1 Conclusions

In this thesis, we studied the performance of STBC over general fading channels. We examined three different kinds of fading channels with diversity: non-identical channels, time-selective channels and relay channels. Exact bit error performance results were derived in closed-form, based on which we proposed new designs of codes, new optimum receiver structures, and adaptive transmission schemes.

For the STBC over non-identical channels, we investigated the performance with both perfect and estimated CSI. If the perfect CSI was available, it was shown that the ML detector is the same as the conventional detector for the case where the channels are identically distributed. With the help of the exact BEP derived, the effects of different degrees of imbalance between channels were studied. These results and observations are helpful to applying STBC's in real environments. Unlike most of the previous works on STBC which assumed that the channels were identically distributed, the OPAS in this study may not be coincidental with EPAS anymore. Therefore, the optimization of power allocation among antennas was necessary. Since the objective function is a convex function, the optimum value can be calculated directly. Depending

on whether the imbalance was caused by the means or the variances of the channel gains, the OPAS emphasized the weaker links, or the stronger links, respectively. The exact BEP results clearly showed that the performance of STBC with OPAS is much better than the one with EPAS, even when the channels are slightly non-identical. Therefore, the OPAS is of considerable value, as the channels in a real environment are mostly non-identical.

On the other hand, if the CSI was imperfect, the structure of the ML detector is different from the case where the channels are identically distributed. Our results showed that the received signals and the estimated channel matrices have to be weighted row-by-row if the channels are non-identically distributed at the receiver end, or weighted column-by-column if the non-identical channels are at the transmit end. This modification of the structure can be attributed to the non-identical channel estimation errors, which lead to non-identical equivalent Gaussian white noise at the receiver. Therefore, the variances of the received signals are not identical when conditioned on the estimated channels. In order to isolate the influences from different sources, we investigated the effects of non-identical channels at the receiver and the at transmitter separately. This study does not include the case when both the transmitter and the receiver are related to non-identical channels, since the performance analysis of this case would be more complex, and closed-form results might not be available. Therefore, further work is needed to obtain the bounds and approximations for the performance in this case. It is also interesting to know whether we should adjust power allocation for the pilot symbols, so as to make the variances of channel estimation identical.

For the STBC over time-selective channels, we also derived the exact BEP. More importantly, based on the BEP, the relationship between the ISI and the row positions in the code matrices was revealed. Since the exact error performance of STBC

over time-selective channels was not available before, it was hard to compare the performances of different designs of STBC. One way to search for the optimum code was to simulate the performances of all the codes, which was time consuming, if not impossible. Having our exact expressions of the error probabilities, it is much easier to obtain the performances of different STBC matrices by numerical computation. Moreover, since the performance results depend on and only on the row positions of the code matrices, the code design problem can be further simplified by obviating the tedious calculation. One proposition and two design criteria were also proposed to design or search for better STBC designs that have less ISI, compared with the original code matrix. The results may be of great importance, not only because the exact BEP results are obtained for the first time, but also because of the standards it built for the code designs in the time-selective channels. In this case, channel estimation was not included, since the channel estimation error is an independent source of performance degradation, which is not expected to change the observations made in this thesis. In future work, the effect of channel estimation errors on the performance of STBC over time-selective channels needs to be studied.

For the STBC over relay channels, the AF strategy was examined. Three existing protocols were considered and exact BEP results were obtained in closed form for the first time. It was shown that our exact result is more accurate than the existing asymptotic BEP results. We also compared the performances of the three protocols in different situations. It was shown that protocol I has the best performance, especially in the fast block fading channel. Protocol II on the other hand, only requires the source to transmit once, which is an advantage when a node's battery lifetime is a concern. And both protocols I and II are quite robust to the deep fading on the $S \rightarrow R$ link. Protocol III appeared to be the worst one among the three, and even an irreducible error floor was observed. We found that the error floor is caused by the noise forwarded from

the relay to the destination, therefore, the condition under which the relay should stop forwarding was carefully checked. Following this condition, we proposed adaptive cooperative STBC schemes with full CSI, partial CSI and no CSI available at the relay. The exact BEP results of these adaptive schemes were also obtained in closed form. The numerical results showed that our adaptive scheme with full CSI provides significant gain when the $S \rightarrow D$ link is stronger than the $S \rightarrow R$ link. Moreover, the irreducible error floor observed with conventional cooperative STBC was eliminated completely. The performance gains of the other two adaptive schemes are relatively small compared with the first one, but they require less/no feedback of the CSI. Finally, we compared the energy consumptions of the conventional and the adaptive cooperative STBC schemes, and showed that the energy efficiency is another advantage of the adaptive cooperative STBC schemes.

In this thesis, the performance of the STBC over three different kinds of diversity fading channels was examined. The analytical results obtained are exact and in closed-form, and can be used to facilitate the implementation of the STBC in a real environment. In this thesis, we considered only one of these three fading channels in one case, therefore, the interaction of two or more kinds of channels in one case remains unknown. And further work is needed to investigate this problem.

6.2 Future Work

6.2.1 STBC with Non-identical Channels at both the Transmitter and the Receiver, with imperfect CSI

As we mentioned above, in Chapter 3, we studied the performance of STBC over non-identical channels with imperfect CSI in two cases: the non-identical channels

are related to receive antennas, and the non-identical channels are related to transmit antennas. By examining the two cases separately, we showed that they have different effects on the ML receiver structure, and lead to different performances as well. Naturally, the next step is to examine the general case with non-identical channels related to both the transmit and the receive antennas. However, this general case is not a simple combination of the two cases studied in this thesis. For the general case, the ML decoder may have a more complicated form and the performance results may not be in closed-form. Therefore, deriving the ML decoder and analyzing the performance for this case can be a direction of future work.

6.2.2 The Optimum Power Allocation for STBC over Non-identical channels with imperfect CSI

Also in Chapter 3, it is assumed that the transmitted energy per symbol is the same for both the information symbols and the pilot symbols. It is interesting to know whether we can improve the performance by optimizing the power allocation. Here, the power allocation can be done in one of two ways.

Optimum Power Allocation for the Pilot Symbols

As we showed that the non-identical channels result in non-identical channel estimation errors, which finally change the structure of the ML decoder. Therefore, the first possibility is to allocate different powers to the pilot symbols, in order to obtain identical channel estimation errors. If identical channel estimation errors can be achieved, then we can use the conventional SBS decoder as the ML decoder. This method is especially attractive for Case II in Chapter 3, as the ML decoder of that case cannot be simplified to a SBS decoder. However, there are two problems we need to solve. First of all, the identical channel estimation errors are not obtained without

cost. We need to feed back the CSI to the transmitter, so the overhead of a feedback channel needs to be considered. Second, this power allocation does not guarantee that the performance will be improved, so we need to carefully compare the performance with that of an equal power allocation scheme.

On the other hand, since the BEP result is a function of the variances of channel estimation errors, the second possibility is to minimize this BEP value by adjusting the powers of the pilot symbols. In this way, we can guarantee that the optimum BEP is obtained. Similarly, we also need a feedback channel here.

Optimum Power Allocation for the Data Symbols

Like what we did in Chapter 2, we can also optimize the power for the data symbols and minimize the BEP value. However, the optimization problem here is more involved, since more parameters need to be taken care of. In this case, the channel estimates are time dependent, so the BEP results also depend on the time. The average BEP needs to be obtained by calculating all the BEP results for the data blocks between two adjacent pilot blocks. Besides, the BEP results obtained for STBC over non-identical channels with imperfect CSI are all bounds and approximations, so the issue of how to minimize the real BEP by minimizing these results should also be considered in future works.

Finally, both the power allocations for pilot symbols and data symbols can be considered together.

6.3 Code Design for $\mathcal{H}_i$ Systems over Time-Selective Channels

In Chapter 4, we have proposed a proposition and design criteria for the $\mathcal{G}_i$ Systems. There is another important generalized design for complex orthogonal STBC, the $\mathcal{H}_i$

design, which can be covered in future works. In order to analyze the performance of $\mathcal{H}_i$ systems over time-selective channels, the key step is to find the corresponding channel matrix for the manipulated received signals. Unlike the channel matrix for the $\mathcal{G}_i$ system, it is not straightforward to obtain the channel matrix for $\mathcal{H}_i$ systems, since both s_i and s_i^* appear in the same row of the code matrix. So, we may need to treat the real and imaginary parts of the transmitted symbols separately. Consequently, the corresponding channel matrices need to be obtained for the real and imaginary parts of the transmitted symbols. Having obtained these channel matrices, the performance of $\mathcal{H}_i$ systems may be similarly analyzed as for $\mathcal{G}_i$ systems, and the relationship between ISI and the code matrices may be obtained.

6.4 STBC over More General Channels

In this thesis, we considered STBC over three different kinds of channels. In the real world, however, two or more kinds of channels may appear together in one single situation. For example, it is possible that the channels are both non-identical and time-selective in the vehicular communications. In the cooperative scenario, if the relays are moving fast, the channels can be time-selective as well. Therefore, analyzing STBC over more general channels can be part of the future work.

Bibliography

[1] A. R. Bahai and B. R. Saltzberg, *Multicarrier Digital Communications: Theory and Applications of OFDM*. Plenum Publishing Corp., 1999.

[2] C. Berrou, A. Glavieux, and P. Thitimajshima, "Near shannon limit errorcorrecting coding: turbo codes," in *Proc. of ICC*, 1993, pp. 1067–1070.

[3] R. Gallager, "Low-density parity-check codes," *IEEE Tran. on on Inform. Theory*, vol. 8, pp. 21–28, Jan. 1962.

[4] R. J. McEllice, *The Theory of Information and Coding*, 2nd ed. Cambridge University Press, 2002.

[5] C. Shannon, "A mathematical theory of communication," *Bell Labs Tech. J.*, vol. 27, pp. 379–423,623–656, 1948.

[6] H. L. V. Trees, *Detection, Estimation and Modulation Theory*. Wiley, 1971.

[7] J. G. Proakis, *Digital Communications*, 4th ed. McGraw-Hill, 2000.

[8] G. J. Foschini and M. J. Gans, "On limits of wireless communications in a fading environment when using multiple antennas," *Wireless Personal Comm.*, vol. 6, pp. 311–335, 1998.

[9] E. Telatar, "Capacity of multi-antenna Gaussian channels," *European Transactions on Telecommunication*, vol. 10, no. 6, pp. 558–595, Nov. 1999.

[10] B. Vucetic and J. Yuan, *Space-Time Coding*. New York: John Wiley & Sons, Inc., 2003.

[11] J. Winters, "On the capacity of radio communication systems with diversity in a Rayleigh fading environment," *IEEE Journal on Selected Areas in Communications*, pp. 871–878, Jun 1987.

[12] A. Wittneben, "Basestation modulation diversity for digital simulcast," in *Proc. Vehicular Technology Conf. (VTC), IEEE*, 1991, pp. 848–853.

[13] ——, "A new bandwidth efficient transmit antenna modulation diversity scheme for linear digital modulation," in *Proc.International Conf. on Communication (ICC), IEEE*, vol. 3, 1993, pp. 1630–1634.

[14] N. Seshadri and J. Winters, "Two signaling schemes for improving the error performance of frequency-division-duplex (FDD) transmission systems using transmitter antenna diversity," in *Proc. Vehicular Technology Conf. (VTC), IEEE*, 1993, pp. 508–511.

[15] G. J. Foschini, "Layered space-time architecture for wireless communication in fading environment when using multi-element antennas,," *Bell Labs. Tech. J.*, vol. 1, no. 2, pp. 41–59, 1996.

[16] P.W.Wolniansky, G. Foschini, G. Golden, and R. Valenzuel, "V-blast: An architecture for realising very high data rates over the rich-scattering wireless channel," in *Proc. ISSSE98*, 1998.

[17] T. K. Y. Lo, "Maximum ration transmission," *IEEE Tran. Commun.*, vol. 16, pp. 1458–1461, Oct. 1999.

[18] S. A. Jafar, S. Vishawanath, and A. J. Goldsmith, "Channel capacity and beamforming for multiple transmit and receive antennas with covariance feedback," in *Proc. of IEEE ICC*, 2001, pp. 2266–2270.

[19] A. Narula, M. J. Lopez, M. D. Trott, and G. W. Wornell, "Efficient use of side information in multiple-antenna data transmission over fading channels," *IEEE J. Select. Areas Comm.*, vol. 16, pp. 1423–1436, Oct. 1998.

[20] D. J. Love and R. W. Health, "Grassmannian beamforming for muliple-input multiple output wireless system," *IEEE Trans. Info. Theory*, vol. 49, no. 10, pp. 2735–2747, Oct. 2003.

[21] S. H. Simon and A. Moustakas, "Optimizing MIMO antenna systems with channel covariance feedback," *Bell Lab. Tech. Memor.*, 2002.

[22] Z. Chen, J. Yuan, and V. B, "Analysis of transmit antenna selection/maximal-ratio combining in Rayleigh fading channels," *IEEE Trans. on Veh. Tech.*, vol. 54, no. 4, pp. 1312–1321, 2005.

[23] V. Tarohk, N. Seshadri, and A. R. Calderbank, "Space-time codes for high data rate wireless communications: perfrmance criterion and code construction," *IEEE Trans. Inform. Theory*, vol. 44, no. 2, pp. 744–765, Mar. 1998.

[24] W. Firmanto, B. Vucetic, and J. Yuan, "Space-time TCM with improved performance on fast fading channels," *IEEE Commun. Lett.*, vol. 5, pp. 154–156, 2001.

[25] J. Yuan, Z. Chen, B. Vucetic, and W. Firmanto, "Performance and design of space-time coding in fading channels," *IEEE Trans. Commun.*, vol. 51, pp. 1991–1996, Dec. 2003.

[26] M. Tao and P. Y. Kam, "Optimal differential detection and performance analysis of orthogonal space-time block codes over semi-identical MIMO fading channels," in *Proc. IEEE VTC*, vol. 4, Sept. 2005, pp. 2403–2407.

[27] J. Zhang, Y. Qiang, J. Wang, and D. Li, "On the design of space-time code for fast fading channels," in *Proc. PIMRC, IEEE*, 2003, pp. 1045–1048.

[28] Q. Yan and R. S. Blum, "Improved space-time convolutional codes for quasi-static slow fading channels," *IEEE Trans. Wireless Commun.*, vol. 1, pp. 563–571, Oct. 2002.

[29] S. M. Alamouti, "A simple transmit diversity technique for wireless communcations," *IEEE Journal select. Areas Commun.*, vol. 16, pp. 1451–1458, Oct. 1998.

[30] V. Tarokh, H. Jafarkhani, and A. R. Calderbank, "Space-time block coding from orthogonal designs," *IEEE Trans. Inform. Theory*, vol. 45, no. 5, pp. 1456–1467, 1999.

[31] ——, "Space-time block coding for wireless communications: Performance results," *IEEE J. Select. Areas Commun.*, vol. 17, no. 4, pp. 451–460, 1999.

[32] G. Ganesan and P. Stioca, "Space-time block codes: A maximum SNR approach," *IEEE Trans. Inform. Theory*, pp. 1650–1656, Apr. 2001.

[33] O. Tirkkonen and A. Hottinen, "Square-matrix embeddable space-time block codes for complex signal constellations," *IEEE Trans. Inform. Theory*, vol. 48, pp. 1122–1126, Feb. 2002.

[34] W. Su and X.-G. Xia, "Two generalized complex orthogonal space-time block codes for rate $7/11$ and $3/5$ for 5 and 6 transmit antennas," *IEEE Trans. Inform. Theory*, vol. 49, pp. 313–316, 2003.

[35] W. Su, X.-G. Xia, and K. J. R. Liu, "A systematic design of high-rate complex orthogonal space-time block codes," *IEEE Commun. Lett.*, vol. 8, pp. 380–382, 2004.

[36] X.-B. Liang, "A high-rate orthogonal space-time block code," *IEEE Commun. Lett.*, vol. 7, pp. 222–223, 2003.

[37] C. Xu, Y. Gong, and K. B. Letaief, "High-rate complex orthoogonal space-time block codes for high number of transmit antennas," in *proc. IEEE ICC*, 2004, pp. 20–24.

[38] M. P. Fitz, J. Grimm, and S. Siwamogshtham, "A new view of performance analysis techniques in correlated Rayleigh fading," in *Proc. IEEE WCNC*, 1999, pp. 139–144.

[39] M. K. Byun and B. G. Lee, "New bounds of pairwise error probability for space-time codes in Rayleigh fading channels," in *Proc. of Wireless Communications and Networking Conf.*, 2002, pp. 89–93.

[40] H. Lu, Y. Wang, P. V. Kumar, and K. M. Chugg, "Remarks on space-time codes including a new lower bound and an imporved codes," *IEEE Trans. Info. Theory*, vol. 49, no. 10, pp. 2752–2757, Oct. 2003.

[41] R. K. Mallik and Q. T. Zhang, "A tight upper bound on the pep of a space-time coded system," *to be appear in IEEE ICC*, 2006.

[42] M. Uysal and C. N. Georghiades, "Error performance analysis of space-time codes over Rayleigh fading channels," *Journal of Commun. and Networks*, vol. 2, no. 4, pp. 351–355, Dec. 2000.

[43] M. K. Simon, "Evaluation of average bit error probability for space-time coding based on a simpler exact evaluation of pairwise error probability," *Journal of Comm. and Network*, vol. 3, no. 3, pp. 257–264, Sept. 2001.

[44] G. Taricco and E. Biglieri, "Exact pairwise error probability of space-time codes," *IEEE Trans. Inform. Theory*, vol. 48, no. 2, pp. 510–513, Feb. 2002.

[45] C. Gao, A. Haimovich, and D. Lao, "Bit error probability for space-time block code with coherent and differential detection," in *Proc. IEEE VTC'02-Fall*, 2002.

[46] J. Yuan, "On the performance of space-time block codes on slow Rayleigh fading channels,," in *Proc. IEEE Personal, Indoor and Mobile Radio Communications (PIMRC)*, vol. 2, Sept. 2003, pp. 1688–1692.

[47] H. Shin and J. H. Lee, "Performance analysis of space-time block codes over keyhole Nakagami-m fading channels," *IEEE Trans. Vehicular Tech.*, vol. 53, no. 2, pp. 351–362, Mar. 2004.

[48] G. R. Mohammad-Khani, V. Meghdadi, J. P. Cances, and L. Azizi, "Maximum likelihood decoding rules for STBC generalized framework for detection and derivation of accurate upperbounds," in *Proc. IEEE ICC*, vol. 5, 2004, pp. 2578–2583.

[49] P. Garg, R. Mallik, and H. Gupta, "Performance analysis of space-time coding with imperfect channel estimation," in *Proc. Personal Wireless Communications, IEEE International Conference on*, Dec. 2002, pp. 71–75.

[50] H. Cheon and D. Hong, "Performance analysis of space-time block codes in time-varying rayleigh fading channels," in *Proc. IEEE ICASSP*, vol. 3, 2002, pp. 2357–2360.

[51] C. Shan, P. Y. Kam, and A. Nallanathan, "Theoretical performance of space-time block coded systems with channel estimation," in *Proc. IEEE Globecom*, 2004, pp. 3666–3670.

[52] J. K. Cavers, "An analysis of pilot symbol assisted modulation for rayleigh fading channls," *IEEE Trans. Veh. Tech.*, vol. 40, pp. 686–693, Nov. 1991.

[53] J. N. Laneman and G. W. Wornell, "Distributed space-time-coded protocols for exploiting cooperative diversity in wireless networks," *IEEE Trans. Inform. Theory*, vol. 49, no. 10, pp. 2415–2425, Oct. 2003.

[54] M. Z. Win and J. H. Winter, "Analysis of hybrid selection/maximal-ratio combining of diversity channels with unequal SNR in Rayleigh fading," in *Proc. IEEE VTC Fall*, vol. 1, 1999, pp. 215–220.

[55] P. Polydorou and P. Ho, "Error performance of MPSK with diversity combining in non-uniform Rayleigh fading and non-ideal channel estimation," in *Proc. IEEE VTC'00-Spring*, 2000, pp. 627 – 631.

[56] H. Fu and P. Y. Kam, "Performance of optimum and suboptimum combining diversity reception for binary DPSK over independent, nonidentical Rayleigh fading channels," in *Proc. IEEE ICC*, vol. 4, May 2005, pp. 2367–2371.

[57] M. Dohler, M. Hussain, and H. Aghvami, "Performance of distributed space-time block codes," in *Proc. VTC*, 2004, pp. 742–746.

[58] G. Scutari and S. Barbarossa, "Distributed space-time coding for regenerative relay networks," *IEEE Trans. Wireless Commun.*, vol. 4, no. 5, pp. 2387–2399, 2005.

[59] H. T. Cheng, H. Mheidat, M. Uysal, and T. M. Lok, "Distributed space-time block coding with imperfect channel estimation," in *Proc. IEEE ICC*, 2005, pp. 583–587.

[60] M. Tao and P. Y. Kam, "Analysis of differential orthogonal space time block codes over semi-identical MIMO fading channels," *IEEE Trans. Commun.*, vol. 55, no. 2, pp. 282–291, Feb. 2007.

[61] Y. Li and P. Y. Kam, "Space-time trellis codes over independent, non-identically distributed, rapid, Rayleigh fading channels with channel estimation," in *Proc. IEEE Globecom*, Nov. 2006.

[62] A. Maaref and S. Aissa, "Capacity and error probability analysis for orthogonal space-time block codes over correlated Rayleigh and Rician fading channels," *IEEE Trans. Wireless Commun.*, pp. 807–817, 2006.

[63] I.-M. Kim, "Exact ber analysis of OSTBCs in spatially correlated MIMO channels," *IEEE Trans. Commun.*, pp. 1365–1373, 2006.

[64] W. Li, H. Zhang, and T. A. Gulliver, "Capacity and error probability analysis of orthogonal space-time block codes over correlated Nakagami fading channels," *IEEE Trans. Wireless Commun.*, pp. 2408–2412, 2006.

[65] T. A. Tran and A. B. Sesay, "A generalized linear quasi-ML decoder of OSTBCs for wireless communications over time-selective fading channels," *IEEE Trans. Wireless Commun.*, vol. 3, no. 3, pp. 855–864, May 2004.

[66] Z. Liu, X. Ma, and G. B. Giannakis, "Space-time coding and kalman filtering for diversity transmissions through time-selective fading channels," in *Proc. IEEE MILCOM*, Oct. 2000, pp. 382–386.

[67] ——, "Space-time coding and kalman filtering for time-selective fading channels," *IEEE Trans. Commun.*, vol. 50, pp. 183–186, Feb. 2002.

[68] F.-C. Zheng and A. G. Burr, "Signal detection for orthogonal space-time block coding over time-selective fading channels: A PIC approach for the $\mathcal{G}_i$ systems," *IEEE Trans. Commun.*, vol. 53, no. 6, pp. 969–972, 2005.

[69] ——, "Signal detection for orthogonal space-time block coding over time-selective fading channels: the $\mathcal{H}_i$ systems," *IEEE Trans. Wireless Commun.*, vol. 5, no. 1, pp. 40–46, Jan. 2006.

[70] A. Vielmon, Y. Li, and J. R. Barry, "Performance analysis of alamouti transmit diversity over time-varying Rayleigh-fading channels," *IEEE Trans. Wireless Commun.*, vol. 3, no. 5, pp. 1369–1373, Sept. 2004.

[71] J. Wu and G. J. Saulnier, "Orthogonal space-time block code over time-varing flat-fading channels: Channel estimation, detection, and performance analysis," *IEEE Trans. Commun.*, vol. 55, no. 5, pp. 1077–1087, May 2007.

[72] J. N. Laneman and G. W. Wornell, "Energy efficient antenna sharing and relaying for wireless networks," in *Proc. IEEE WCNC*, Oct. 2000, pp. 7–12.

[73] A. Sendonaris, E. Erkip, and B. Aazhang, "User cooperation diversity-part I: System description," *IEEE Trans. Commun.*, vol. 51, pp. 1927–1938, 2003.

[74] ——, "User cooperation diversity-part II: Implementation aspects and performance analysis," *IEEE Trans. Commun.*, vol. 51, pp. 1939–1948, 2003.

[75] R. U. Nabar, H. Bolcskei, and F. W. Kneubuhler, "Fading relay channels: Performance limits and space-time signal design," *IEEE J. Select. Areas Commun.*, vol. 22, no. 6, pp. 1099–1109, Aug. 2004.

[76] A. Ribeiro, X. Cai, and G. B. Giannakis, "Symbol error probabilities for general cooperative links," *IEEE Trans. Wireless Commun.*, vol. 4, no. 3, pp. 1264–1273, May 2005.

[77] P. A. Anghel and M. Kaveh, "On the performance of distributed space-time coding systems with one and two non-regenerative relays," *IEEE Trans. Wireless Commun.*, vol. 5, no. 3, pp. 682–692, Mar. 2006.

[78] L. Xian and H. Liu, "An adaptive power allocation scheme for space-time block coded MIMO systems," in *Proc. IEEE WCNC*, 2005, pp. 504–508.

[79] M. Seo and S. W. Kim, "Power adaption in space-time block code," in *Proc. IEEE Globecom*, 2001, pp. 3188–3193.

[80] J. Cheng, H. Wang, J. Lilleberg, and S. Cheng, "Unequally powered STBC for slow flat Rayleigh fading channel," in *Proc. IEEE WCNC*, 2002, pp. 291–295.

[81] J. H. Horng, L. Li, and J. Zhang, "Adaptive space-time transmit diversity for MIMO systems," in *Proc. IEEE VTC'03-Spring*, 2003, pp. 1070–1073.

[82] G. Ganesan, P. Stioca, and E. G. Larsson, "Diagonally weighted orthogonal space-time block codes," in *Proc. Asilomar*, 2002, pp. 1147–1151.

[83] P. Y. Kam, "Optimal detection of digital data over the nonselective Rayleigh fading channel with diversity reception," *IEEE Trans. Commun.*, vol. 39, pp. 214–219, Feb. 1991.

[84] J. W. Craig, "A new, simple and exact result for calculating the probablity of error for two-dimensional signal constellaions," in *Proc. IEEE MILCOM*, Boston, MA, 1991, pp. 571–575.

[85] J. M. Wozencraft and I. M. Jacobs, *Principles of Communication Engineering*. Wiley, 1965.

[86] I. S. Gradshteyn and I. M. Ryzhik, *Table of integrals, Series, and Products*, 5th ed. Academic Press, 1994.

[87] J. He and P. Y. Kam, "On the performance of orthogonal space-time block codes over independent, nonidentical Rayleigh/Ricean fading channels," in *Proc. IEEE Globalcom*, Nov. 2006.

[88] G. Moniak, M. Berbineau, and J. F. Pardonche, "Robust and high data rate transmissions for security between a bus and a control center," in *Proc. IEEE VTC*, 2004, pp. 1377–1381.

[89] S. Biswas, R. Tatchikou, and F. Dion, "Vehicle-to-vehicle wireless communication protocols for enhancing highway traffic safety," *IEEE Communications Magazine*, vol. 44, pp. 74–82, Jan. 2006.

[90] W. Xiang, P. Richardson, and J. Guo, "Introduction and preliminary experimental results of wireless access for vehicular environments (WAVE) systems," in *the Third Annual International Conference on Mobile and Ubiquitous Systems: Networking and Services*, 2006, pp. 1–8.

[91] S. Eichler, "Performance evaluation of the IEEE 802.11p WAVE communication standard," in *Proc. IEEE VTC*, 2007, pp. 2199–2203.

[92] M. Wellens, B. Westphal, and P. Mahonen, "Performance evaluation of IEEE 802.11-based WLANs in vehicular scenarios," in *Proc. IEEE VTC*, 2007, pp. 1167–1171.

[93] W. C. Jakes, *Microwave Mobile Communication*. Wiley, 1974.

[94] F.-C. Zheng and A. G. Burr, "Receiver design for orthogonal space-time block coding for four transmit antennas over time-selective fading channels," in *Proc. IEEE Globecom*, vol. 1, 2003, pp. 128–132.

[95] ——, "Double diagonalization: an improved zero-forcing detector for orthogonal STBC over time-selective fading channels," in *Proc. IEEE VTC*, 2005, pp. 1060–1064.

[96] T. Cui and C. Tellambura, "Efficient signal detection for space-time block coding over time-selective fading channels," in *Proc. of IEEE WCNC*, 2006, pp. 1771–1775.

[97] L. Y. Song and A. G. Burr, "Successive interference cancelation for space-time block codes over time-selective channels," *IEEE Commun. Lett.*, vol. 10, no. 12, pp. 837–839, Dec. 2006.

[98] D. Yu and J. H. Lee, "A robust detection scheme of orthogonal space-time block codes over vey fast fading channels," *IEICE Trans. Commun.*, no. 1, pp. 171–175, Jan. 2007.

[99] G. P. Villardi, G. T. F. Abreu, and R. Kohno, "Modified orthogonal space-time block codes for time-selective fading channels," in *Proc. Asilomar*, 2005, pp. 1243–1247.

[100] M. K. Simon and M. S. Alouini, *Digital Communication over Fading Channel*, 2nd ed. Wiley, 2004.

[101] J. Lu, K. B. Letaief, C.-I. Chuang, and M. L. Liou, "M-PSK and M-QAM BER computation using signal-space concepts," *IEEE Trans. Commun.*, vol. 47, no. 2, pp. 181–184, 1999.

[102] P. A. Anghel, G. Leus, and M. Kaveh, "Multi-user space-time coding in cooperative networks," in *Proc. ICASSP*, vol. 4, 2003, pp. 73–76.

[103] S. Barbarossa and G. Scutari, "Cooperative diversity through virtual arrays in multihop network," in *Proc. ICASSP*, vol. 5, 2003, pp. 209–212.

[104] M. Dohler, A. Gkelias, and H. Aghvami, "A resource allocation strategy for distributed MIMO multi-hop communication systems," *IEEE Commun. Lett.*, vol. 8, no. 2, pp. 99–101, Feb. 2004.

[105] S. Barbarossa and G. Scutari, "Distributed space-time coding strategies for wideband multihop networks: regenerative vs. non-regenerative relays," in *Proc. ICASSP*, 2004, pp. 501–504.

[106] A. Stefanov and E. Erkip, "On the performance analysis of cooperative space-time coded systems," in *Proc. WCNC*, 2003, pp. 729–734.

[107] M. Uysal and H. Mheidat, "Maximum-likelihood detection for distributed space-time block coding," in *Proc. IEEE VTC'04-Fall*, 2004, pp. 2419–2423.

[108] M. O. Hasna and M. Alouini, "End-to-end performance of transmission systems with relays over Raleigh-fading channels," *IEEE Trans. Wireless Commun.*, vol. 2, no. 6, pp. 1126–1131, Nov. 2003.

List of Publications

1. J. He, and P. Y. Kam, “Performance Analysis of Orthogonal Space-Time Block Codes over Time-Selective Channels, and Applications to Code Design of $\mathcal{G}_i$ Systems”, *IEEE Transaction on Communications*, Vol. 57, Issue 3, pp. 707-715, Mar. 2009.

2. J. He, and P. Y. Kam, “Orthogonal Space-Time Block Codes in Vehicular Environments: Optimum Receiver Design and Performance Analysis”, *EURASIP Journal on Wireless Communications and Networking*, Special issue on Wireless Access in Vehicular Environment, vol. 2009, 2009.

3. J. He, and P. Y. Kam, “Cooperative Space-Time Block Coding with Amplify-and-Forward Strategy: Exact Bit Error Probability and Adaptive Forwarding Schemes”, *ELSEVIER Journal on Physical Communications*, Vol. 1, Issue3, pp. 209-220, Sep 2008

4. J. He, and P. Y. Kam, “Orthogonal Space-Time Block Codes over Semi-Identical Channels with Channel Estimation”, in *Proc. IEEE Global Communications Conference (GLOBECOM08)*, New Orleans, LA. USA, Nov. 30 - Dec. 4, 2008.

5. J. He, and P. Y. Kam, “Optimum Space-Time Block Codes over Time-Selective Channels”, in *Proc. IEEE Global Communications Conference (GLOBECOM08)*, New Orleans, LA. USA, Nov. 30 - Dec. 4, 2008.

6. J. He, and P. Y. Kam, “Exact Bit Error Probability of Cooperative Space-Time Block Coding with Amplify-and-Forward Strategy”, in *Proc. IEEE International Conference on Communications (ICC08)*, Beijing, China, May. 19 - 23, 2008.

7. J. He, and P. Y. Kam, “Adaptive Cooperative Space-Time Block Coding with Amplify-and-Forward Strategy”, *Proc. IEEE Vehicular Technology Conference (VTC08Spring)*, Singapore, May. 11–14, 2008.

8. J. He, and P. Y. Kam, “On the Performance of Distributed Space-Time Block Coding over Nonidentical Ricean Channels and the Optimum Power Allocation”, in *Proc. IEEE International Conference on Communications (ICC07)*, Glasgow, UK, Jun. 24 - 28, 2007.

9. J. He, and P. Y. Kam, “Bit Error Performance of Orthogonal Space-Time Block Codes over Time-Selective Channel”, in *Proc. IEEE International Conference on Communications (ICC07)*, Glasgow, UK, Jun. 24 - 28, 2007.

10. J. He, and P. Y. Kam, “On the Performance of Orthogonal Space-Time Block Codes over Independent, Nonidentical Rayleigh/Ricean Fading Channels”, in *Proc. IEEE Global Communications Conference (GLOBECOM06)*, San Francisco, CA. USA, Nov. 27 - Dec. 1, 2006.

Appendix A

Proof of Inequality (2.39)

We first bound the BEP (2.28) with inequality (2.35) as

$$P_{k'}(e) \geq \frac{1}{\pi}\int_0^{\frac{\pi}{2}} \frac{\exp\left(-\sum_{m=1}^{M_T}\sum_{n=1}^{N_R}\left(\frac{\mu_m|M_{m,n}|^2}{\sin^2\theta+2\sigma_{m,n}^2\mu_m}\right)\right)}{\left(1+\frac{A_1}{\sin^2\theta}\right)^{M_T N_R}} d\theta. \tag{A.1}$$

Now the numerator term can be further written as

$$\begin{aligned} & \exp\left(-\sum_{m=1}^{M_T}\sum_{n=1}^{N_R}\left(\frac{2\sigma_{m,n}^2\mu_m K_o}{\sin^2\theta+2\sigma_{m,n}^2\mu_m}\right)\right) \\ = \; & \exp\left(-\sum_{m=1}^{M_T}\sum_{n=1}^{N_R}\left(K_o-\frac{K_o\sin^2\theta}{\sin^2\theta+2\sigma_{m,n}^2\mu_m}\right)\right) \\ = \; & \exp\left(-M_T N_R K_o + K_o\sin^2\theta\sum_{m=1}^{M_T}\sum_{n=1}^{N_R}\left(\frac{1}{\sin^2\theta+2\sigma_{m,n}^2\mu_m}\right)\right). \end{aligned} \tag{A.2}$$

Applying the arithmetic mean-harmonic mean inequality [86], we can obtain the inequality

$$\sum_{i=1}^{Q}\frac{1}{a+x_i} \geq \frac{Q}{a+x_{am}}, \tag{A.3}$$

where a and the x_i's are positive numbers and x_{am} is the arithmetic mean of the x_i's.

Therefore, the numerator term is lower bounded as

$$\begin{aligned} & \exp\left(-\sum_{m=1}^{M_T}\sum_{n=1}^{N_R}\left(\frac{2\sigma_{m,n}^2\mu_m K_o}{\sin^2\theta + 2\sigma_{m,n}^2\mu_m}\right)\right) \\ \geq\ & \exp\left(-M_T N_R K_o + \left(\frac{M_T N_R K_o \sin^2\theta}{\sin^2\theta + \frac{\sum_{m=1}^{M_T}\sum_{n=1}^{N_R} 2\sigma_{m,n}^2\mu_m}{M_T N_R}}\right)\right) \\ =\ & \exp\left(-\frac{M_T N_R K_o A_1}{\sin^2\theta + A_1}\right), \end{aligned} \tag{A.4}$$

and inequality (2.39) is proved.

Appendix B

Performance Approximation of Some $\mathcal{G}_4$ Systems

In section 4.3.1, we use the optimum $\mathcal{G}_4$ code matrix. The variance of the interference contains the common term $\|\mathbf{h}_1\|^2$, therefore, we can cancel this common term in the denominator and the numerator in (4.18). If other $\mathcal{G}_4$ code matrices are used, the variance of the interference may not be directly related to $\|\mathbf{h}_1\|^2$. For example, for the hand-designed $\mathcal{G}_4$ code (4.53), the variance of the interference is given by

$$\begin{aligned}&\left(1-|R(1)|^2\right)\left(\|\mathbf{h}_1\|^2+|h_2(2)|^2+|h_2(7)|^2+|h_3(3)|^2+|h_3(6)|^2\right)E_s\\&+\left(1-|R(3)|^2\right)\left(|h_1(1)|^2+|h_1(8)|^2+|h_2(2)|^2+|h_2(7)|^2+2|h_4(4)|^2+2|h_4(5)|^2\right)E_s\\&+\left(1-|R(5)|^2\right)\left(|h_1(1)|^2+|h_1(8)|^2+|h_3(3)|^2+|h_3(6)|^2\right)E_s.\end{aligned}$$

In such a case, however, we can approximate this variance. Noting that the $|h_i(t)|^2$'s are identically distributed and $\|\mathbf{h}_1\|^2$ is the sum of eight different $|h_i(t)|^2$'s, we approximate each $|h_i(t)|^2$ as $\|\mathbf{h}_1\|^2/8$. Thus, the variance of the interference can be approximated as

$$\frac{3}{2}\left(1-|R(1)|^2\right)\|\mathbf{h}_1\|^2E_s+\left(1-|R(3)|^2\right)\|\mathbf{h}_1\|^2E_s+\frac{1}{2}\left(1-|R(5)|^2\right)\|\mathbf{h}_1\|^2E_s. \quad \text{(B.1)}$$

All the remaining steps are then similar to those from (4.18) to (4.24). This method leads to a very close approximation to the average BEP, as shown in Fig 4.8.

Appendix C

Derivation of Equation (5.41)

The conditional BEP (5.40) has two exponential terms, which include variables $|h_{SR}|^2$ and $|h_{SD}|^2$, separately. Therefore, we can average over them one by one. Noticing that $|h_{SD}|^2$ and $|h_{SR}|^2$ are central chi-square distributed, we first average over $E_{SR}|h_{SR}|^2$ from $E_{SD}|h_{SD}|^2$ to infinity, and obtain

$$\begin{aligned}
&P_{\alpha}^{STBC}\left(e|h_{RD},h_{SR},E_{SR}|h_{SR}|^2>E_{SD}|h_{SD}|^2\right)\\
&=\frac{1}{\pi}\int_0^{\frac{\pi}{2}}\exp\left(-\frac{E_{SD}|h_{SD}|^2\cos^2\alpha}{(E_{RD}|h_{RD}|^2+1)N_o\sin^2\theta}\right)\\
&\quad\cdot\int_{E_{SD}|h_{SD}|^2}^{\infty}\frac{\exp\left(-\frac{xE_{RD}|h_{RD}|^2\cos^2\alpha}{(E_{RD}|h_{RD}|^2+1)N_o\sin^2\theta}-\frac{x}{2\sigma_{SD}^2E_{SD}}\right)}{2\sigma_{SR}^2E_{SR}}dxd\theta\\
&=\frac{1}{\pi}\int_0^{\frac{\pi}{2}}\frac{\exp\left(-\frac{E_{SD}|h_{SD}|^2\cos^2\alpha}{N_o\sin^2\theta}-\frac{E_{SD}|h_{SD}|^2}{2\sigma_{SR}^2E_{SR}}\right)}{\frac{E_{SR}2\sigma_{SR}^2E_{RD}|h_{RD}|^2\cos^2\alpha}{(E_{RD}|h_{RD}|^2+1)N_o\sin^2\theta}+1}d\theta.
\end{aligned}\tag{C.1}$$

Similarly, averaging over $|h_{SD}|^2$, we have

$$\begin{aligned}
&P_{\alpha}^{STBC}\left(e|h_{RD},\ E_{SR}|h_{SR}|^2>E_{SD}|h_{SD}|^2\right)\\
&=\frac{1}{\pi}\int_0^{\frac{\pi}{2}}\frac{\frac{g}{1+ag}}{\frac{E_{SR}2\sigma_{SR}^2E_{RD}|h_{RD}|^2\cos^2\alpha}{(E_{RD}|h_{RD}|^2+1)N_o\sin^2\theta}+1}d\theta
\end{aligned}\tag{C.2}$$

where a and g are defined in (5.14) and (5.42), respectively. Averaging equation (C.2) with the help of Lemma 5.1, the average BEP is given by (5.41).

Appendix D

Derivation of Equation (5.44)

Since equation (5.43) is independent of $|h_{RD}|^2$, we first average over $E_{SD}|h_{SD}|^2$ from $E_{SR}|h_{SR}|^2$ to infinity, and obtain

$$\begin{aligned} & P_{\alpha}^{STBC}\left(e|h_{SR},\ h_{SR} < h_{SD}\right) \\ &= \frac{1}{\pi}\int_0^{\frac{\pi}{2}} \int_{E_{SR}|h_{SR}|^2}^{\infty} \frac{\exp\left(-\frac{x\cos^2\alpha}{N_o\sin^2\theta} - \frac{x}{2\sigma_{SD}^2 E_{SD}}\right)}{2\sigma_{SD}^2 E_{SD}} dx d\theta \\ &= \frac{1}{\pi}\int_0^{\frac{\pi}{2}} \frac{1}{a}\exp\left(-\frac{E_{SR}|h_{SR}|^2\cos^2\alpha}{N_o\sin^2\theta} - \frac{E_{SR}|h_{SR}|^2}{2\sigma_{SD}^2 E_{SD}}\right) d\theta. \end{aligned} \tag{D.1}$$

Averaging the above equation over $|h_{SR}|^2$, the average BEP is given by (5.44).

Appendix E

Derivation of Equation (5.48)

Averaging over $|h_{SR}|^2$ and $|h_{SD}|^2$, the conditional BEP is given as

$$\begin{aligned} & P_{\alpha}^{STBC}\left(e|h_{RD},|h_{SR}|^2>|h_{th}|^2\right) \\ &= \frac{\exp\left(-\frac{|h_{th}|^2}{2\sigma_{SR}^2}\right)}{\pi}\int_0^{\frac{\pi}{2}}\left(1+\frac{2\sigma_{SR}^2E_{SR}E_{RD}|h_{RD}|^2\cos^2\alpha}{(E_{RD}|h_{RD}|^2+1)N_o\sin^2\theta}\right)^{-1} \\ &\qquad \cdot\left(1+\frac{2\sigma_{SD}^2E_{SD}\cos^2\alpha}{(E_{RD}|h_{RD}|^2+1)N_o\sin^2\theta}\right)^{-1} \\ &\qquad \cdot\exp\left(-\frac{E_{SR}E_{RD}|h_{RD}|^2|h_{th}|^2\cos^2\alpha}{(E_{RD}|h_{RD}|^2+1)N_o\sin^2\theta}\right)d\theta. \end{aligned} \tag{E.1}$$

We need to average the above equation over $|h_{RD}|^2$, but it is hard to obtain a closed-form result. Under the high SNR assumption $E_{RD}|h_{RD}|^2 \gg 1$, we have

$$\exp\left(-\frac{E_{SR}E_{RD}|h_{RD}|^2|h_{th}|^2\cos^2\alpha}{(E_{RD}|h_{RD}|^2+1)N_o\sin^2\theta}\right)\approx\exp\left(-\frac{E_{SR}|h_{th}|^2\cos^2\alpha}{N_o\sin^2\theta}\right). \tag{E.2}$$

Now, the average of (E.1) can be approximated with the help of Lemma 5.1, which is given in (5.48).